Thesis submitted for the degree of Doctor of Philosophy

Trinity Term 2012

UNDERSTANDING THE LINK BETWEEN INTERLEUKIN 17 AND VACCINE-INDUCED PROTECTION IN TUBERCULOSIS

Kristin Lisa Griffiths

Lincoln College

Jenner Institute & Medical Sciences Doctoral Training Centre

University of Oxford

Word count: 27 700 words

CLARENDON FUND

wellcome trust

Understanding the Link Between Interleukin 17 and Vaccine-Induced Protection in Tuberculosis

Kristin Griffiths, Lincoln College

Thesis submitted for the degree of Doctor of Philosophy, Trinity Term 2012

Abstract

Tuberculosis (TB), caused by infection with *Mycobacterium tuberculosis* (*M.tb*), remains a global health problem and although BCG offers some protection against childhood disseminated disease and other mycobacterial infections, its efficacy against pulmonary TB varies between 0 and 80%. Modified Vaccinia virus Ankara expressing antigen 85A (MVA85A) is a novel TB vaccine designed to boost mycobacterium-specific $CD4^+$ T cell response primed by BCG. MVA85A induces strong interferon (IFN)-γ responses, a cytokine known to be essential for protection following *M.tb* infection. A strong IFN-γ response is not a correlate of protection and in terms of the adaptive response, interleukin (IL)-17 is emerging as an important cytokine following vaccination as it is thought to help boost IFN-γ production by $CD4^+$ T cells. This thesis shows that MVA85A induces IL-17 in PBMC and whole blood of human BCG – MVA85A vaccinees. This is replicated in mice receiving BCG – MVA85A intranasally. The administration of cholera toxin (CT) with BCG enhances IL-17 and confers improved protection following *M.tb* challenge, which is partially dependent on IL-17 and on the mucosal route of administration. Since CT is not a suitable adjuvant in humans, an alternative IL-17-inducing pathway was investigated. In human BCG – MVA85A-vaccinated volunteers, blocking the hydrolysing ability of the CD39, an apyrase responsible for hydrolysing pro-inflammatory ATP, enhances IL-17 production. Challenge of BCG – MVA85A-vaccinated $CD39^{-/-}$ mice with *M.tb* slightly improved the protective capacity of the vaccine, suggesting that a pathway dependent on ATP-driven inflammation may be a target for improving the immunogenicity of a vaccine against *M.tb* disease. Overall, this thesis has confirmed the important role of IL-17 in vaccine-induced protection against TB disease and identifies a possible target pathway for improvement of a novel vaccine.

ACKNOWLEDGEMENTS

First and foremost I would like to thank my supervisors Professor Helen McShane and Dr Helen Fletcher for their encouragement, enthusiasm, support and guidance throughout my project, even providing me with a roof over my head when I needed it. This DPhil has been a very positive experience and I will never forget these last four years. I hope I have managed to contribute to the lab even a fraction of what I have gained from being here.

This thesis could not have happened without the friendship, patience and many hours of assistance during the interminable challenge and takedown experiments, especially from Elena Stylianou and Hazel Poyntz, as well as Rachel Kandt and Gareth Betts. Thanks also to Iman Satti for invaluable help throughout and to Elena Stylianou and Magali Matsumiya for always being there as a sounding board for thoughts and ideas, scientific or otherwise. And thanks to the rest of the TB group for making this a great place to work.

Thanks also to Drew Worth for help with flow cytometry, and Julie Furze for running smooth lab and helping me find things when they're right in front of me!

None of the animal work could have taken place without the assistance of the FGF staff, in particular Carol Williams, Viv Clark, Heather Gray, Stacy and Douglas.

I would like to thank Professors Keith Gull and Fiona Powrie, along with the Wellcome Trust and the Clarendon Fund for accepting me onto the IITM programme and giving me this opportunity to come to Oxford for my DPhil.

The animal experiments would not be complete without the generous donation of knockout mouse strains: CD39null animals from Dr Simon Robson from the Beth Israel Deaconess Medical Centre, and IL-17KO animals from Prof Fiona Powrie and Dr Kevin Maloy from the University of Oxford.

My four years here would not have been the same without the friendships of Ivy Christou, Beatrice Krebs, Tumena Corrah and Anne Grijzenhout. Thanks also to rowing and the various permutations of Lincoln W1 for keeping me sane and organised.

I would never have got here without the support of my parents Anne and Cedge – thank you for bringing me up to be the person I am today, for always being there, believing in me, pushing me and being proud of me. And thanks to my hermanita Kari Griffiths for being the best sister a girl could ask for.

I couldn't have got through the writing without Meg's kind offer of her cottage in Spaxton where I spent my most productive two weeks.

And finally, thank you Abhi not only for helping with the MATLAB-related analysis, but also for putting up with me and always finding ways/places for us to meet to make our four years apart go that little bit faster – I'm lucky to have you in my life now and for the rest of our lives.

TABLE OF CONTENTS

Abstract ii

Acknowledgements iii

Table of Contents v

List of figures x

List of tables xi

List of abbreviations xii

Introduction 1

1 Introduction 2

1.1 Tuberculosis as a global problem 2

1.1.1 Epidemiology of tuberculosis disease 2

1.1.2 Pathogenesis, immunology and pathology of TB infection 3

1.1.3 Current measures for TB control 9

1.1.4 Vaccination as a means of controlling TB 13

1.2 $CD4^+$ T cell subsets 21

1.2.1 The Th1/Th2 paradigm 21

1.2.2 Th17 cells 23

1.2.3 T cell memory 25

1.2.4 Regulatory T cells 27

1.2.5 Other T cell subsets 30

1.3 Interleukin 17 and vaccine-induced control of TB disease 31

1.3.1 IL-17 is essential in vaccine-induced control in mice 32

1.3.2 IL-17 correlates with protection-associated pathology in vaccinated cattle 35

1.3.3 Evidence of a protective role for IL-17 in human TB 37

1.3.4 MVA85A induces IL-17 in human volunteers 38
1.4 Cholera toxin as an IL-17-inducing adjuvant 39
1.5 Aims of the project 42
1.6 Experimental approaches 42
1.6.1 Samples from volunteers vaccinated with MVA85A 42
1.6.2 Murine studies using an M.tb aerosol challenge model 42
Materials & Methods 44
2 Materials & Methods 45
2.1 Human samples 45
2.1.1 Vaccine study participants 45
2.1.2 Thawing of cryopreserved peripheral blood mononuclear cells 45
2.1.3 Stimulation of PBMC 45
2.1.4 Flow cytometry 46
2.1.5 ATP assay 46
2.2 Animal work 47
2.2.1 Animals 47
2.2.2 Anaesthesia 47
2.2.3 Bacille Calmette-Guérin and Mycobacterium tuberculosis 47
2.2.4 Modified Vaccinia virus Ankara with Antigen 85A 48
2.2.5 Vaccination 48
2.2.6 Dissection and organ preparation 48
2.2.7 Stimulation 49
2.2.8 Flow cytometry 49
2.2.9 Mycobacterium tuberculosis challenge 50
2.2.10 Organ homogenisation and plating 50
2.2.11 Challenge takedown 51
2.2.12 Organ fixation for histology and preparation of paraffin sections 51

2.2.13 Immunohistochemical staining of lung sections 51
2.2.14 Analysis of lung sections 52
2.2.15 IL-17 ELISA 53
2.2.16 Antibody blocking and testing 54
2.2.17 RT-qPCR 54
2.3 Statistical analyses 56
Results 57
3 Induction of IL-17 following vaccination of healthy volunteers with MVA85A 58
3.1 Introduction 58
3.2 ATP hydrolysis following MVA85A vaccination follows a distinct pattern and can be inhibited using an apyrase inhibitor 58
3.3 IFN-γ and IL-17 double positive cells peak 2 weeks post-vaccination 60
3.4 IL-17$^+$ and IFN-γ$^+$IL-17$^+$ cells are present at a higher frequency in whole blood compared to PBMC of vaccinated subjects 62
3.5 Discussion 63
4 Evaluating the immunogenicity of a BCG prime – MVA85A boost vaccination regime in mice 66
4.1 Introduction 66
4.2 Timecourse of BCG-induced IFN-γ and IL-17 following intranasal vaccination of Balb/c mice 66
4.3 Timecourse of BCG – MVA85A-induced IFN-γ and IL-17 following *i.d.* vs. *i.n.* vaccination of Balb/c mice 70
4.4 Timecourse of BCG – MVA85A-induced IFN-γ and IL-17 following intranasal vaccination in C57BL/6 mice 73
4.5 Induction of CD8$^+$ T cells following BCG or BCG – MVA85A vaccination 77
4.6 Discussion 79

5 Cholera toxin treatment 81
5.1 Introduction 81
5.2 The effect of cholera toxin administration with BCG ± MVA85A on immunogenicity 82
5.2.1 CT administered with BCG 82
5.2.2 CT with BCG followed by MVA85A 84
5.2.3 BCG followed by CT with MVA85A 86
5.3 The effect of cholera toxin administration with BCG on vaccine efficacy 91
5.3.1 CT administered with BCG 91
5.3.2 Cholera toxin with BCG followed by MVA85A 92
5.4 The effect of cholera toxin administration with BCG on lung pathology following challenge 94
5.5 The effect of blocking IL-17 following challenge of BCG + CT – MVA85A-vaccinated animals 96
5.6 The effect of CT administration with BCG *i.d.* on *M.tb* challenge outcome 99
5.7 The effect of cholera toxin administration with BCG in animals lacking IL-17A 101
5.8 Discussion 103
6 Vaccination and challenge of CD39$^{-/-}$ animals 107
6.1 Introduction 107
6.2 Immunogenicity of BCG – MVA85A in CD39$^{-/-}$ mice 108
6.3 Vaccinated CD39$^{-/-}$ animals are better protected against *M.tb* challenge compared to WT animals 109
6.4 Pathology 111
6.5 Post-challenge gene expression 112
6.6 Discussion 114
Conclusions & Future Work 117

7 Conclusions & Future work 118

Appendix ..... a

8 Appendix ..... b

8.1 Table of reagents ..... b

8.2 Table of solutions ..... e

8.3 Testing the blocking activity of the anti-IL-17 antibody MAB421 from R&D Systems ..... e

9 References ..... g

10 Published papers ..... w

LIST OF FIGURES

Figure 1.1.3 Prevalence of TB and estimated projections for 2015 12
Figure 1.4 CT pathway resulting in cytokine production.....40
Figure 3.2.1 ATP hydrolysis by PBMC and $CD39^+$ Treg percentages dip 2 weeks post-vaccination.....59
Figure 3.3.1 IL-17 and IFN-γ production in PBMC peaks 2 weeks post-vaccination.....61
Figure 3.4.1 IL-17 and IFN-γ production in whole blood peaks 1 week post-vaccination.....63
Figure 4.2.1 Immunogenicity of BCG delivered *i.n*.....67
Figure 4.3.1 Immunogenicity of BCG – MVA85A following *i.d.* and *i.n.* administration.....71
Figure 4.4.1 Immunogenicity of BCG – MVA85A delivered *i.n.* in C57BL/6 mice.....75
Figure 4.5.1 $CD8^+$ T cell induction following *i.n.* BCG vaccination.....77
Figure 4.5.2 Boosting of BCG-induced $CD8^+$ T cell responses with MVA85A.....78
Figure 5.2.1 Effect of cholera toxin on BCG immunogenicity.....83
Figure 5.2.2 Immunogenicity of BCG + CT followed by MVA85A.....85
Figure 5.2.3 Administration of CT with MVA85A either *i.n.* or *i.d.* following an intranasal BCG prime.....88
Figure 5.3.1 Vaccine efficacy of BCG *i.n.* + CT.....91
Figure 5.3.2 Effect of CT on vaccine efficacy in a BCG – MVA85A vaccine regime.....93
Figure 5.4.1 Histological analysis of *M.tb*-exposed lung.....95
Figure 5.5.1 Effect of blocking IL-17 on vaccine efficacy following *M.tb* challenge.....98
Figure 5.6.1 Effect of BCG *i.d.* + CT on *M.tb* challenge outcome.....100
Figure 5.7.1 Effect of BCG ± CT in IL-$17^{-/-}$ mice following *M.tb* challenge.....102
Figure 6.2.1 Immunogenicity of BCG – MVA85A in $CD39^{-/-}$ mice.....108
Figure 6.3.1 Challenge of $CD39^{-/-}$ animals with *M.tb*.....110
Figure 6.4.1 Histological analysis of lung section from WT and $CD39^{-/-}$ animals challenged with *M.tb*.....111
Figure 6.5.1 Gene expression in lungs of *M.tb*-challenged WT and $CD39^{-/-}$ mice.....113
Figure 7.1.1 Comparison of CT and ATP adjuvanting pathways.....121
Figure 8.3.1 Effect of the anti-IL-17 blocking antibody MAB421.....f

LIST OF TABLES

Table 1.2.17 Primer sequences……56
Table of reagents……b
Table of solutions……e

LIST OF ABBREVIATIONS

AC	adenyl cyclase
Ad85A	adenovirus expressing antigen 85A
ADP	adenosine diphosphate
Ag85A	antigen 85A
Ag85B	antigen 85B
AMP	adenosine monophosphate
APC	antigen-presenting cell
APC	allophycocyanin
ART	anti-retroviral therapies
ATP	adenosine triphosphate
BAL	bronchoalveolar lavage
BCG	Bacille Calmette-Guérin
BMMΦ	bone marrow-derived macrophage
C.albicans	*Candida albicans*
cAMP	cyclic AMP
CCR	C-C motif receptor
CD	cluster of differentiation
cDNA	complementary DNA
CFP-10	culture filtrat protein 10
cfu	colony forming units
cholera toxin	CT
CR3	complement receptor 3
CREB	cAMP response element binding unit
CTLA4	cytotoxic lymphocyte antigen 4
CXCL	C-X-C chemokine ligand
CXCR	C-X-C chemokine receptor
dbcAMP	dibutyryl cAMP
DC	dendritic cell
DMSO	dimethylsulphoxide
DNA	deoxyribonucleic acid
DOTS	directly-observed therapy short course
EAE	experimental autoimmune encephalomyelitis
EDTA	ethylenediaminetetraacetic acid
ELISA	enzyme-linked immunosorbant assay

ELISpot	enzyme-linked immunosorbant spot
ESAT-6	early secreted antigenic target 6
EU	European Union
FITC	fluorescein isothiocyanate
Foxp3	forkhead box P3
FSC	forward scatter
GPCR	G protein-coupled receptor
GSK	Glaxo Smith Kline
H&E	haemotoxylin and eosin
HIV	human immunodeficiency virus
i.d.	*intradermal*
i.n.	*intranasal*
i.p.	*intraperitoneal*
i.v.	*intravenous*
ICS	intracellular cytokine staining
IFN-γ	interferon gamma
IGRA	IFN-γ release assay
IL	interleukin
iNOS	inducible nitric oxide synthase
IRF	interferon regulatory factor
IRIS	immune reconstitution inflammatory syndrome
iTreg	inducible regulatory T cell
KO	knockout
L.monocytogenes	*Listeria monocytogenes*
LN	lymph node
LPS	lipopolysaccharide
M.bovis	*Mycobacterium bovis*
M.leprae	*Mycobacterium leprae*
M.lepromatosis	*Mycobacterium lepromatosis*
M.smegmatis	*Mycobacterium smegmatis*
M.tb	*Mycobacterium tuberculosis*
MBL	mannose-binding lectin
MDR-TB	multi-drug resistant tuberculosis
MHC	major histocompatibility complex
MPL	monophosphoryl lipid
MR	mannose receptor

mRNA	messenger RNA
MS	multiple sclerosis
MVA	modified Vaccina virus Ankara
MVA85A	MVA expressing antigen 85A
NADPH	nicotinamide adenine dinucleotide phosphate
NALP3	NACHT, LRR and PYD domains-containing protein 3
NF-κB	nuclear factor κB
NTM	non-tuberculous mycobacteria
nTreg	natural regulatory T cell
OCHRe	Oxford Centre for Histopathology Research
OVA	ovalbumin
PBMC	peripheral blood mononuclear cells
PBS	phosphate buffered saline
PCR	polymerase chain reaction
PE	phycoerythrin
PE-Cy5	phycoerythrin cychrome 5
PE-Cy7	phycoerythrin cychrome 7
pfu	plaque forming units
PGE_2	prostaglandin E_2
PMA	phorbol myristate acetate
PPD	purified protein derivative
PRR	pattern recognition receptor
RNA	ribonucleic acid
RNI	reactive nitrogen intermediates
ROI	reactive oxygen intermediates
RORγt	RAR-related orphan receptor gamma t
RT-qPCR	real time quantitative polymerase chain reaction
s.c.	*sub cutaneous*
SSC	side scatter
STAT	signal transducer and activator of transcription
T-bet	T-box expressed in T cells
TB	Tuberculosis
T_{cm}	central memory T cell
TCR	T cell receptor
TDM	trehalose dimycolate
TDR-TB	totally drug resistant tuberculosis

T_{eff}	effector T cell
T_{em}	effector memory T cell
TGF-β	transforming growth factor beta
Th	T helper
TLR	toll-like receptor
TNF-α	tumour necrosis factor alpha
Treg	regulatory T cell
TST	tuberculin skin test
UK	United Kingdom
WHO	World Health Organisation
WT	wild type
XDR-TB	extensively-drug resistant tuberculosis
ZN	Ziehl-Neelsen

INTRODUCTION

1 INTRODUCTION

1.1 Tuberculosis as a global problem

1.1.1 Epidemiology of tuberculosis disease

Tuberculosis (TB) is a disease most commonly caused by infection with the acid-fast bacterium (so named because it is not de-colourised during acid-based staining procedures [1]) *Mycobacterium tuberculosis* (*M.tb*). Currently, one third of the world's population is infected with *M.tb* [2], with an estimated 9 million new infections occurring each year [3]. Areas endemic for the disease are located largely in tropical and sub-tropical areas of the world, such as in Africa and on the Indian sub-continent, although there are high-burden centres in Eastern Europe, Russia and South America. Furthermore, countries such as the United Kingdom (UK), with a high influx of immigrants from endemic countries, are also experiencing an increase in the number of cases of TB disease within these populations. Poor nutrition and co-infection with human immunodeficiency virus (HIV) are risk factors for development of pulmonary TB, the most common and devastating form of the disease [3, 4]. This global problem is also confounded by the emergence of multi-, extensively- and totally-drug resistant (MDR, XDR and TDR, respectively) TB. MDR-TB is classified as infection with bacteria that do not respond to treatment with the two key drugs, isoniazid and rifampicin, while XDR-TB is infection with bacteria that do not respond to the two drugs listed above as well as fluoroquinolones and at least one of the injectable second line drugs [5]. Totally-drug resistant TB has been identified in patients in Iran and India, and is classified as bacteria that do not respond to any tested anti-TB drugs [5]. The implications of any form of drug-resistant TB are three-fold: the health of the patient is compromised and their life expectancy reduced; the risk of spread of infection is increased due to lack of control of bacterial growth; and the cost and duration of treatment and therefore economic burden on the country is increased.

Tuberculosis already places a large economic burden on countries with high rates of incidence and prevalence due to a long and costly treatment regime that, under the directly-observed treatment short (DOTS) course, requires significant manpower (discussed in more detail below). The disease also reduces the availability of able-bodied adults capable of contributing effectively to the economy due to chronic infection causing a wasting disease.

Another mycobacterial species, *Mycobacterium bovis* (*M.bovis*), infects cattle, causing lesions in the animals and rendering the milk and meat unfit for human consumption. It was estimated in 1995 that bovine TB costs the world over USD3 billion since infected cattle have to be culled [6]. Bacille Calmette-Guérin (BCG) can be used as a vaccine against bovine TB, however due the lack of longevity of vaccine efficacy and the fact that it confounds diagnostic tests, it is not widely used [7]. Due to the homology between the two mycobacterial strains (*M.tb* and *M.bovis*), this animal population is therefore also a valid target population for an improved vaccine.

1.1.2 Pathogenesis, immunology and pathology of TB infection

Transmission of *M.tb* occurs through inhalation of bacteria-containing aerosols produced when a patient with active pulmonary TB coughs or expels infected mucous. In the airways and lungs, the bacteria are taken up by lung macrophages into phagosomes. Normally, these phagosomes would mature into lysosomes, producing an acidic environment designed to kill and breakdown invading pathogens. *Mycobacterium tuberculosis*, however, is able to prevent the acidification of the phagosome and survive and multiply within the macrophage [8]. In most cases, once infection occurs, the host is either able to clear the disease or control the infection as a latent infection. This stage of the disease is not detectable by x-ray-imaging of the lungs, the only diagnosis being the patient's immune response to *M.tb* antigens. This is assessed either by performing a tuberculin skin test (TST) by injecting purified protein derivative (PPD) – a cocktail of secreted mycobacterial proteins – under the skin, or by using interferon (IFN)-γ release

assays (IGRAs) such as the T-spot (an enzyme-linked immunosorbant spot (ELISpot) assay detecting responses to the mycobacterial antigens early secreted antigenic target (ESAT)-6 and culture filtrate protein (CFP)-10) or Quantiferon (an enzyme-linked immunosorbant assay (ELISA) detecting serum levels of IFN-γ produced in response to ESAT-6, CFP-10 and TB7.7) [9]. IGRAs were initially designed as a tool for diagnosis of latent TB, and while their specificity for this diagnosis is good, there is an increase in the use of IGRAs for diagnosis of active disease for which the specificity of the tests is poor [10]. Unlike a TST, however, IGRAs can distinguish between BCG vaccination and exposure to most environmental (non-tuberculous) mycobacterial (NTM) species, and exposure to tuberculous mycobacteria, as the antigens used are present only in the latter. Reactivation of latent infection, leading to active TB disease occurs, in 10% of latently infected individuals and is marked by the development of granulomas with necrotic centres in the lungs, a breakdown of the lung vasculature, and a cough producing bacteria-containing sputum. The symptoms of active disease include coughing, lack of energy and wasting, and diagnosis is made based on either a smear- or culture-positive result. A smear test is the staining of sputum obtained from the patient for acid-fast bacilli using a Ziehl-Neelsen (ZN) stain, whilst a culture test is culturing of sputum in conditions conducive to mycobacterial growth [9]. Although results from a smear test are available immediately, these tests are less sensitive due to the low prevalence of bacteria in sputum, and therefore only highly infected individuals can be diagnosed by this method. Furthermore, the drug susceptibility of the bacteria TB cannot be determined via smear testing. The drawback to culturing the bacteria is that it takes approximately 8 weeks to diagnosis. Consequently, as with every other aspect of TB prevention, diagnosis and treatment, new diagnostic tests are needed, such as polymerase chain reaction (PCR)-based methods, although current versions of these still require a culture step.

Death from active TB is finally due to pneumonia-like disease caused by large volumes of fluid in the lungs, or from generalised systemic inflammation.

As reviewed in Zuñiga *et al.* [11], there are generally accepted to be 4 stages in the pathogenesis of TB disease, outlined below and discussed in further detail later:

I. Inhalation of *M.tb* and its phagocytosis by alveolar macrophages. Control at this stage relies on the innate capacity of the infected macrophages to kill the bacteria.

II. Recruitment of other inflammatory cells, including dendritic cells (DCs) and monocytes, to the site of infection through macrophage-produced cytokines such as interleukin (IL)-12 and tumour necrosis factor (TNF)-α. This leads to further cytokine production by the incoming cells to further enhance the bactericidal activity of the infected cells, however it also provides a reservoir of monocytes for further infection by *M.tb*.

III. Development of the adaptive immune response with the influx of T cells from the mediastinal lymph nodes (lung LN) and the development of structured granulomas. This is where infection is contained during latent infection.

IV. In 10% of infected patients, the granulomas become necrotising and cavitation, tissue damage and liquefaction occurs leading to dissemination to other areas of the lung through damage to the bronchi.

In stage I, the mycobacteria are phagocytosed by alveolar macrophages and lung-resident DCs. Phagocytosis can occur through several pathways, as reviewed in van Crevel *et al.* [12]. One mechanism involves recognition of the *M.tb* through receptors on the surface of the antigen-presenting cells (APC). Mannose receptor (MR), expressed on APCs, recognises the 19kDa protein Rv3763 on the bacterial surface and induces phagocytosis [13], while the glycolipid trehalose dimycolate (TDM) is recognised by Mincle [14]. Complement receptors bind to bacteria coated with complement factor C3 [15, 16]. The complement pathway is a system in which pathogens are opsonised by

complement components that recognise residues such as sugars and glycolipids on the bacterial cell surface. Complement receptors expressed on the APC cell surface then mediate phagocytosis through binding to the complement components. Complement receptor 3 (CR3), which is implicated in *M.tb* phagocytosis can also directly recognise bacterial products and skip the need for opsonisation of the bacteria (reviewed in [17]). The complement pathway can also be activated by mannose-binding lectins (MBL), free-floating proteins produced by the liver, which bind to mannose residues on the bacterial cell surface. C3 then recognises the MBL-coated mycobacteria, leading to complement receptor-mediated phagocytosis [18].

The immune response in stage I revolves around cytokines produced by the infected alveolar macrophages. *In vitro* experiments culturing naïve splenic $CD4^+$ T cells with either splenic or bone marrow-derived macrophages (BMMϕ) infected with *M.tb* showed that IL-10 was induced following infection in the macrophages, which lead to a 'Th0' phenotype, with the cells expressing both IL-4 and IFN-γ in a non-polarised fashion [19]. This was in contrast to splenic DCs, which produced IL-12 and induced a strong Th1 phenotype. Furthermore, Garcia-Romo *et al.* [20] showed that alveolar macrophages express low levels of costimulatory molecules such as CD40, CD80 and CD86 following infection with *M.tb* and produce no IL-12. These data suggest that the macrophages initially infected by the mycobacteria do not have a strong pro-inflammatory phenotype, and are likely modulated by the *M.tb* in order to delay the development of an immune response. That *M.tb* can avoid destruction within the phagosome is well established. It does this through preventing fusion of the phagosome with the lysosome, thereby preventing acidification of the vacuole, which would normally induce lysis of the bacterium [21]. This not only prevents destruction of the bacteria, but also impairs antigen presentation on major histocompatibility complex (MHC) class II molecules. Prevention of phagolysosomal fusion is thought to be mediated by the mycobacterial cell-surface glycolipid lipoarabinomannan, which is able

to inhibit the upregulation of early endosome autoantigen 1 and therefore the recruitment of late endosomal proteins to the phagosome (reviewed in [22]).

The protected state of the bacterium within the phagosome can be overcome through autophagy. Autophagy can be initiated by the cell's exposure to IFN-γ and is the process of the cell degrading its own components. With respect to *M.tb* infection, autophagosomes containing cytosolic proteins such as ubiquitin and rps30 are able to fuse with the phagosome. This leads to the release of these proteins into the phagosome and the generation of anti-microbial peptides that are able to kill the *M.tb* [23, 24].

As well as preventing phagosomal fusion, *M.tb* also prevents apoptosis of infected cells [25], further hindering effective antigen presentation, this time by limiting the uptake of *M.tb*-containing cell debris by DCs for cross-presentation on MHC-I. The immediate immune response following detection therefore relies on the response induced by signalling through pattern recognition receptors (PRRs), including toll-like receptors (TLRs). TLR2, TLR4 and TLR9 have been implicated in detection of mycobacteria. Toll-like receptors are expressed on or within antigen-presenting cells and recognise different components of infectious agents, including sugar moieties such as lipopolysaccharide (LPS), RNA and DNA. In the case of *M.tb*, TLR2 recognises glycolipids in the bacterial cell wall and induces IL-1β production by the macrophage. TLR4 is the receptor for heat shock protein 60/65, which is secreted by *M.tb*. Toll-like receptor 9 is an intracellular receptor and recognises unmethylated bacterial CpG DNA within the phagosome. The receptors activated by *M.tb* make use of the MyD88 and IRAK signalling pathway, activating transcription factors involved in immunological gene expression, such as nuclear factor (NF)-κB and interferon regulatory factor (IRF), leading to the transcription of tumour necrosis factor (TNF)-α, IL-1β and IL-12, reviewed in Kleinnijenhuis *et al*. [26]. It has also recently been shown that recognition of *M.tb* by Mincle not only induces phagocytosis of the bacteria but also activates the macrophage, prompting production of Th17-inducing cytokines by the infected cells

[27]. These cytokines then initiate the recruitment of other inflammatory cells including DCs, monocytes and neutrophils, leading to the onset of stage II.

Stage II marks the beginning of the assembly of inflammatory cells at the site of infection for the early stages of granuloma formation. During this stage, the infiltrating monocytes provide further targets for mycobacterial infection, meaning the bacteria undergo exponential replication. Some killing of bacteria occurs at this stage, mediated by the infected cells themselves and their production of TNF-α, which promotes apoptosis (in place of necrosis), facilitating killing of the mycobacteria [28]. TNF-α may also act through an as yet undefined mechanism to inhibit mycobacterial replication within the cell, such as promoting phagosome/lysosome fusion or inducing reactive oxygen intermediates (ROI). This is also the stage at which infected DCs migrate to the lung LN in order to present mycobacterial antigens to $CD4^+$ T cells and initiate the adaptive immune response and progression to stage III.

At stage III, mycobacterial proliferation slows with the arrival of T cells into the lungs. $CD4^+$ T cells are known to be essential in the control of *M.tb* infection as evidenced by the increased risk of HIV-infected individuals of developing active TB [29, 30]. Interferon γ production by *M.tb*-specific $CD4^+$ T cells has been shown to be important in control of *M.tb* infection both from studies in IFN-$\gamma^{-/-}$ mice [31] and from the increased susceptibility of humans with mutations in IFN-γ-related genes [32]. The cytokine is induced by IL-12 produced by infected APCs and acts along with TNF-α to promote the generation of a respiratory burst within the infected cell. This leads to the production of ROI (through activation of nicotinamide adenine dinucleotide phosphate (NADPH)) and reactive nitrogen intermediates (RNI; through activation of inducible nitric oxide synthase (iNOS)). The exact role of ROI and RNI in mycobacterial killing is unclear, however they are likely to act both through direct killing of the bacteria, for example through DNA damage or through interfering with bacterial proteins (reviewed in [33, 34]), or through initiating further signalling within the infected cell and production of

cytokines such as TNF-α through the NF-κB pathway ([35] and reviewed in [36]) TNF-α has been well-established as being an important cytokine in protection against TB disease in both animal knock out studies [37] and in the observation of reactivation of disease in humans receiving anti-TNF antibody treatment [38].

Stage III is the stage at which latent infection remains and the host and *M.tb* are in a state of equilibrium. In 10% of cases, however, patients progress to stage IV, where bacterial growth can no longer be controlled. In these cases, the granulomas that formed in stages II and III begin necrotising into liquefied cavitary granulomas and the necrotic macrophages release *M.tb* into the extracellular environment. If these granulomas happen to be located close to bronchi, they can be transmitted via aerosols produced upon patient coughing. In terms of immunology, this stage of the disease is highly inflammatory, with an abundance of cells such as neutrophils and cytokine-producing T cells.

1.1.3 Current measures for TB control

Drugs

According to the World Health Organisation (WHO; [39]) treatment for primary TB disease should aim to do the following:

- Cure the patient and restore quality of life and productivity
- Prevent death from active TB or its late effects
- Prevent relapse of TB
- Reduce transmission of TB to others
- Prevent the development and transmission of drug resistance.

Upon diagnosis of active pulmonary TB, the WHO guidelines recommend a 6 month course comprising 2 months with isoniazid, rifampicin, pyrazinamide and ethambutol, followed by 4 months on isoniazid and rifampicin. This treatment regime should be administered under the DOTS strategy, whereby intake of every dose of drugs is observed by another party, be it a family member or a health worker. This strategy is

vitally important to the prevention of drug resistance as 32% of patients defaulting on treatment develop drug-resistant TB [39]. Adherence to the 6 month course is confounded not only by the length of the course but also by the side effects of the drugs, including nephrotoxicity, effects on hearing and balance, hepatotoxicity and perturbances in blood sugar levels.

The long treatment regime and multiple drugs are essential for preventing the development of drug resistance and ensuring complete clearance of the bacterial load. Isoniazid interferes with mycolic acid elongation and is thought to target rapidly-growing bacteria, whereas rifampicin targets RNA-polymerase, killing bacteria undergoing rapid metabolic bursts. Pyrazinamide targets bacteria in a low metabolic state in an acidic microenvironment by increasing the cellular concentration of pyrazinoic acid within the bacterium, which interferes with fatty acid synthesis [40], and ethambutol prevents cell wall synthesis.

As described above, MDR-TB is classified as infection with *M.tb* that is resistant to isoniazid and rifampicin [39]. Recommended treatment for MDR-TB is with 8-10 drugs for at least 6 months and should continue 4 months after the patient is smear- or culture-negative. XDR-TB treatment is difficult due to cross-resistance between different drug groups and the risk that treatment with a wide range of drugs will simply lead to even broader resistance. Current guidelines, however, recommend treatment with drugs that are not in wide use in the region in question, therefore limiting the chance of previous exposure and therefore desensitisation to the drug [41].

HIV and *M.tb* co-infection presents another problem in treatment due to drug interactions between TB drugs and anti-retroviral therapies (ART; particularly rifampicin interference with protease inhibitors) and the risk of development of immune reconstitution inflammatory syndrome (IRIS). IRIS is thought to develop following reconstitution of the $CD4^+$ T cell population following ART and is a strong reactivity of these cells to the *M.tb* infection. Symptoms include fever, occasional

development of disseminated TB and worsening lung pathology. For this reason, and because TB progresses faster than HIV, TB treatment is carried out first in HIV/*M.tb* co-infected individuals [39, 42].

For these reasons (length of treatment, side effects, risk of the development of drug-resistance, complex treatment regimes for HIV/*M.tb* co-infection), there is a desperate need for the development of both novel drugs for the treatment of TB disease, and a vaccine that will either provide sterilising protection or prevent the development of active disease. In the long term, an effective vaccine is the most cost-effective and desirable method of disease control.

STOP TB

The Stop TB Partnership was developed in 2000 with the aim of raising public awareness of TB and to 'accelerate social and political action to stop the spread of TB around the world' [43]. The Partnership is made up of over 1200 organisations and includes donors, government and non-government organisations, both national and international, and research groups. The Global Plan to Stop TB was launched by the Partnership in 2006 with the following objectives:

- Achieve universal access to high-quality care for all people with TB
- Reduce the human suffering and socioeconomic burden associated with TB
- Protect vulnerable populations from TB, TB/HIV and drug-resistant TB
- Support development of new tools and enable their timely and effective use
- Protect and promote human rights in TB prevention, care and control

These are linked with the objectives of the Millennium Development Goals for TB, which were to halt and reverse 'incidence, prevalence and death rates associated with TB' by 2015 (www.un.org/millenniumgoals).

These objectives were to be achieved by expanding the DOTS strategy; addressing the needs of those at risk of developing a TB/HIV co-infection, and of developing MDR-TB; contributing to strengthening the health system; engaging all care providers;

empowering people with TB and their communities; and enabling and promoting research into both drug and vaccine development.

As shown in figure 1.1.3, by 2010 prevalence of TB had begun to decline across the world, with most regions, with the exception of Africa and South-East Asia, set to reach the target by 2015 [43]. This marked difference in rate of decline in Africa and South-East Asia is likely due to HIV co-infection (Africa) and the emergence of MDR- and XDR-TB (South-East Asia). The fact that these regions remain the most severely affected by TB means significant efforts should be put into addressing these issues in the future.

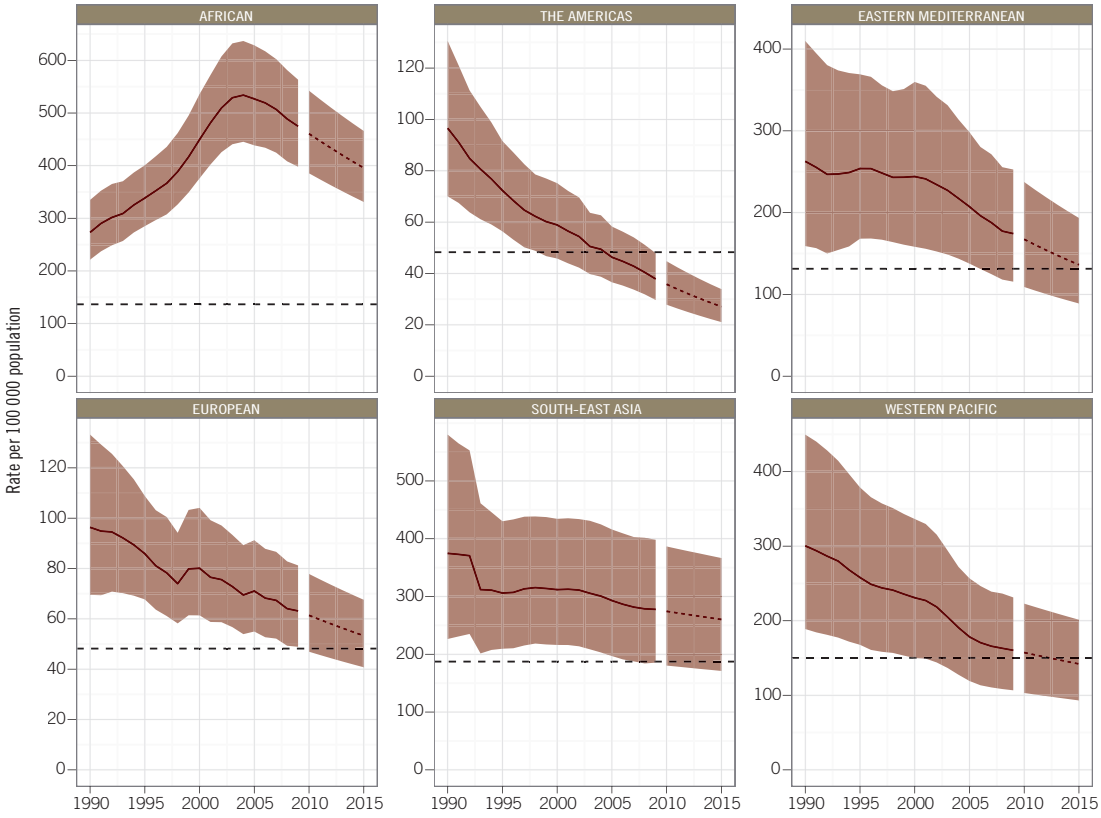


Figure 1.1.3 Prevalence of TB and estimated projections for 2015. This figure was taken from the Global Plan to Stop TB (2010) and shows the projected prevalence of TB for 2015 by WHO region. Dotted lines represent target prevalence for 2015.

1.1.4 Vaccination as a means of controlling TB

Aims of vaccination

When developing any vaccine, it is important to consider the goals one wishes to achieve through vaccination. The ideal goal would be to provide sterile protection, meaning the bacterium would never have the opportunity to colonise the lungs and establish an infection. In such a case, the vaccine would have to be administered to an uninfected population and would have to induce an immune response that could be effectively recalled upon initial infection. In the case of TB, the target population for such a vaccine would be infants, since in endemic areas most of the adult population is latently infected.

Alternatively, or additionally, one could develop more of a therapeutic or post-exposure vaccine targeted at the infected population. With respect to TB, such a vaccine would be designed to either clear a current latent infection or ensure the immune system remains capable of maintaining a latent infection and preventing the development of active TB, since this is the infectious stage of the disease as well as the stage causing mortality. The most at-risk population in this case are HIV-infected individuals with latent TB. Unfortunately, this population is immunosuppressed, so a vaccine would have to be administered either at the early stages of the HIV infection while $CD4^+$ T cells are still at healthy levels, or following commencement of anti-retroviral therapy. Furthermore, a live vaccine such as BCG would not be recommended for HIV-infected individuals due to their immunosuppressed state and the risk of the vaccine itself becoming an infection. Indeed, in South Africa BCG is withheld at birth in babies born to HIV^+ mothers until the HIV status of the infant is established [44]. Another factor to consider when designing a post-exposure vaccine is the Koch phenomenon. This was a phenomenon observed by Robert Koch upon re-exposure of *M.tb*-exposed individuals to mycobacterial antigens, whereby a delayed-type hypersensitivity reaction occurs due to a strong reaction at the site of disease leading to further necrosis and disease progression (reviewed in [45]).

Potential vaccine candidates for such a population would therefore have to be either a non-replicating attenuated bacterium or virus, or a protein/particle-based vaccine. If we can ensure the population is vaccinated with a vaccine such as BCG at birth, then this non-replicating or protein vaccine could be safely administered as a boost.

Various vaccination strategies and candidate vaccines against TB are discussed below.

BCG – the current TB vaccine

BCG is an attenuated form of *M.bovis* developed by Albert Calmette and Camille Guérin during the first two decades of the 20th Century. Compared to *M.bovis* and *M.tb,* BCG has lost the region of difference (RD)-1 locus, which contains many of the genes responsible for the virulence of the parent strain and *M.tb,* including ESAT-6 and CFP-10. BCG has been in use as a vaccine against TB disease since 1921, when it was first administered to humans. It is administered intradermally (*i.d.*), usually in the upper arm. Since BCG is a slow-growing bacterium, a localised pus-secreting lesion forms at the site of injection over a period of about four weeks, resolving eventually into a dimpled scar.

BCG is recommended as a vaccine administered to infants at birth in endemic countries, with the exception of the recommendation that it not be administered to babies born to HIV^+ mothers until their HIV status is known. As estimated in 2004, BCG is currently administered to ~100 million infants worldwide [46]. Its efficacy against pulmonary TB, however, varies between 0 and 80% depending on geographical location. The reason for this variation is unknown, and there have been several theories put forward, including genetic factors, poor nutrition, exposure to environmental mycobacteria or other asymptomatic infections such as helminths, differences in vaccine strain/storage, and, in the case of infants vaccinated at birth with no environmental exposure, maternal immunological and nutritional factors (reviewed in [47]). None of these, however, has been shown conclusively and solely to account for the variability in BCG efficacy.

Although BCG rarely protects against pulmonary TB in adolescents and adults in endemic areas, it is still in place as a recommended vaccine due to its ability to protect

against other forms of TB, such as disseminated TB and TB meningitis, in childhood [48]. It also offers protection against leprosy, a disease caused by *M.leprae* or *M.lepromatosis.* The fact that BCG is already widely administered and that it offers some protection to non-pulmonary mycobacterial disease, as well as evidence suggesting the ability of BCG to confer reduced overall mortality in low-income countries (reviewed in [49] and [50]), means that any novel vaccine designed against TB would likely be designed either to boost a previous BCG vaccination or be based on a mycobacterial species such as *M.bovis* or *M.smegmatis* so that the benefits of mycobacterial exposure could be maintained.

Vaccination approaches

There are two main approaches used in the development of TB vaccines. The first is to further modify BCG or another mycobacterial species to increase its immunogenicity and/or safety in the hope of inducing a longer-lasting response and/or a safer vaccine. Current vaccines in the pipeline that employ this mechanism include two developed/funded by Aeras: BCG over-expressing antigen 85B (Ag85B) [51], and BCG expressing perfringolysin O from *Clostridium perfringens*, and over-expressing Ag85A, Ag85B and Rv3407 [52]. Development of the former was stopped due to instability of the vaccine construct and lack of immunogenicity, and the latter vaccine has been withdrawn from clinical development due to two cases of shingles in vaccinated volunteers [53]. Another vaccine with a similar approach was more successful in safety trials: BCG expressing listeriolysin from *Listeria monocytogenes* (*L.monocytogenes*) [54]. The purpose of this vaccine was to encourage the escape of BCG from the phagosome with the effect of inducing apoptosis of the infected cell and increasing uptake of bacterial particles by DCs as well as access of the antigen to the cross-presentation pathway for presentation to $CD8^+$ T cells on MHC-I, a subset of cells whose importance in protection against TB disease is still under investigation.

Another approach using a modified mycobacterium is IKEPLUS. Here, *M.smegmatis* has had the conserved pathogenic *esx-3* secretion system removed and has been engineered to express the *M.tb* antigens *Rv02788 – Rv0303* [55]. In preliminary murine challenge studies, this vaccine shows potential as a vaccine to replace BCG.

Using a similar approach, but this time with *M.tb*, another group has developed an *M.tb* mutant lacking PhoP, a protein required for the synthesis of virulence-related lipids. Administration of the mutant, named SO2, to mice, guinea pigs and non-human primates prior to *M.tb* challenge conferred protection against TB disease and a strong $CD4^+$ T cell response [56].

The second approach is to maintain BCG (or one of the modified versions discussed above) as a prime and use either a vectored or a protein vaccine as a boost.

A number of protein-based vaccines are currently in the pipeline. The one furthest along in development is perhaps M72, developed by Glaxo Smith Kline (GSK). This is a fusion of two *M.tb* proteins: Mtb39a and Mtb32a [57, 58]. The proteins were chosen based on their immunogenicity in PPD-responsive humans and their capacity for protection in murine *M.tb* challenge models. Mtb32a is a secreted protein and is thought to be a serine protease [59], while Mtb39a is not secreted [60]. M72 is administered along with the GSK adjuvant AS01A, a liposome containing monophosphoryl lipid (MPL) and QS-21, which is designed to skew the immune response towards Th1 through TLR4. M72/AS01 is currently in Phase IIa immunogenicity studies.

Three subunit vaccines developed by Staten's Serum Institut are in Phase I clinical trials. The first of these is Hybrid I, which is a fusion protein consisting of Ag85B and ESAT-6, two proteins secreted by most mycobacterial species, both of which are highly immunogenic in BCG-vaccinated individuals [61, 62]. However, due to the presence of ESAT-6, which would confound diagnostic tests for TB as this antigen is used in tests such as Quantiferon and T-Spot, HyVac4 was designed as a replacement for Hybrid I, and consisted of the same fusion protein, but with ESAT-6 being replaced with a protein

from the same family: TB10.4 [63, 64]. Both of these vaccines were adjuvanted with IC31, an adjuvant made up of the anti-microbial peptide KLK and an oligodeoxynucleotide for TLR activation. The third vaccine is Hybrid56, which is a fusion protein consisting of Ag85B and ESAT-6 as well as *Rv2660c*, a gene transcribed during latency [65]. Hybrid56 is designed to protect both pre- and post-infection due to the inclusion of a latency antigen, and has shown promising results in pre-clinical mouse studies [65]. This vaccine was adjuvanted with CAF01, an adjuvant known to induce strong memory cell populations, and consisting of a lipid shell enclosing trehalose dibehenate, a synthetic version of the mycobacterial TDM [66].

The final class of boosting vaccines is viral vectors. Two viruses expressing *M.tb* antigens are currently in Phase IIa/b immunogenicity and efficacy trials. Aeras, in collaboration with Crucell, has developed a human adenovirus, serotype 35, expressing a fusion protein made up of Ag85A, Ag85B and TB10.4 (Aeras-402) [67]. In Phase I and IIa immunogenicity trials this vaccine has been shown to efficiently boost responses primed by BCG, with the best effect seen 3 months post-BCG in healthy adults [67, 68]. This vaccine also induces primarily strong $CD8^+$ T cell responses to the antigens in question.

Finally, MVA85A, developed by the Jenner Institute, is a Modified Vaccinia virus Ankara (MVA) expressing Ag85A. MVA85A has been shown to improve protection against TB disease in several animal models. In mice, DNA encoding Ag85A followed by MVA85A conferred improved protection compared to BCG following *M.tb* aerosol challenge [69]. Similarly, when used following DNA encoding Ag85A, or in a regime of BCG – MVA85A – fowl pox expressing Ag85A, MVA85A conferred improved survival in guinea pigs [70, 71]. Furthermore, in a non-human primate model, BCG – MVA85A vaccination showed improved survival compared to unvaccinated animals [72]. Finally, in cattle, MVA85A administered following BCG confers improved protection as determined by lung pathology compared to unvaccinated animals [73].

MVA85A has been used in several safety and immunogenicity trials in humans and has been shown to be safe and induce good immunogenicity in all trials to date, including in the most at-risk populations: infants, children, and HIV-infected adults [74-76]. MVA85A is designed to boost post-natal BCG, and has been administered *i.d.* 3 – 6 months after BCG in infants. In adults, it is also administered *i.d.* but since most adults in endemic areas have previously had BCG, no extra BCG is given, and $CD4^+$ T cell responses to Ag85A are boosted significantly regardless of time post-BCG. It is likely that MVA85A in adults is boosting all mycobacterial immunity, which is made up of BCG-, *M.tb*- and NTM-induced immunity. As well as inducing strong IFN-γ, TNF-α and IL-2 responses in peripheral blood mononuclear cells (PBMC), MVA85A can also induce IL-17 from $CD4^+$ T cells [77, 78], both in PBMC and whole blood, and induces $CD8^+$ T cell responses in whole blood ([79], Satti and Griffiths, unpublished).

In cattle, IL-17 induced following either BCG, BCG – MVA85A or BCG – Ad85A vaccination has been correlated with protection against challenge with *M. bovis*, as measured by lung pathology score [73].

Animal challenge models

Given the long and unpredictable time between infection with *M.tb* and development of TB disease, and the long and complex treatment period required for *M.tb*, controlled *M.tb* challenge studies in humans are not possible. Furthermore, field efficacy studies with natural *M.tb* exposure require large numbers of volunteers and long follow-up periods. In the absence of the above tools as well as a correlate of protection for vaccine efficacy, animal models form an important part of vaccine development for TB. Most vaccines are tested in mice. In the majority of mouse challenge studies, either C57BL/6 or Balb/c mice are used. These strains are classed as resistant strains, as following aerosol exposure they are able to contain the bacteria in a mid-term infection [80], and the outcome of chronic infection can be monitored. C57BL/6 and Balb/c mice, however, are not necessarily the ideal mouse strains for comparisons to human disease. First of

all, BCG protects very well in these strains, unlike in humans, always giving 1 – 2 log lower lung colony forming units (cfu) compared to unvaccinated controls. This means that sensitivity to see improvement in vaccine efficacy is reduced. Furthermore, whilst advanced TB disease in humans is marked by necrosis, caseation and cavitation within the granuloma, mice do not develop caseating necrosis and death occurs due to expansion of the granuloma, consisting largely of lymphocytes and macrophages, with this structure taking over surface area for gas exchange [81]. In humans, necrosis occurs due to damage to surrounding tissues by inflammatory factors, however in mice, *M.tb*-infected macrophages are killed with little effect on surrounding tissue [82]. Strains such as C3H/HeJ, CBA and I/St on the other hand, are susceptible and succumb to disease, eventually developing necrotic granulomas (reviewed in [80, 83]). Strains such as these may therefore be more useful for monitoring drug efficacy and the development of active TB.

In general, mice are relatively cheap to maintain and there is a large range of reagents available for immunological study in mice, as well as a wealth of information on and tools for manipulating genetics. The mouse is therefore a very useful challenge model, albeit with some limitations. The strain of mouse should be chosen carefully in relation to the aspect of human disease to be studied.

Guinea pigs, rabbits and monkeys have also been used as challenge models for TB, although the cost of running the experiments and the lack of immunological reagents available has meant these species are used less often than mice. In terms of replicating human disease, guinea pigs, rabbits and monkeys appear to develop more features typical of human active TB than mice do. For example, guinea pigs develop caseous granulomas similar to those observed in human active TB, however liquefaction rarely occurs in this species (reviewed in [84]). Rabbits are thought to develop disease that most resembles that in humans, with the development of caseous granulomas, which can also form liquefied cavitary centres (also reviewed in [84]).

Non-human primates, in particular *Macacca fasicularis,* not only develop disease that has the same features as human disease, including caseous necrotising granulomas and cavitation [85], but also provide a model for latent infection [86]. Immunological reagents often cross react between human and non-human primate samples, meaning there is an increasing amount of immunological investigation that can be performed in this species. The main limitation of non-human primate research is cost of containment level III facilities for such animals.

Finally, cattle represent a relevant animal model for TB. In this species, *M.bovis,* a mycobacterium closely related to *M.tb,* naturally infects cattle, causing pulmonary tuberculosis resembling that observed in humans. The route of infection in cattle is thought to be either oral or respiratory, depending on the exposure [87]. Granuloma formation in cattle is heterogeneous, like that observed in humans, although cavitation does not develop except in severe infection [88]. Furthermore, the immunological parameters necessary for controlling *M.bovis* infection are similar to those identified to date in human *M.tb* infection, including a strong IFN-γ response from $CD4^+$ T cells [88, 89]. As discussed above, bovine TB is a growing problem in the UK and throughout the world. BCG could be used as a vaccine in cattle, although legislation does not currently allow this in the UK/EU. Furthermore, we are faced with the same problems with reliable protection as in humans, as BCG-induced protection does not persist over time [7]. Cattle have already been used in a number of vaccine development studies, and an aerosol method of *M.bovis* challenge has been developed [90]. Although not as cheap or convenient as the mouse model, there is increasing availability of reagents for immunological studies in cattle. It would therefore be of interest to both the medical and the agricultural world to make use of *M.bovis* infection in cattle as a model for testing vaccine efficacy. However, as with study in non-human primates, the cost of running a containment level 3 facility for large numbers of such large animals is prohibitive for large-scale and frequent studies.

There are several animal models for TB available, each with their own caveats and advantages that must be taken into account when interpreting results and translating them to human disease progression and vaccine or treatment efficacy.

1.2 CD4+ T cell subsets

1.2.1 The Th1/Th2 paradigm

In 1986 it was confirmed by Mosmann *et al.* that there are two subsets of CD4+ T cell, identifiable by their expression of cytokines: Th1 cells produced IL-2 and IFN-γ, whilst Th2 cells did not produce these cytokines, but did produce 'several less defined [cytokine] activities', including IL-4 [91]. That the two subsets had different functional roles in the immune system became apparent in the study of leishmaniasis in mice. These studies found that IFN-γ-producing but not IL-4-producing T cells were responsible for control of *Leishmania major* infection, and that blocking IL-4 production could ameliorate disease progression, suggesting that the different cell types had distinct roles during infection [92]. Since then, these subsets have been further defined. Th1 cells produce IFN-γ in response to APC-derived IL-12 [93], and their role is to assist in the clearance of intracellular pathogens by activating APCs [94] and, for some pathogens such as Herpes Simplex Virus, assisting in the activation and migration of CD8+ T cells [95, 96]. T-box expressed in T cells (T-bet) is the transcription factor responsible for the expression of IFN-γ by Th1 cells [97] and is itself induced by signal transducer and activator of transcription (STAT) 4, which is induced by IL-12 [98, 99].

Expression of the transcription factor STAT6, induced by IL-4 produced by APCs [100], followed by GATA-3 [101, 102], leads naïve CD4+ T cells down the Th2 path. Th2 cells produce IL-4, IL-5 and IL-13, which help with isotype-switching in B cells, largely through IL-4 production [103], as well as recruitment of granulocytes such as eosinophils to the site of infection with pathogens such as helminths through production of IL-5 [104]. Th2 cells are usually induced following infection with

extracellular pathogens and parasites. If directed against self- or non-inflammatory antigens, Th2 responses can be associated with allergy and asthma, which arise from the recognition of otherwise harmless antigens by IgG antibodies which then activate mast cells and basophils to release inflammatory mediators such as histamines and heparin [105].

The effect of over-active Th1 cells is not clear. It was initially thought that autoimmune diseases such as multiple sclerosis (MS) and rheumatoid arthritis were driven by Th1 cells, since the lesions in these diseases were described as resembling 'delayed type hypersensitivity' lesions for which Th1 cells were considered responsible [91]. Experimental results, however, revealed that knocking out [106] or blocking IFN-γ [107] worsened disease outcome in the mouse model of MS, experimental autoimmune encephalomyelitis (EAE), while adding in IFN-γ ameliorated disease [108]. Perhaps confusingly at the time, blocking IL-12 using an anti-IL-12p40 antibody reduced EAE severity, leading to the conclusion that IL-12 was involved with the pathogenesis of autoimmunity [109]. This discrepancy between IL-12p40 but not IFN-γ involvement was clarified once it became apparent that the IL-12p40 subunit also forms part of the cytokine IL-23 [110]. Interleukin 23 has since been found to be responsible for the expansion of Th17 cells (see below), which have now been found to be key mediators of autoimmune diseases [111].

As evidenced by the increased risk of developing TB disease following HIV infection, a disease characterised by a severe drop in $CD4^+$ T cell numbers, it is clear that $CD4^+$ T cells are vitally important in protection against TB. In particular, a Th1 IFN-γ-mediated response, rather than a Th2 IL-4 mediated response is important, with IFN-γ playing a central role in driving the downstream activation of *M.tb*-infected macrophages [112]. Indeed, skewing of the T cell response away from a Th1 response may be a mechanism employed by mycobacteria in order to evade or direct a less-effective immune response,

widening the window immediately post-infection during which bacteria can establish an infection [19].

1.2.2 Th17 cells

As mentioned above, a third class of effector $CD4^+$ T cell has recently been identified. Th17 cells are marked by their production of IL-17A and F [113], as well as IL-21 and IL-22 [114]. This thesis will focus on IL-17A, which will be referred to as IL-17 from here on. Although it was initially thought that these cells were induced by IL-23 produced by APCs [113], it later became apparent that IL-23 expands the population of already-differentiated Th17 cells, and that a combination of IL-1β, IL-6 and transforming growth factor (TGF)-β are necessary for their induction from naïve $CD4^+$ T cells [115-117]. The role of Th17 cells is thought to be in protection against fungal infections, for example *Candida albicans* (*C.albicans*) [118], some intracellular pathogens such as *Francisella tularensis* [119] and *Bordetella pertussis* [120], as well as some extracellular pathogens, for example *Klebsiella pneumoniae* [121]. The transcription factors responsible for the development of Th17 cells are STAT3 [122], and RAR-related orphan receptor (ROR)γt [123], both of which are upregulated by IL-6 and have binding sites within the *IL17* gene.

As reflected by the pathogens to which they respond, Th17 cells are mucosa-associated cells, being induced in sites such as the gut or the lungs, as evidenced by expression of integrins and C-C motif receptors (CCRs) associated with mucosal sites, such as CCR6 [124, 125].

Interleukin 17 is a highly inflammatory cytokine with several roles, including activation of endothelial cells and subsequent recruitment of neutrophils to the site of infection [126, 127], recruitment of T lymphocytes through induction of chemokines such as CXCL9, CXCL10 and CXCL11 [128], and, on a more macro scale through these mechanisms, the formation of granulomas [129]. There is also evidence to suggest that IL-17 induces production of pro-inflammatory cytokines such as IL-12, IL-1β and IL-6

from macrophages [130-132]. As such, its production must be both temporally and spatially regulated in order to avoid adverse pathogenic effects.

Interleukins 17A and F are thought to have similar functions. Both bind to and signal through the IL-17RA receptor, and IL-17F has a similar capacity to IL-17A for inducing chemokines and cytokines such as CXCL10 and IL-6 [133]. There are some differences in their function, however, as, unlike in IL-17A knock out (KO) animals, progression of EAE is not affected in IL-17FKO mice [133].

One hypothesised role for IL-21, produced by Th17 cells, is to act along with TGF-β in the absence of IL-6 and in a STAT3-dependent manner to promote differentiation of Th17 cells [134-136], which would be important for maintenance of the subset once IL-6 production by APCs dissipates. Interleukin 21 has also been implicated in pathology; in an animal model of Crohn's disease in the gut, IL-21 was found to be responsible for the onset of chemically-induced disease [137].

Finally, IL-22 is another cytokine produced by Th17 cells [114], although another cell subset producing IL-22 but not IL-17 or IFN-γ has now emerged and been named Th22 [138, 139]. Unlike IL-21, IL-22 produced by Th17 cells has no effect on IL-17 production by Th17 cells [114]. Its role instead seems to be to mediate the production of anti-microbial peptides such as β-defensin 2 [114] as well as to induce production of pro-inflammatory cytokines such as IL-6 and IL-8 [140].

Throughout the development of the theory of the Th17 subset of cells, there has been on-going discussion regarding how well what is known about Th17 cells in mouse, where most of the work has been done, can be translated to humans. Initially it was thought that mechanisms of induction differed in that human Th17 cells did not require TGF-β, whilst mouse cells did [115], however it has now been shown that this is not the case and TGF-β is in fact necessary for human Th17 development [141, 142]. Furthermore, it was initially thought that Th17 cells with the ability to produce IFN-γ as well as IL-17 were unique to humans [143], however IFN-γ^{+}IL-17^{+} cells have now been

identified in mice [144, 145]. Studying Th17 cells in mice should therefore provide a good indication of the process of their development and their effector functions in humans.

It should be noted that although immunologists have quite readily classified $CD4^+$ T cells into various subsets based on their function and cytokine expression, it is now becoming apparent that these classifications are plastic and can change depending on the environment of the cells. It is generally accepted that there is a 'downhill slope' associated with this plasticity and that Th1 cells are 'terminally differentiated', however there is evidence that there is interplay between the different subsets, for example cells can express both the regulatory transcription factor Foxp3 (see below) and RORγt, and there is evidence for Th17 cells converting to IFN-γ-producing Th1-like cells as reviewed in [146]. This potential plasticity should be taken into account when designing vaccines targeted at the induction of a particular cell type.

As will be discussed in more detail below, Th17 cells are emerging as playing an important role in vaccine-induced protection against TB disease through either mediating induction of Th1 cells at the time of vaccination and/or mediating early recruitment of protective Th1 cells following infection.

1.2.3 T cell memory

As well as $CD4^+$ T cells being grouped into different subsets based on their cytokine profile, they can also be characterised based on their 'memory phenotype'. As reviewed in [147], a naïve unactivated T cell expresses a T cell receptor (TCR) specific for a certain peptide presented on an MHC-II molecule on an APC. Upon contact with the APC, if the affinity of the TCR with the peptide : MHC complex is correct, the T cell will be activated and mature into an effector T (T_{eff}) cell. Depending on its phenotype (which will depend on the cytokine signals associated with its activation, which in turn depends on the pathogen activating the APC and the location of this encounter), the T cell will then either migrate to the site of infection to carry out its function on location, or remain

in the lymph node to provide assistance to the APCs for either B cell activation and class-switching or for $CD8^+$ T cell activation. Most $CD4^+$ T cells will die either once the infection has cleared or the cells are exhausted. A small fraction of the cells, however, will remain alive and develop into memory T cells, although whether the cells develop from T_{eff} cells or are induced directly from naïve T cells to become memory cells is still unclear. Central memory T (T_{cm}) cells, characterised by their expression of the lymphoid homing marker CCR7, as well as CD62L, CD27 and CD28, remain in the secondary lymphoid organs with the role of either activating antigen-carrying APCs upon their entry into the lymph nodes or proliferating and becoming effector cells [148]. Effector memory T (T_{em}) cells have a very low threshold for activation and lower proliferative capacity and are located in non-lymphoid tissue and as such express homing markers relevant for the tissue in which they are found. Here, they patrol for re-infection by the pathogen for which they are specific [148]. In 2010, Pepper *et al.* [149] showed that following infection with *L.monocytogenes*, Th1 cells induced following intravenous (*i.v.*) infection preferentially develop into $CCR7^-$ T_{em} cells, whereas Th17 cells develop into T_{cm} cells following intranasal (*i.n.*) infection, suggesting that the route of infection as well as the phenotype of the cell may play a role on which memory phenotype is induced. A T_{cm} subset with a 'non-effector' phenotype has also been described. These cells express CD62L and CCR7 and show no bias towards any of the described subsets, however, under polarising conditions and antigenic stimulation they can rapidly proliferate and respond to infection [149].

In relation to vaccination, one would expect that it is important to induce both T_{em} and T_{cm} cells. In particular in cases such as *M.tb* where the recall response is likely delayed by the bacterium, it would be important to have a mucosal population of T_{em} cells as a frontline defence, as well as a population of T_{cm} cells that could proliferate once the APCs reach the draining LNs.

1.2.4 Regulatory T cells

Another relatively recent subset of T cells to be described is the regulatory T (Treg) cell. In mice, these cells are characterised by expression of the transcription factor Foxp3 and high levels of surface CD25, however in humans, Foxp3 can be transiently expressed by naïve T cells immediately following activation, meaning it cannot be reliably used as a marker for Treg cells [150]. As the name suggests, the role of Treg cells is to modulate the inflammatory immune response. The cells employ numerous mechanisms in order to do this, including secretion of cytokines such as IL-10, which is especially important in gut-related inflammatory diseases [151, 152]. Alternatively, Treg cells can act in a cell-cell contact-dependent manner through cytotoxic T lymphocyte antigen (CTLA)4 expression. CTLA4 binds to CD80 or CD86 expressed DCs, an interaction that sends an inhibitory signal through the DCs and prevents their maturation into APCs for activation of effector T cells [153].

There are thought to be two origins of Treg cells. Both subsets are characterised by Foxp3 expression, however natural Treg (nTreg) cells originate in the thymus and emerge after selection, although the process of their selection is unknown. Inducible Treg (iTreg) cells on the other hand can be induced from naïve T cells to upregulate Foxp3 expression, however little is known of these cells, and most Treg-related functional studies revolve around nTreg.

Just as there have emerged different subsets of effector T cells, so there are different subsets of Treg cells identifiable by their transcription factor expression and their suppression capabilities. The transcription factors T-bet and STAT3 were discussed earlier in relation to Th1 and Th17 cells respectively. Studies have shown that Treg cells can be induced by IFN-γ to express T-bet [154] and, in a mucosal environment, to express STAT3 [155], and that these Treg cells have the specific roles of regulating the activity of their corresponding effector cells. The result of this transcription factor expression is the expression of tissue-specific chemokine receptors, for example CXCR3

on T-bet$^+$ Treg cells [154], and CCR6 on STAT3$^+$ Treg cells [155]. Furthermore, there is evidence of a developmental link between Treg cells and Th17 cells: TGF-β alone induces expression of Foxp3 and the development of iTreg cells, whereas if IL-6 is present, Th17 cells preferentially develop [156]. This phenomenon may be necessary for the control of pathology in the gut, where enough of a response is required to maintain the intestinal flora, but this response requires regulation to avoid the development of pathology.

In terms of antigen-specificity, one would expect that cell-cell contact-mediated suppression would require the Treg cell to be specific for the antigen they are repressing responses to, and that nTreg cells are generally specific for self-antigens [157]. Perhaps this is the difference between nTreg and iTreg cells: nTreg cells are present to prevent autoimmunity from developing during both the steady state and during an infection, and iTreg are induced during the infection in order to dampen antigen-specific responses to prevent the development of immunopathology.

Another marker for Treg cells has recently been identified. CD39 is an ectonucleosidase whose role it is to hydrolyse extracellular adenosine triphosphate (ATP) and adenosine diphosphate (ADP) to adenosine monophosphate (AMP). AMP then breaks down to adenosine, which can act through the A2A receptors on responding T cells to suppress them, possibly through inhibiting their ability to produce pro-inflammatory cytokines [158]. CD39 is expressed on 80% of Foxp3$^+$ cells in mice and these Foxp3$^+$CD39$^+$ cells have the ability to suppress CD4$^+$CD25$^-$ cells, suggesting that most Treg cells are CD39$^+$ and that this is a reliable marker for this subset of cells [159]. Furthermore, Foxp3 appears to drive the expression of CD39 on Treg cells [160]. The Foxp3$^-$CD39$^+$ cells have an effector phenotype [159, 161].

As well as mediating the generation of adenosine, the CD39 on Treg cells could also be acting through removal of ATP from the local microenvironment. ATP is known to be pro-inflammatory as it binds to the P2X7 receptor on the surface of APCs [162]. This

binding causes a potassium (K^+) efflux from the cell, thereby activating the NACHT, LRR and PYD domains-containing protein-3 (NALP3) inflammasome. The NALP3 inflammasome recruits the enzyme Caspase-1 to the complex, which drives the cleavage of pro-IL-1, induced through TLR activation, to IL-1β, which can then be secreted. The removal of ATP from the extracellular environment by CD39 would therefore have a local suppressive effect, especially in a highly inflammatory environment consisting of a high concentration of dead or damaged host cells, all of which would be contributing to extracellular ATP, as suggested in [160].

In humans, it is more complex, with CD39 being expressed on only a subset of Treg cells expressing CCR6 [160], suggesting there may be a link between $CD39^+$ Treg cells and Th17 regulation, and possibly mucosal disease. Indeed, it has been shown in a couple of studies that MS patients have fewer and less functional $CD39^+$ Treg cells [160, 163].

It is important to consider the role of Treg cells following vaccination, as vaccination is unlikely to be effective if too many Treg cells are present. Importantly, vaccination with MVA85A has been shown to decrease levels of TGF-β in serum of vaccinated volunteers, suggesting overriding of regulatory responses [164].

Following *M.tb* infection, Treg cells have been shown to be induced at the site of infection, thereby delaying the development of an adaptive immune response to the pathogen [165], and the immunogenicity of MVA85A has been shown to depend on the number of circulating Treg cells prior to vaccination [77].

Treg cells are likely an important factor in the balance of immunity vs. pathology during TB disease, especially in the latent phase, where containment within granulomas in the lungs requires an immunogenic cellular cuff. Regulation of cellular activity within this cuff, as well as recruitment of new cells to this site, needs to be such that there is enough of a response to contain the bacteria, but not so much as to cause pathology, tissue destruction, and possible progression of disease.

1.2.5 Other T cell subsets

CD8⁺ T cells

CD4⁺ T cells recognise exogenous peptide presented on MHC-II on APCs and respond by producing cytokines designed to modify their environment by acting on both lymphoid and non-lymphoid cells in order to propagate the immune response to invading pathogens. CD8⁺ T cells, on the other hand, recognise peptides presented on MHC-I molecules, which are present on all nucleated cells. Peptides presented on MHC-I molecules are endogenous peptides derived from proteins being translated within the presenting cell. In the case of infection, these peptides would derive from viruses or bacteria infecting the presenting cells. Activated CD8⁺ T cells bind to the peptide : MHC complex and kill the infected cell [166, 167] via a variety of mechanisms including production of cytotoxic pore-forming toxins such as perforin or granzyme A [168] or by inducing apoptosis through Fas/FasL binding (reviewed in [169]). CD8⁺ T cells are also capable of acting in a manner similar to CD4⁺ T cells by producing IFN-γ in order to activate the infected cells they are recognising.

Although CD4⁺ T cells take up most of the limelight in relation to *M.tb* infection, it is clear that CD8⁺ T cells are important for control of *M.tb* infection, as is evidenced by a decreased ability to control infection in mice lacking CD8⁺ T cells [170]. As well as producing IFN-γ in order to activate *M.tb*-infected macrophages, CD8⁺ T cells may also act against *M.tb* infection by inducing apoptosis of infected cells that are not able to contain the infection alone, a function that may be important during the latent stage of disease [171].

γδ T cells

γδ T cells have been shown to be important in the initial control of infection by several pathogens, including *M.tb* [172] (see below) *Staphylococcus aureus* [173], *C.albicans* [174], and *L.monocytogenes* [175]. γδ T cells differ from CD4⁺ T cells because instead of expression of the αβ TCR on the cell surface, their TCR is made up of a γ and a δ chain.

Furthermore, compared to the high heterogeneity of the αβ TCR, γδ TCRs are relatively homogeneous (reviewed in [176]), possibly reflecting less of a role for antigen recognition in their activation and reflecting their innate rather than adaptive nature.

As for αβ T cells, γδ T cells can be divided into subsets based on marker expression and cytokine production. γδT1 cells express NK1.1 and CD27 and produce IFN-γ, whilst γδT17 cells express the scavenger receptor Scart-2 and CCR6 and produce IL-17 [177, 178]. Phenotypic commitment of γδ T cells appears to occur in the thymus, from where they emerge as cells resembling 'antigen-experienced' cells [178], leading to a lower threshold for activation, another clue that these cells are involved in the innate rather than the adaptive immune response.

Little is known about receptor recognition by the γδ TCR, however it is thought that γδ T cells can respond to non-protein antigens such as lipids presented on certain MHC-Ib molecules such as CD1c, T10 and T22 [179-181], and that they can become activated through expression and ligation of TLRs 1 & 2 [182].

M.tb infection has been shown to induce γδ T cells, and they have been implicated in both mice and humans as being important in protection following infection, most likely through production of cytokines such as IFN-γ and IL-17 [183, 184].

1.3 Interleukin 17 and vaccine-induced control of TB disease

The importance of IFN-γ in the control of *M.tb* infection in both mice and humans is well established. A strong IFN-γ response, however, is not a correlate of protection either following infection or as a predictor for vaccine efficacy.

As discussed earlier, IL-17 is a pro-inflammatory cytokine produced by a variety of cell types, including $CD4^+$ T cells and γδ T cells. The importance of this cytokine during *M.tb* infection has gradually been emerging over the past decade, with most evidence pointing towards a positive role in vaccine-induced protection against TB disease.

1.3.1 IL-17 is essential in vaccine-induced control of M.tb *in mice*

The first evidence for IL-17 as a protective cytokine in vaccine-induced protection during *M.tb* infection comes from a study in mice. In this study, mice were either unvaccinated or vaccinated subcutaneously (*s.c.*) with an ESAT-6 peptide (adjuvanted with monophosphoryl lipid A, TDM and dimethyl dioctadecylammonium bromide) prior to *M.tb* challenge [128]. The results showed that vaccination accelerated the accumulation of $CD4^+$ T cells in the lungs and that IL-17-producing cells appeared earlier than IFN-γ-producing cells in vaccinated mice. The experiment was then repeated in IL-12p35$^{-/-}$ (the subunit belonging to IL-12 only) and IL-12p40$^{-/-}$ (the subunit shared between IL-12 and IL-23) mice. In IL-12p35$^{-/-}$ animals, vaccination with the ESAT-6 peptide gave 0.5 log protection, however vaccination of the IL-12p40$^{-/-}$ animals offered no protection, suggesting IL-23 but not IL-12 is essential for vaccine-induced protection following *M.tb* infection. Interleukin 23, responsible for mediating expansion of Th17 cells, is made up of the IL-12p40 subunit and the IL-23p19 subunit. The above vaccination/challenge experiment was therefore repeated in IL-23p19$^{-/-}$ animals, and here the cfu counts from vaccinated and unvaccinated lungs were the same. Furthermore, the accelerated vaccine-induced recruitment of IFN-γ^+ cells to the lungs was not observed in the IL-23p19$^{-/-}$ mice, and virtually no IL-17^+ cells entered the lungs. The phenotype of the IFN-γ^+ cells recruited following infection of wild type (WT) vaccinated mice was $CXCR3^+$. CXCR3 is the receptor for the ligands CXCL9 and CXCL10, suggesting that the lack of IL-23-expanded IL-17-producing $CD4^+$ T cells in the lungs led to a lack of CXCL9 and CXLC10 induction and therefore a lack of recruitment of $CXCR3^+$ IFN-γ-producing T cells to the lungs. Although the mechanism of induction of CXCL9 and CXCL10 is not known, the authors speculated that the presence of IL-17 binding sites in the promoters for both genes and the fact that antibody neutralisation of IL-17 led to a decrease in their expression meant that IL-17 was driving this expression of chemokine ligands

The same group went on to investigate BCG-induced protection and the relationship to IL-17 [185]. Similar to their previous observations following vaccination with the adjuvanted ESAT-6 peptide, *s.c.* BCG vaccination of IL-23p19$^{-/-}$ mice showed reduced vaccine efficacy. As a step towards elucidating the mechanism behind this, they found that BCG vaccination of mice lacking the IL-17RA receptor had reduced frequencies of CD4^{+} T cells following vaccination compared to WT controls. Furthermore, in the absence of responsiveness to IL-17, DCs produced less IL-12, which led to a lower frequency of IFN-γ-producing CD4^{+} T cells, in keeping with the ability of IL-17 to induce IL-12 production by DCs [131, 132]. The kinetics of the immune response was such that IL-17-producing cells in WT mice peaked earlier than IFN-γ-producing cells, which along with the dependency of IL-12 production on IL-17, suggests that a strong early IL-17 response is required for priming of an IFN-γ response.

As suggested in [185], the delayed IFN-γ response to BCG is likely down to the induction of IL-10 through prostaglandin E2 (PGE_2) induction by BCG. Interleukin 10 is an inhibitor of the Th1 pathway, however exposure of the DCs to IL-17 overcomes this IL-10-mediated inhibition. This was confirmed by vaccination and challenge of IL-10$^{-/-}$ animals. BCG-vaccinated IL-10$^{-/-}$ mice had higher expression of IL-12 and higher frequencies of Th1 cells, which was not affected by administration of an anti-IL-17 blocking antibody. Following challenge, no difference in bacterial burden was observed in naïve animals, but there was a significantly lower bacterial burden in IL-10$^{-/-}$ vaccinated animals. Another group has recently showed that blocking IL-10R at the time of vaccination in both the resistant C57BL/6 mice and the susceptible CBA/J mice improves protection following *M.tb* challenge [186]. This was associated with an increase in both IL-17 and IFN-γ-producing cells in the spleen pre-vaccination, and in the lungs following long-term infection with *M.tb.* The main producers of IL-17 following infection were CD4^{+} T cells and Thy1.2^{+}CD3^{-} cells, which may represent innate-lymphoid cells or NKT cells.

Data from the above studies show that IL-23-mediated IL-17 production following vaccination and *M.tb* challenge plays a role during the induction of the responding cells during vaccination in promoting the ability of IFN-γ-producing $CD4^+$ T cells to respond to vaccination. Interleukin 17 likely also plays a role following challenge, since IL-17-producing cells are the first cells to arrive 'on the scene' following infection, and effective recruitment of IFN-γ-producing cells to the lungs is dependent on the initial arrival of these IL-17-producing cells. One could argue, however, that the vaccine-induced IL-17-mediated effect observed post-challenge is due to a larger pool of IFN-γ^+ cells available post-vaccination for entry into the lungs upon infection, and that post-challenge IL-17 plays a different role, for example in the recruitment of neutrophils to the lungs for the formation of the granuloma.

Indeed, in studies using both *M.bovis* (intratracheal infection) [187] and *M.tb* infection [129], IL-17 has been shown to recruit neutrophils to the lungs and be instrumental in the formation of granulomas through this recruitment. In these studies, in which the mice were not vaccinated, γδ T cells were the main producers of IL-17, and infection of $V\gamma4/6^{-/-}$ mice, which lack γδ T cells, with *M.bovis* showed impaired granuloma formation. In studies involving vaccination, such as those described above, $CD4^+$ T cells are key producers of IL-17 in the lungs following challenge, so it could be that upon initial encounter with mycobacteria in the lungs, the more innate γδ T cells are the key IL-17-producers, but following vaccination, a primed population of $CD4^+$ T cells are instrumental in producing IL-17 in the lungs.

Given that IL-17 is such a highly inflammatory cytokine it is important to consider potential pathologic effects of this cytokine in *M.tb* infection. Several studies have shown that persistent presence of IL-17, whether through extended exposure to antigen in a repeated exposure model [188], or through neutrophil recruitment by IL-17 in susceptible and resistant mouse strains [189, 190], leads to adverse lung pathology. In the first of these studies, *M.tb*-infected mice were repeatedly vaccinated with BCG *s.c.* By

the third administration of BCG, although the bacterial loads in the lungs were no different to mice receiving phosphate buffered saline (PBS), there was significantly worse lung pathology in the BCG-vaccinated compared to the PBS control animals, which coincided with increased IL-17 and IL-23 production in the lungs and could be reversed by treatment with an anti-IL-17 blocking antibody [188].

The other two studies investigated the differences in granulocyte recruitment to the lungs in six different mouse strains: three susceptible strains (I/St, DBA/2 and CBA/J) and three resistant strains (A/Sn, C57BL/6 and Balb/c) [189, 190]. Both studies observed an increase in granulocytes in the lungs of the susceptible strains, and depletion of granulocytes led to an increase in survival [190].

It is therefore clear that while IL-17 undoubtedly plays a protective role in mouse models of *M.tb* infection, its production and downstream effects need to be tightly regulated. Since early expression of IL-17 following infection of vaccinated animals is associated with an influx of IFN-γ-producing cells, it is likely that under normal infection circumstances in an immunocompetent animal, IL-17-mediated effects are naturally regulated, since IFN-γ has been shown to be able to negatively regulate IL-17 [191]. Furthermore, it is even possible that Th17 cells recruited to the lung following infection may acquire IFN-γ production and eventually differentiate into Th1 cells, as has been described in [192].

1.3.2 IL-17 correlates with protection-associated pathology in vaccinated cattle

The other animal model in which the role of IL-17 in TB disease has been studied is cattle. As mentioned above, this is a highly relevant model of TB disease as cattle are naturally exposed to *M.bovis* and develop TB-like disease. Furthermore, similar levels of protection can be seen against bovine TB following BCG vaccination.

Viral-vectored vaccines (adenovirus 5 and MVA) expressing Ag85A as boosts for BCG have been used alongside BCG in a bovine challenge model of TB [73]. Results from these experiments showed that cultured IFN-γ ELISpot responses using PBMC pre-

challenge correlated inversely with pathology score. Furthermore, IL-17 expression following stimulation with Ag85A (measured by RT-qPCR) both pre- and post-challenge correlated inversely with pathology score. When the animals were broken down into protected animals (those with reduced pathology scores compared to unvaccinated controls) and non-protected animals (pathology scores equal to the control animals), IL-17 production was significantly higher pre-and post-challenge in the protected animals. This suggests that IL-17 is important in vaccine-induced protection against *M.bovis* challenge. Since levels both pre- and post-challenge are important, it would suggest that the IL-17 is coming from cells involved in the adaptive immune response, such as $CD4^+$ T cells, rather than more innate cells such as γδ T cells.

Similar to mouse studies [129], IL-17 has been implicated as having a role in the initial formation of the granuloma in *M.bovis* infection of unvaccinated cattle [193]. In these experiments, the mRNA for the chemokines CXCL9 and CXCL10, both involved in initiation of granuloma formation, steadily decreased as the *M.bovis*-induced lymph node granulomas progressed. Interleukins 17 and 22 were the only cytokines whose pattern of mRNA expression followed a similar pattern, leading to the suggestion that these cytokines are involved in the induction of granulomas following infection.

Also similar to studies of *M.tb* infection in unvaccinated mice in which IL-17 drives pathology, a separate study in cattle has recently found that gross lung pathology following *M.bovis* infection was associated with a greater percentage of highly-activated lymphocytes [194]. Although IL-17 was not highly expressed in PBMC post-challenge (as measured by RT-qPCR following PPD-B stimulation), it was the only cytokine measured that clearly distinguished between animals with macroscopic lesions and those without, with higher expression in the animals with macroscopic lesions. Since these animals were not vaccinated, it is likely that these observations relate more to those described in [189, 190] in which neutrophil recruitment was negatively associated with *M.tb*-induced pathology in mice.

Therefore, it would seem that IL-17 in cattle, as in mice, is important for the induction of vaccine-induced immunity against TB disease, as well as in the induction of protection structures in the lung. Also as is the case in mice, IL-17 is a risk factor for the development of pathology.

1.3.3 Evidence of a protective role for IL-17 in human TB

Given the difficulty of diagnosing either initial infection or the exact time of onset of active disease in humans, as well as difficulty in obtaining lung tissue, not much is known about the cytokines directly involved in protection against TB disease or those induced in lungs following vaccination. Data from whole blood, PBMC, pleural effusions and bronchoalveolar lavage fluid (BAL), however, suggest that IL-17 is induced both following vaccination and during active disease. How this relates to either vaccine efficacy or disease outcome is still unknown.

Pleurisy can occur during active TB and is characterised as inflammation in the pleura, the membrane that separates the lungs from the ribcage. There have been varied reports regarding cytokine production by cells from pleural fluid, although all studies have detected little to no IL-17 by ELISA in the fluid. One study looked at IL-17 and IL-22 production by $CD4^+$ T cells from pleural fluid following stimulation with ESAT-6 and CFP-10, and found that approximately 0.1 – 0.2% of $CD4^+$ T cells expressed IL-17 or IL-22 [195]. Another study stimulated the cells with PPD and found no IL-17-producing cells [196]. This study also detected high levels of IL-22 in the pleural fluid from these patients. Two other studies [197, 198] reported high percentages of IL-17-producing cells in pleural effusions, however these cells were stimulated with phorbol myristate acetate (PMA) and ionomycin, which reflects the cells' capacity to produce IL-17 rather than their antigen-specificity.

Another study looked at cytokine production in PBMC and BAL in healthy individuals compared to patients with active TB [199]. Here, $IL\text{-}17^+$ and $IL\text{-}22^+$ cells were reduced in PBMC from patients with active TB compared to healthy controls, however levels of free

IL-22 in the BAL from patients were increased, whilst IL-17 was undetectable. Flow cytometry was not performed on cells from the BAL samples, however one could speculate that responses to *M.tb*-derived antigens may be increased at the site of disease due to migration of antigen-specific cytokine-secreting cells to the lungs. Interestingly, no cytokine production by γδ T cells was observed.

Similar results were observed when comparing PMA-stimulated whole blood from healthy donors with blood from patients with latent and active TB. Here, percentages of IL-17- and IL-22-producing $CD4^+$ T cells were lower in patients with active TB, however the ability of their circulating PBMC to respond to mycobacterial antigens during a 7 day culture was increased [200].

Finally, a study in Argentina found that clinical signs of disease correlated inversely with IFN-γ production by $CD4^+$ T cells in BAL samples, but positively with percentages of cells producing IFN-γ and IL-17 simultaneously [201]. IL-17 alone showed no correlation. This is of particular interest, since vaccine-induced polyfunctional $CD4^+$ T cells have been reported following MVA85A vaccination in both humans (see below) and mice.

Overall, it is clear that *M.tb* infection induces IL-17-producing cells at the site of disease. Whether these are protective or pathogenic is hard to tell without data on clinical disease, however the one study in which clinical disease was taken into account suggests that IL-17 is pathogenic. It is worth noting that the patients in whom the IFN-γ^+IL-17^+ cells correlated with worsened disease had been infected for longer, so it is possible that late in disease IL-17 is a mediator or marker of pathology, as can be seen in mice, but that early on it could be having a positive effect.

1.3.4 MVA85A induces IL-17 in human volunteers

MVA85A administered to volunteers across different ages and geographical locations with a history of BCG vaccination has been shown to induce high levels of IFN-γ production by $CD4^+$ T cells as detected by both ELISpot and flow cytometry. Interleukin 17 production by $CD4^+$ T cells has also been reported in two studies with MVA85A-

vaccinated volunteers. The first of these was an age de-escalation study in South Africa, in which adolescents and children with a history of BCG received MVA85A *i.d.* Interleukin 17 was detected by flow cytometry in whole blood, albeit at low percentages [76]. Furthermore, polyfunctional responses were reported in this trial, with most cells expressing IFN-γ, IL-2 and TNF-α, but a small percentage also producing IL-17. A second dose escalation study in the UK described detection of IL-17 by ELISpot in PBMC from the higher dose group, which is the dose now given as the standard dose of MVA85A [77]. The age de-escalation study made use of the lower dose of MVA85A, however because flow cytometry was performed on whole blood rather than PBMC, IL-17 responses were more readily detectable. The differences in detection of $CD4^+$ T cell cytokine responses between whole blood and PBMC as well as further work performed on samples from the dose-escalation trial will be discussed later in this thesis.

1.4 Cholera toxin as an IL-17-inducing adjuvant

Cholera toxin (CT), produced by the bacterium *Vibrio cholerae*, acts through the cyclic adenosine monophosphate (cAMP) pathway. Under normal circumstances this pathway is activated by external ligands such as chemokines or PGE_2 binding to a G protein-coupled receptor (GPCR) on the cell surface. In the case of a stimulatory signal, this activates the release of the intracellular $G_{\alpha s}$ subunit, which in turn activates adenyl cyclase (AC). The role of AC is to cyclise intracellular ATP to cAMP. Cyclic AMP can be negatively regulated by phosphodiesterase (PDE), which breaks it down to 5'AMP. The roles of cAMP within the cell are numerous and depend on the cell type and the stimulus. One of its roles is to convert the inert protein kinase A (PKA) tetramer into an active kinase by binding to the two inactive subunits. Active PKA is then able to phosphorylate and activate transcription factors such as cAMP response element binding unit (CREB). There is also evidence that cAMP regulates the NF-κB pathway [202]. Summarised in Figure 1.4.

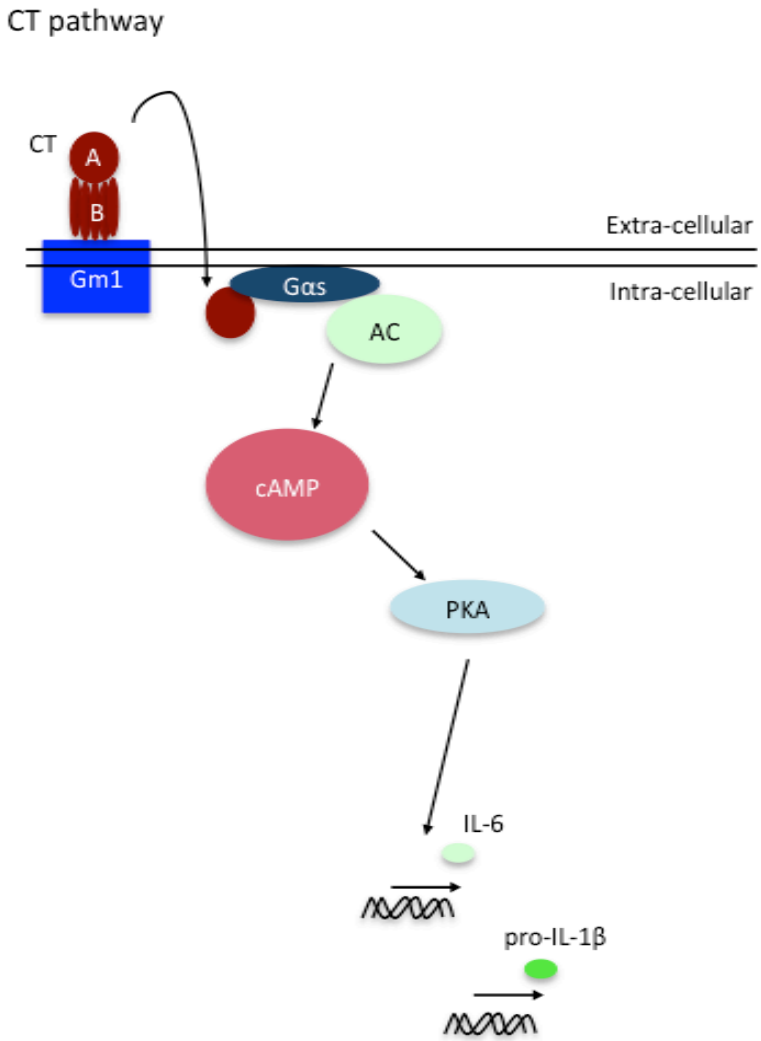


Figure 1.4 CT pathway resulting in cytokine production. In brief, the B subunit binds to the ganglioside receptor GM1, facilitating translocation of the A subunit into the cytoplasm. Binding to Gαs causes constitutive activation of AC, leading to high cellular concentrations of cAMP and activation of PKA. PKA activation mediates production of the pro-inflammatory cytokines IL-6 and pro-IL-1β.

Cholera toxin exists as a holotoxin, with a B subunit that binds to the ganglioside GM1 on the cell surface. This facilitates translocation of the A subunit through the endoplasmic reticulum and into cytosol where it binds to ADP ribosylation factor 6, which ribosylates AC, rendering it constitutively active, resulting in increased levels of cAMP in the cytosol and therefore an increase in events downstream of cAMP [203].

With respect to modulation of the immune function of cells, CT has been shown to directly affect IL-12 production by preventing binding of IRF8 to the IL-12p40 promoter in dendritic cells [204]. The same effect was also observed using dibutyryl cAMP

(dbcAMP), a cell-permeable analogue of cAMP, suggesting this pathway is cAMP-mediated [204]. Furthermore, increased intracellular cAMP in dendritic cells, induced either through CT treatment or through administration of dbcAMP or forskolin, a cAMP-inducing agent, increases IL-17 production from $CD4^+$ T cells following culture with the treated DCs and was found to act through the PKA pathway [205]. The same study also found that IL-6 and IL-1β secreted by CT-treated DCs are responsible for enhanced IL-17 production [205]. Cholera toxin can also increase production of IL-10, a negative regulator of the Th1 pathway but a cytokine to which Th17 cells are refractory.

More generally, CT increases maturation of antigen presenting cells, increasing expression of MHC-I and MHC-II on their cell surface and therefore their antigen-presenting ability, as well as increasing expression of costimulatory molecules such as CD86 [206].

Cholera toxin has previously been used as an IL-17-inducing adjuvant in murine models. In the first study, transgenic mice with a TCR specific for ovalbumin (OVA) given CT either with OVA peptides or adenovirus expressing OVA yielded more IL-17-producing $CD4^+$ T cells than mice receiving OVA alone [207]. This was shown to occur in an IL-6-dependent manner and was mediated by the B subunit. A second study vaccinated mice with irradiated anthrax spores with and without CT and observed improved protection following anthrax challenge in the animals receiving CT. The only cytokine upregulated following vaccination was IL-17, suggesting this was the mediator of the improved protection [205]. In contrast to the previous group's findings, the CT B subunit did not induce IL-17 responses.

A CT-like toxin, *E.coli*'s heat labile toxin has been used in a human vaccine trial as an adjuvant for intranasally-delivered vaccines against *M.tb* and HIV. The trial had to be terminated, however, due to the development of a Bell's palsy in two of the volunteers [208]. Therefore, due to its toxicity in humans, CT cannot be used as an adjuvant in vaccines, however alternatives that target the cAMP pathway could be used instead.

1.5 Aims of the project

Since it has been found that MVA85A vaccination in humans was able to induce IL-17 production by $CD4^+$ T cells, the aims of this project were

a) To further investigate IL-17 production in samples from human volunteers and investigate *in vitro* enhancement of IL-17 production
b) To investigate IL-17 production by $CD4^+$ T cells in mice vaccinated with a BCG – MVA85A vaccine regime
c) To investigate enhancement of IL-17 production in mice vaccinated with BCG alone or followed by MVA85A
d) To investigate the effect of enhanced IL-17 production in mice on *M.tb* aerosol challenge outcome
e) To investigate the lack of the proposed regulatory protein CD39 on the outcome of *M.tb* challenge in BCG – MVA85A-vaccinated mice

1.6 Experimental approaches

1.6.1 Samples from volunteers vaccinated with MVA85A

Initial experiments identifying the induction of IL-17 by MVA85A vaccination in human volunteers were performed on samples from a dose-escalation study. Results showed that only the higher dose, which is now routinely used in the trials, induced IL-17. Further experiments investigating this phenomenon were therefore performed on these samples. Flow cytometry was used to quantify cytokine expression, and stimulation in the presence of CD39 inhibitors was performed in order to determine the effect of this on the capacity of cells to produce IL-17.

1.6.2 Murine studies using an M.tb *aerosol challenge model*

The timecourse of IL-17 production by $CD4^+$ T cells following vaccination by the BCG – MVA85A regime was studied in both Balb/c and C57BL/6 mice. As for the human

samples, study of cytokine expression was performed using flow cytometry following stimulation with PPD and an Ag85A peptide pool.

Cholera toxin was used as an adjuvant for IL-17 production, and the effect of this on protection against TB disease was investigated using an *M.tb* aerosol challenge model. Blocking antibodies against IL-17 were used in order to determine the contribution of this cytokine to protection.

Two knockout mouse strains were used during this project. IL-17$^{-/-}$ animals were obtained from Prof. Fiona Powrie and Dr Kevin Maloy. The effect of the lack of this cytokine on challenge outcome was studied in both vaccinated and naïve animals, and the effect of CT on vaccine efficacy was also investigated in these animals.

Based on the results performed on human samples relating to the relationship between CD39 and IL-17 production by CD4^{+} T cells, CD39$^{-/-}$ mice were obtained from Dr Simon Robson in order to investigate the effect of BCG – MVA85A vaccination on these animals' ability to control *M.tb* infection.

MATERIALS & METHODS

2 MATERIALS & METHODS

A table of reagents and their sources is presented in the Appendix on page b.

A table of solutions and their recipes is presented in the Appendix on page e.

2.1 Human samples

2.1.1 Vaccine study participants

Subjects were recruited for clinical trials approved by the Oxfordshire Research Council, ClinicalTrials.gov ID: NCT00465465 (TB009). The dose of MVA85A administered in both trials was $1x10^8$ plaque-forming units (pfu), administered *i.d.* All participants in the trials were BCG vaccinated adults (maximum Heaf test reaction grade II, negative on *ex vivo* ELISPOT for ESAT-6 and CFP-10) between 18-50 years of age who tested seronegative for HIV as well as hepatitis B and C virus. Eight subjects were selected from TB009 and samples were investigated at time-points of week 0 (day of MVA85A vaccination), 1, 2, 4 and 24.

2.1.2 Thawing of cryopreserved peripheral blood mononuclear cells

Peripheral blood mononuclear cells obtained from subjects were frozen down in freezing mix at the time of sample acquisition in aliquots containing approximately $5x10^6$ PBMC per mL. Samples selected for investigation were removed from long-term storage in liquid nitrogen and placed on dry ice in preparation for thawing. Vials were flash thawed at 37°C and then transferred into 9ml of R10 medium. Cells were then washed twice and left to rest with Benzonase for two hours at 37°C, 5% CO2. Cells were resuspended at approximately $2x10^6$ PBMC per ml and counted using a CASY Counter (Schärfe System, GmbH).

2.1.3 Stimulation of PBMC

Cells were resuspended at $1x10^6$ cells/mL and each sample divided into seven 1mL aliquots in 5mL polystyrene round bottom tubes. Cells were stimulated for 18 hours at

37°C in 5% CO_2 with one of the following: no stimulation, no stimulation + 100uM ATP, no stimulation + 100uM ARL67156, 0.2ug/mL PMA and 2ug/mL ionomycin, 2ug/mL Ag85A peptide pool, 2ug/mL Ag85A peptide pool + 100uM ATP, 2ug/mL Ag85A peptide pool + 100uM ARL67156. After 2 hours, 5ug/mL Brefeldin A and 0.7uL GolgiStop were added.

2.1.4 Flow cytometry

Following stimulation, cells were pelleted at 1300rpm for 5 min at 4°C and transferred to a 96 well plate for staining.

Cells were stained for 10 min on ice with 10µL ViViD Live/Dead cell stain diluted in dH_2O prior to surface staining in 45µL of an antibody cocktail containing eFluor450 anti-CD19, eFluor450 anti-CD14, APC anti-CD25 and PE-Cy7 anti-CD39 diluted in FACS buffer. 150µL Cytofix/Cytoperm was used to permeabilise cells prior to staining intracellularly with PE-Cy5 anti-CD3, Qdot655 anti-CD4, APC-AlexaFluor780 anti-CD8, FITC anti-IFN-γ and PE anti-IL-17.

Stained cells were analysed using an LSR II flow cytometer (BD Biosciences).

2.1.5 ATP assay

ATP hydrolysis was measured as described in Borsellino *et al.* [160]. Briefly, PBMC from subjects were resuspended at $1x10^6$ cells/mL and aliquoted into 6 wells/sample of a white 96 well plate at $5x10^4$ cells/well. Cells were treated with either nothing, 50uM ATP or 50uM ATP + 100uM ARL67156 for 10 min at room temperature. One volume CellTiter-Glo solution was added to each well and cells were incubated for a further 10 min at room temperature in the dark. Luminescence was recorded using a Varioskan Flash spectral scanning multimode reader (Thermo Scientific). ATP hydrolysis was calculated using a standard curve of known ATP concentrations and expressed in nmol.

2.2 Animal work

2.2.1 Animals

Six to eight week old Balb/c and C57BL/6 mice were obtained from Harlan, UK. $CD39^{-/-}$ animals were obtained from Dr Simon Robson at the Beth Israel Deaconess Medical Centre, Harvard, USA. $IL\text{-}17^{-/-}$ animals were obtained from Prof. Fiona Powrie and Dr Kevin Maloy at the University of Oxford, Oxford, UK. Both knockout strains were on a C57BL/6 background.

All work was done under the UK Home Office PPLs 30/2412 and 30/2889. All procedures were performed by me (PIL 30/8774) in accordance with the UK Animals (Scientific Procedures) Act 1986.

2.2.2 Anaesthesia

Vaccinations were performed under anaesthetic. For inhalational anaesthesia, animals were given 2-3.5% IsoFlo (isofluorane) with 2L/min oxygen in air. Animals given systemic anaesthesia received a 100µL intraperitoneal (*i.p.*) injection of 75mg/kg Ketaset (ketamine hydrochloride) plus 1mg/kg Dormitor (medetomidine hydrochloride) diluted in endotoxin-free water. For recovery, Balb/c mice received 100µL 1:9 dilution Antisedan (atipamezole hydrochloride) *i.p.* while C57BL/6 mice received a 100µL 1:99 dilution of the same.

2.2.3 Bacille Calmette-Guérin and Mycobacterium tuberculosis

BCG was of the strain Pasteur. It was cultured in-house by growing up to log phase in 7H9 medium with Tween80, glycerol and ADC enrichment before aliquoting and freezing down at -80°C in PBS. For vaccinations, BCG was thawed and pelleted at 3000rpm for 25 min and resuspended at the required concentration in PBS.

M.tb strain Erdman K01 isolated from human sputum was donated by BEI Resources, Virginia, USA (NR-15404). Bacteria were removed from the glass vial and sonicated three times prior to use.

2.2.4 Modified Vaccinia virus Ankara with Antigen 85A

Modified Vaccinia virus Ankara with an Antigen 85A insert (MVA85A) was made in-house by the Vector Core at the Jenner Institute [69].

2.2.5 Vaccination

BCG was administered at $4x10^5$ cfu/vaccination. MVA85A was administered at $1x10^6$ pfu/vaccination. Cholera toxin was administered at 2μg/mouse in 50μL given either with the vaccine or alone.

For *i.n.* vaccination, animals received the vaccine in a 50μL bolus administered using a pipette held over the nose.

Intradermal vaccinations were administered using a U-100 29G needle. 25μL was injected into each ear dorsum.

Intraperitoneal administration of substances was done on restrained animals and delivered in 100-200μL using a 1mL 29G syringe.

2.2.6 Dissection and organ preparation

Prior to sacrifice, animals were placed in a warmer heated to 38°C and 8-10 drops blood collected into 200μL PBS with 10mM ethylenediaminetetraacetic acid (EDTA) if blood was to be used for leukocyte isolation, or into empty tubes if used for serum. Animals were sacrificed by cervical dislocation. The chest cavity was opened and BAL taken by injecting 3x500μL PBS using 0.3mm x 0.6mm tubing attached to a 2mL syringe. Lungs, spleen and lung LN were excised and placed in PBS. Prior to excision, lungs were perfused with 5mL PBS through the right ventricle.

Blood collected into PBS + EDTA was processed by adding 1mL ammonium chloride potassium (ACK) lysis buffer centrifuged at 4000rpm in for 4 min. This step was repeated and cells resuspended in 500μL R10 (Dulbecco's Modified Eagle Medium supplemented with 10% foetal calf serum, 2mM L-glutamine and 100U Penicillin/100μg Streptomycin).

For serum, blood was centrifuged at top speed for 10 min and supernatant (serum) collected.

Spleens and lung LN were passed through a 70µm sieve into 5mL R0 (Dulbecco's modified Eagle Medium supplemented with 2mM L-glutamine and antibiotic as described above) and transferred to a 15mL tube. Cells were sedimented at 1500rpm for 5 min. Lung LN were resuspended in R10 and counted using the Casy Counter.

Splenocytes were treated for 5 min with 5mL ACK lysis buffer for red blood cell lysis before sedimenting as above and counted on the Casy Counter.

Lungs were minced and placed in 2.5mL R0. A DNase/collagenase mix was made up using 1.4mg/mL collagenase and 60µg DNase in R0. The mix was added to the lungs in 2.5mL and the cells incubated at 37°C for 40 min. Following incubation, 5mL R10 was added to each tube and cells were passed through a 70µm sieve followed by 5mL R10. Cells were sedimented at 1500rmp for 5 min and the red blood cells lysed as described above.

2.2.7 Stimulation

Cells from blood, lung LN and spleen were resuspended at $1.3x10^7$ cells/mL and plated in a round bottom 96 well plate in 150µL. Antigen 85A peptide pools and PPD-T were made up to 8µg/mL and 50µL added to the relevant wells to give a final concentration of 2µg/mL. Brefeldin A was added at 25µg/well two hours after the addition of the antigen and cells were stimulated for another 16 hours.

2.2.8 Flow cytometry

Following stimulation, cells were sedimented at 300xg for 5 min. Cells were stained with 10µL Live/Dead stain for 10 min on ice. 45µL surface staining cocktail was added and cells incubated for 30 min on ice. Cells were washed 2x with 150µL FACS buffer (PBS with 1% FCS) sedimenting at 300xg for 5 min between each wash. Fixation/Permeabilisation solution was added in 150µL and cells incubated on ice for

20 min. Two washes were performed with 150µL Perm/Wash diluted 1:9 in water, sedimenting as above between each wash. Following permeabilisation, the intracellular stain was applied in 45µL and cells incubated for 30 min on ice. Two washes in Perm/Wash were performed as above. Cells were resuspended in 100µL FACS buffer and transferred to cluster tubes. Samples were analysed using an LSR II flow cytometer.

2.2.9 Mycobacterium tuberculosis challenge

Animals were challenged using a Biaera AeroMP-controlled nebuliser contained in a Category Level 3 TCOL isolator. Prior to challenge, samples of the sonicated stock were plated at the following dilutions: $1x10^{-4}$, $1x10^{-5}$ and $1x10^{-6}$. For challenge, the *M.tb* was made up to $5x10^{6}$ cfu/mL in 10 mL PBS. This was transferred to the nebuliser in the isolator. An AGI-4 glass impinger was filled with 10mL PBS containing 0.01% Tween80. Animals were loaded into nose-only restrainers and fitted to the exposure unit. The programme was run for 10 min plus a 5 min purge. The airflow was set to 12L/min at a pressure of 20psig. After the run, animals were unloaded from the challenge unit and placed in cages. A 1mL sample of the impinger was taken and plated out neat and at a $1x10^{-1}$ dilution in 50µL. If a second run was necessary, a new impinger was used and the nebuliser was washed out with PBS before addition of another 10 mL of *M.tb*. In order to determine challenge dose (the aim was for 100-200 cfu/mouse), two naïve animals from each run were sacrificed 24 hrs post-challenge and lungs aseptically removed.

Where animals received antibody treatment post-challenge, 100µg antibody (anti-IL-17A) or isotype control antibody (Rat IgG2A) was administered *i.p.* every 3-4 days for 4 weeks.

2.2.10 Organ homogenisation and plating

Lungs and spleens removed from challenged animals were placed in reinforced 2mL tubes containing 2.8mm ceramic beads. Organs were homogenised at 5500rpm for 20

seconds using a Precellys 24 tissue homogeniser. Lungs from 24 hrs were plated neat in 100µL on 6-7 plates/mouse. Plates were counted 4 weeks post-plating.

Plates were made using Middlebrook 7H10 Agar Base with 2.5mL glycerol added/500mL. After autoclaving for sterilisation, 50mL OADC enrichment was added/500mL and plates poured at 15-20mL agar/plate.

2.2.11 Challenge takedown

Animals were sacrificed 4 weeks post-challenge and lungs and spleens aseptically removed into tubes and homogenised as described above. Lungs from naïve animals were plated at the following dilutions: $1x10^{-2}$, $1x10^{-3}$ and $1x10^{-4}$. Lungs from vaccinated animals were plated either the same as the naïve animals or at $1x10^{-1}$, $1x10^{-2}$ and $1x10^{-3}$ dilutions. Spleens were plated at $1x10^{-1}$, $1x10^{-2}$ and $1x10^{-3}$ dilutions or neat and diluted $1x10^{-1}$ and $1x10^{-2}$. Plates were counted 4 weeks after plating.

2.2.12 Organ fixation for histology and preparation of paraffin sections

If a lung lobe was to be taken for histology, animals were killed by cervical dislocation. Spleen and the other lung lobe were removed and placed in tubes as described above for cfu quantitation. A hole was cut in the trachea using a blade and 500µL 10% Neutral Buffered Formalin (NBF) injected using 0.3mmx0.6mm tubing attached to a 23G needle on a 2mL syringe. The lung was removed and placed in 7.5mL 10% NBF overnight. The following day the lobes were transferred to 70% ethanol and stored at 4°C. Embedding, sectioning, and ZN and haematoxylin and eosin (H&E) staining were performed by Histopathox.

2.2.13 Immunohistochemical staining of lung sections

Formalin-fixed paraffin-embedded sections were immunohistochemically stained for CD3, B220 and F4/80. Slides were warmed at 60°C for 10 min to ensure fixation to the slide. Slides were incubated in for 5 min in Histo-Clear twice, followed by 2x 5 min in 100% ethanol then once in 50% ethanol before incubating in water for 5 min. Slides

were placed in Cytomation Target Retrieval solution at pH 6 for 2 min at pressure at 125°C in a Biocare Medical Decloaker. Slides were then placed in PBS. Antibodies were made up to a 1/100 dilution separately in RPMI containing azide and 10% FCS. Slides were dried and sections circled using a water-repellent pen. One drop of 2.5% horse serum was added to each slide and incubated for 5 min. Serum was knocked off and antibody solution dropped on to the relevant sections. Slides were incubated for 1 hour at room temperature in a humidified chamber. Antibody was knocked off and slides washed in PBS for 5 min. One drop of Histofine Simple Stain Mouse MAX PO Rat and Rabbit Universal Immuno-peroxidase Polymer was added to the relevant slides and incubated 30 min as above. Polymer was knocked off and slides washed in PBS for 5 min. Development solution (DAB peroxidase substrate kit 3,3'-diaminobenzidene) was made up at 50µL/1mL diluent. One drop of development solution was added to each slide and slides left to develop for 8 min before washing in PBS. Slides were counter-stained in haematoxylin stain. Slides were mounted using Aquatex aqueous mountant and left to dry overnight. Slides were scanned using a Hamamatsu NanoZoomer 2.0-HT (Hamamatsu, Japan) at x20 magnification.

2.2.14 Analysis of lung sections

Stained sections were scanned by the Oxford Centre for Histopathology Research (OCHRe) at x20 magnification using a Hamamatsu slide scanner. Files were provided as .ndpi files, which were converted to .tif files using the ndip2tiff software provided by Dr Christophe Deroulers (NDPITools; http://www.imnc.in2p3.fr/pagesperso/deroulers/software/ndpitools/). MATLAB (MATLAB 7.13.0, The MathWorks Inc., Natick, MA 2000) was used to determine exclusive k-means clustering of three colours (broadly white, pink and purple) in the H&E-stained tissue. Clustering is the process of separating similar elements in a dataset from its non-similar elements. There are four main approaches to mathematically determining clustering: exclusive clustering in which every element is assigned to one

cluster and one cluster only; overlapping clustering in which elements can belong to multiple clusters; hierarchical clustering where an element's grouping depends on neighbouring clusters; and probabilistic clustering in which an element's grouping is determined probabilistically.

K-means clustering is a is a tool for exclusive clustering and can be used for automated image analysis based on assignment of each pixel in an image to a pre-defined colour, or cluster, thereby simplifying the image from thousands of colours to, in this case, 3 colours. Should a pixel not exactly match any of the pre-defined colours, its assignment will be based on its composition of primary colours. Here, this effect was minimised by further defining each cluster by selecting 10 hues for each, giving the programme a range of hues to work with. For this analysis, an algorithm for k-means clustering originally proposed by MacQueen [209] and modified for colour analysis by Shoelson [210] was used.

Furthermore, a statistical module was programmed in order to determine the percentage contribution of each cluster to the overall image.

2.2.15 IL-17 ELISA

A 96 well MaxiSorp plate was coated with 1µg anti-IL-17 antibody and incubated at room temperature overnight. The following day the plate was washed 6x in PBS + 0.05% Tween (PBS-T) and blocked for 1 hr using 100µL PBS + 10% FCS at room temperature. Standards of recombinant IL-17 were made up at 2-fold serial dilutions in PBS. Eight standards starting at 1µg/mL were added in duplicate in 50µL. Two wells were filled with 50µL PBS as blanks. 50µL PBS was added in rows B-D and F-H except the standard wells. 75µL serum was added to each well in rows A and E, except the standard well. One in 3 serial dilutions were made down the plate by transferring 25µL serum from A to B and so on. The plate was incubated for 2 hrs at room temperature, then washed 6x in PBS-T. 50µL biotinylated detection antibody diluted to 1µg/mL in PBS was added followed by incubation for another 1 hr at room temperature. The plate

was washed as described above and 50µL ExtrAvidin alkaline phosphatase diluted 1/5000 in PBS-T was added for 30 min at room temperature. A p-Nitrophenyl Phosphate Substrate disodium salt hexahydrate (pNPP) tablet was dissolved in 20mL milliQ water. The plate was washed as described above and 100µL substrate solution added to each well. The plate was left to develop and read at 405nm every 5 min using a BioTech Microplate Reader on Gen5 software until the absorbance of the highest standard was 1.

2.2.16 Antibody blocking and testing

For *in vivo* testing of anti-IL-17A antibody efficacy, animals previously vaccinated with BCG – MVA85A received 100µg anti-IL-17A or PBS in the same volume *i.p.* either 1 week or 4 weeks post-MVA85A. Two days post-antibody administration, animals were bled and serum isolated and used in an IL-17A ELISA as described above.

Alternatively, naïve animals received 100µg anti-IL-17 antibody or PBS *i.p.* Twenty four hours later, animals received 2µg CT *i.n.* Animals were sacrificed 15 hours post-CT administration and lungs taken and examined for granulocyte infiltration by flow cytometry.

2.2.17 RT-qPCR

Lungs from *M.tb*-infected mice were homogenised as described in section 1.2.10 and 200µL of the homogenate placed in 2mL RLT buffer from the RNeasy Fibrous Tissue kit. Samples were stored at -20°C until ready for use. Samples were thawed and 300µL placed in a 1.5mL Eppendorf tube. 590µL RNase-free water was added along with 10µL proteinase K. Tubes were incubated for 10 min at 55°C before centrifuging for 3 min at 10000xg. Supernatant was transferred to a new tube containing 450µL 100% ethanol. 700µL were transferred to an RNeasy mini column and columns were centrifuged at 8000xg for 15 s. Flow through was discarded and the procedure repeated until all the sample was transferred to the column. Buffer RW1 was added (350µL) and the column

centrifuged as above. For each sample, 10µL DNase was mixed with 70µL buffer RDD and added to the column. Columns were incubated for 15 min at room temperature. Column was washed with Buffer RW1 as described above. 500µL RPE was added to each column and column centrifuged for 15 s at 8000xg. Wash with RPE was repeated but this time the spin was for 2 min at 8000xg. The column was transferred to a new collection tube and the column centrifuged for 1 min at full speed. Column was placed in a new collection tube and the sample eluted in 50µL RNase-free water with a spin at 8000xg.

RNA was converted to cDNA as follows. A mix was made up with (per reaction) 4µL 10x Buffer RT, 4µL dNTP mix (5mM each), 4µL Oligo-dT primer (1µg), 2µL Ominscript Reverse Transcriptase, 6µL RNase-free water. The reaction mix was vortexed, then pulsed in a microfuge and 20µL aliquoted to 1.5mL Eppendorf tubes. Template RNA was added in 20µL and tubes vortexed briefly before placing in a heat block at 37°C for 1 hr. cDNA was stored at -20°C.

Primers were ordered from Sigma Aldrich as shown in Table 1.2.17 and made up to 100µM as instructed on the accompanying data sheet. Primers were diluted a further 1/10 by combining 50µL each of forward and reverse primer for each gene in 400µL RNase-free water.

The qPCR mastermix was made up with 10µL QuantiTect SYBR Green PCR mix, 2µL primer mix, 7µL RNase-free water. Each well of a PCR plate was filled with 19µL mastermix followed by 1µL of the relevant cDNA. Plates were run on a LightCycler 480 system (Roche Applied Science). Primers were tested and standard curves made up from 1/10 serial dilutions of the PCR product from the test runs, starting at 10^6 copies/mL.

HPRT was used as the housekeeping gene for normalisation.

Gene	Primer sequence	Melting temp (°C)	Product length (bp)
IL-17AF	AACATGAGTCCAGGGAGAGCTTCA	59.5	117
IL-17AR	AGTGTTTGGACACGCTGAGCTTTG	59.8	
IL-23p19F	AGCACCTGCTTGACTCTGACATCT	59.8	156
IL-23p19R	TAGAACTCAGGCTGGGCATCTGTT	59.8	
IFNgF	ACACACTGCATCTTGGCTTTGCAG	60.2	81
IFNgR	TAGGCTTTCAATGACTGTGCCGTG	59.3	
TNFF	TTCCGAATTCACTGGAGCCTCGAA	60	144
TNFR	TGCACCTCAGGGAAGAATCTGGAA	59.8	
CXCL10F	TGGCTAGTCCTAATTGCCCTTGGT	59.9	100
CXCL10R	TCAGGACCATGGCTTGACCATCAT	60.1	
IL-10F	GCTCTTGCACTACCAAAGCCACAA	59.8	144
IL-10R	TGCAGTTATTGTCTTCCCGGCTGT	60.5	
RorcF	AGCATCTATAGCACTGACGGCCAA	59.9	129
RorcR	ACTGCAGAAACTGGGAATGCAGTG	59.6	
IL-17FF	GTGAATTCCAGAACCGCTCCAGTT	59.2	172
IL-17FR	ACCAGGATTTCTTGCTGAATGGCG	59.7	
IL-23RF	GCAACATGACATGCACCTGGAACA	60	192
IL-23RR	TGCCTAGGGAATTGACAGCTTGGA	60	
Foxp3F	TACACCCAGGAAAGACAGCAACCT	59.9	137
Foxp3R	CTGCTTGGCAGTGCTTGAGAAACT	59.8	
CXCL9F	ATGGATTGCCACATCAGGCTAGGA	60	167
CXCL9R	AATGCTTGCAGAGGCCAGAAGAGA	60.4	

Table 1.2.17 Primer sequences. mRNA sequences for each gene of interest were found in the NCBI gene database and primers designed using the IDT PrimerQuest tool (http://eu.idtdna.com/Scitools/Applications/PrimerQuest/Default.aspx?SequenceWarning=True). Sequences were selected and tested for specificity in the mouse genome using the Basic Sequence Alignment Tool (BLAST) for nucleotides (blast.ncbi.nlm.nih.gov).

2.3 Statistical analyses

Wilcoxon Sign Rank Tests were used for comparison of paired data. Two data sets belonging to different groups were analysed using a t test (parametric) or Mann-Whitney test (non-parametric). One way ANOVA or Kruskal-Wallis tests were used for comparing 3 or more groups of parametric or non-parametric data respectively. Correlations were determined using Spearman Rank Correlations. Analyses were performed using statistical analysis tools in GraphPad Prism.

RESULTS

3 INDUCTION OF IL-17 FOLLOWING VACCINATION OF HEALTHY VOLUNTEERS WITH MVA85A

3.1 Introduction

It has previously been shown that MVA85A can induce IL-17 production in both human whole blood [76] and PBMC [77], as well as in cattle [73]. In MVA85A- or adenovirus expressing Ag85A (Ad85A)-vaccinated cattle, vaccine-induced IL-17 production both pre- and post- *M.bovis* challenge has been correlated with vaccine-induced protection against TB disease [73].

Furthermore, in human PBMC, vaccine-induced IL-17 was found to correlate negatively with percentages of $CD4^{+}CD25^{hi}CD39^{+}$ Treg cells pre-vaccination [77].

Here I sought to further investigate a possible link between ATP hydrolysis by $CD39^{+}$ Treg cells and potentially protective IFN-γ and IL-17 production in PBMC from volunteers vaccinated with MVA85A.

3.2 ATP hydrolysis following MVA85A vaccination follows a distinct pattern and can be inhibited using an apyrase inhibitor

Hydrolysis of extracellular ATP was measured in PBMC from vaccinated subjects at 0, 1, 2, 4 and 24 weeks post-vaccination using the CellTiter-Glow cell viability assay and plotting against a standard curve. There was a significant difference in ATP hydrolysis 2 weeks post-vaccination compared to baseline ($p = 0.008$) (Fig. 3.2.1A). Paired analysis between 0 and 2 weeks is shown in figure 3.2.1B. In order to verify that ATP hydrolysis was attributable to the action of an apyrase, cells were treated with ARL67156 at the time of ATP addition, which reduced ATP hydrolysis (Fig 3.2.1C).

Treg cells, defined here as $CD4^{+}CD25^{hi}CD39^{+}$, have previously been shown to decrease in number post-vaccination with MVA85A. Since CD39 is an eNDTPase metabolising ATP, percentages of these cells in PBMC of vaccinated subjects were compared to levels of

ATP hydrolysis. There was a small dip in percentages of CD39+ Treg cells between 1 and 2 weeks post-vaccination, which followed the pattern of ATP hydrolysis (Fig 3.2.1D).

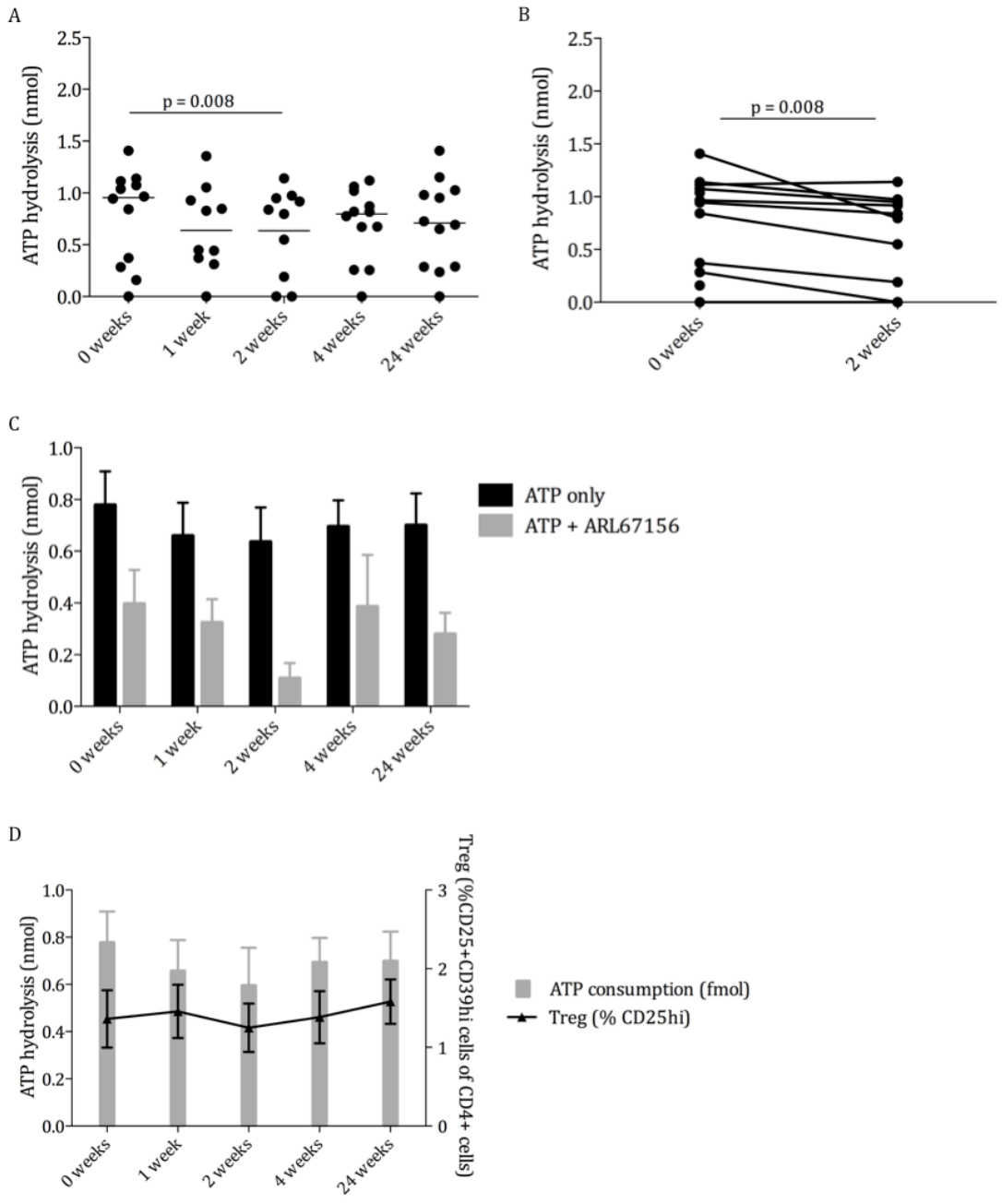


Figure 3.2.1 ATP hydrolysis by PBMC and CD39$^+$ Treg percentages dip 2 weeks post-vaccination. PBMC from MVA85A-vaccinated subjects were plated out at 5x10^4 cells/well in 50µL. Cells were incubated with either 50µM ATP or 50µM ATP + 100µM ARL67156 before addition of the luciferase reagent. A standard curve starting at 50µM ATP was set up. Negative controls were cells with no ATP added. (**A**) Shows change in ATP hydrolysis over time post-vaccination. (**B**) Paired representation of change in ATP hydrolysis between 0 and 2 weeks post-MVA85A. Effect of addition of ARL67156 is shown in (**C**). (n = 10-12). Note that the observation of a greater effect of the inhibitor is potentially due to saturation of binding sites for ATP by the inhibitor at this timepoint, whereas the greater percentage of CD39$^+$ cells present at other timepoints meant the concentration of ARL67156 was not

high enough to completely block all available binding sites. Percentages of $CD25^+CD39^+$ Treg in MVA85A-vaccinated subjects were calculated as a percentage of $CD4^+$ T cells and shown in (**D**), plotted over ATP hydrolysis.

3.3 IFN-γ and IL-17 double positive cells peak 2 weeks post-vaccination

In PBMC from healthy MVA85A-vaccinated subjects, $CD4^+$ T cells producing only IL-17 were not detectable by intracellular cytokine staining (ICS), using a peptide pool of 66 Ag85A peptides as the stimulant (data not shown). In contrast, $CD4^+$ T cells producing both IFN-γ and IL-17 simultaneously were readily detected in response to the same stimulant. IFN-γ^+IL-17^+ cells (gating shown in figure 3.3.1A) peaked 2 weeks post-vaccination (Fig 3.3.1B). Since there appeared to be CD39 activity in the PBMC samples (Fig 3.3.1C), the effect of ARL67156 treatment on antigen-specific cytokine production was examined. Addition of ARL67156 enhanced production of both cytokines both 1 and 2 weeks post-vaccination and the change in cytokine production compared to baseline in this experiment was significant ($p = 0.047$ at 1 week and 0.02 at 2 weeks post-vaccination) (Fig 3.3.1C).

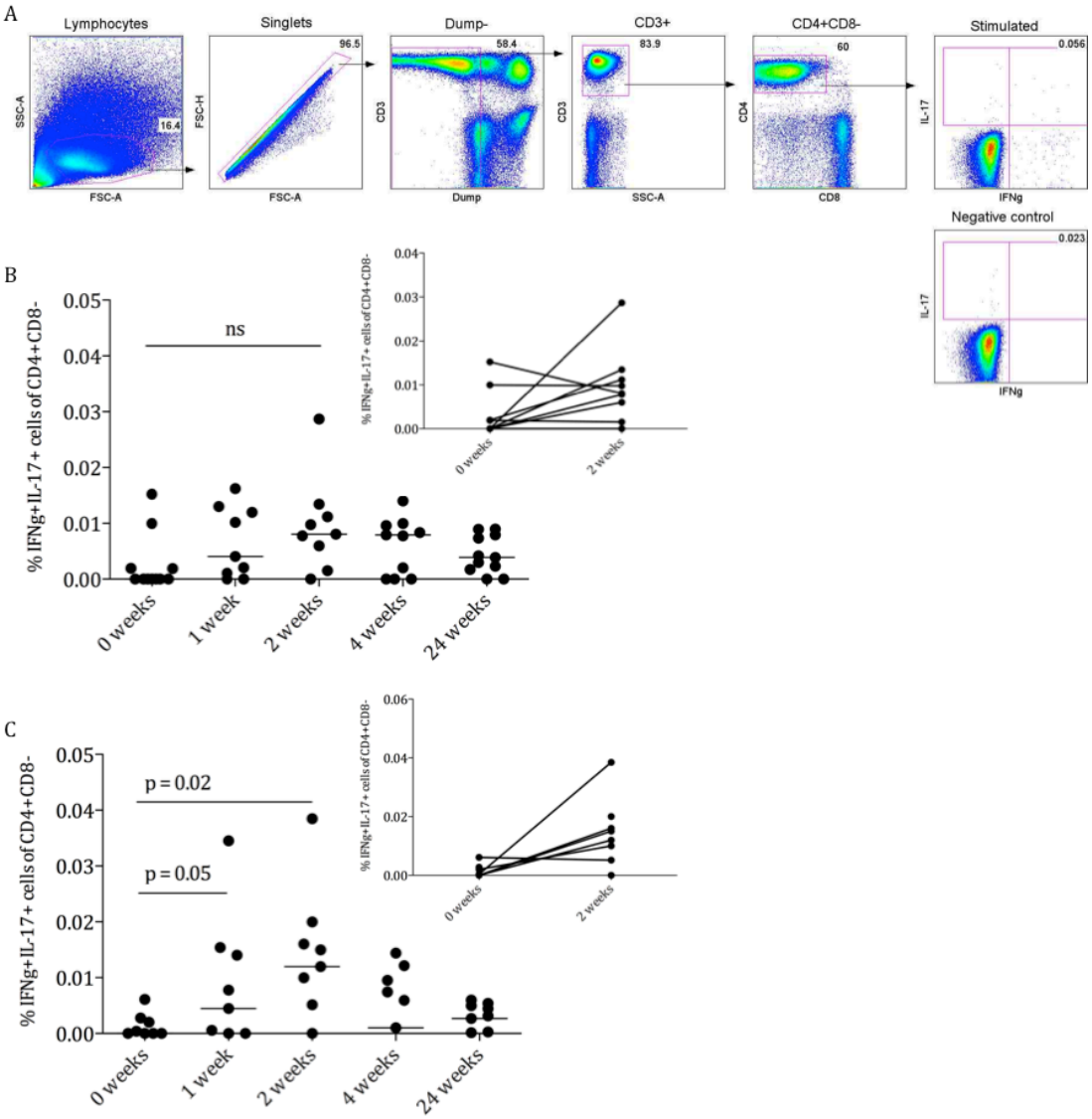


Figure 3.3.1 IL-17 and IFN-γ production in PBMC peaks 2 weeks post-vaccination. PBMC from vaccinated subjects were stimulated with Ag85A peptide pools with or without 100uM ARL67156. No stimulation and phorbol 12-myristate 13-acetate with ionomycin were used as negative and positive controls. Percentages shown are unstimulated subtracted from Ag85A stimulation. Following staining, cells were gated as shown in (**A**): Lymphocytes were gated for on forward scatter (FSC) vs. side scatter (SSC). Singlets were then gated and dead cells, B cells and monocytes were gated out. $CD3^+$ cells were selected for $CD4^+CD8^-$ cells. Antigen-specific cytokine expression from these cells was evaluated. Cells expressing both IL-17 and IFN-γ were quantified and shown in (**B**). The effect of ARL67156 on cytokine expression was investigated by addition during ICS stimulation (**C**).

3.4 IL-17$^+$ and IFN-γ$^+$IL-17$^+$ cells are present at a higher frequency in whole blood compared to PBMC of vaccinated subjects

Other trials involving vaccination with MVA85A have investigated cytokine responses in whole blood as opposed to PBMC. One marked difference between these two compartments is that IFN-γ-producing CD8$^+$ T cells are readily detectable in whole blood but not in PBMC following vaccination ([79] and Satti, unpublished data). To directly compare CD4$^+$ T cell cytokine production in these two compartments, I investigated IL-17 and IFN-γ production following stimulation with Ag85A peptides in whole blood and PBMC from the same BCG – MVA85A-vaccinated healthy subjects. Both IL-17$^+$ and IFN-γ$^+$IL-17$^+$ cells peaked 1 week post-vaccination (Figs. 3.4.1A & B), in contrast to the undetectable IL-17 response and the peak of IFN-γ$^+$IL-17$^+$ cells observed 2 weeks post-vaccination in PBMC (Fig 3.3.1B). The magnitude of response was also significantly higher one week post-vaccination in whole blood, with a median of 0.041% compared to 0.004% for PBMC, p = 0.001. Furthermore, there was a significant difference in peak response comparing whole blood and PBMC (Fig 3.4.1C) (median for WB (1 week post-vaccination): 0.041%; PBMC (2 weeks post-vaccination): 0.008%; p = 0.0003).

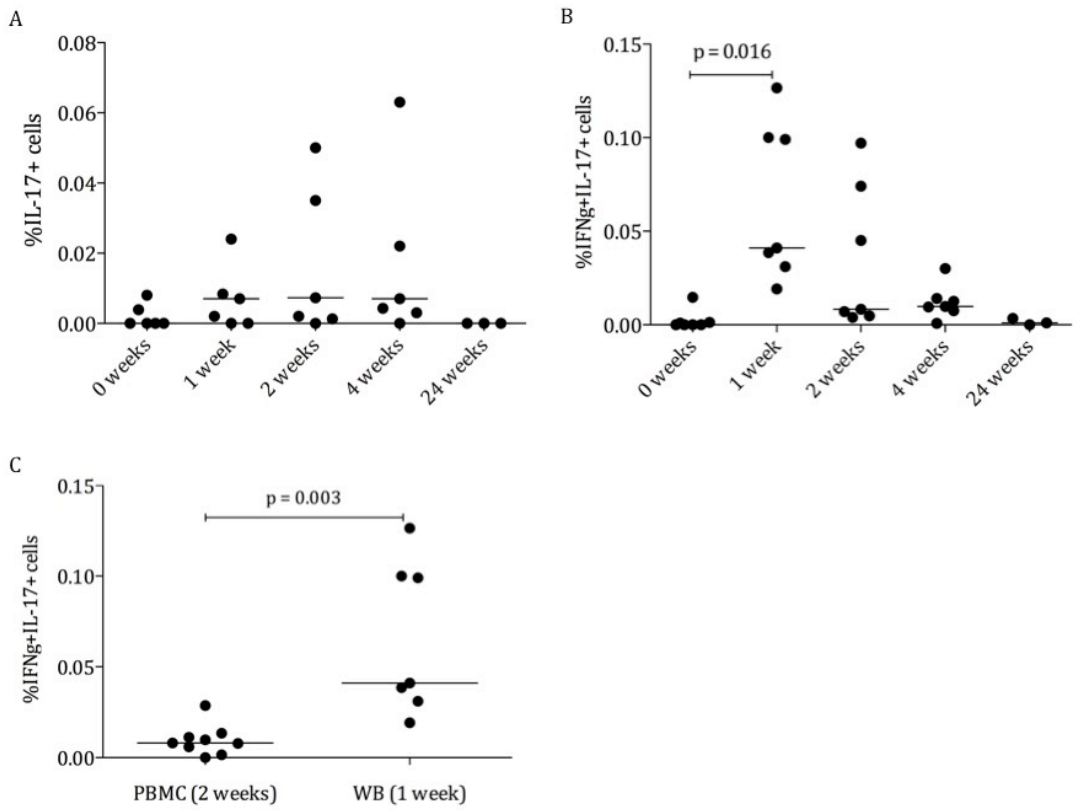


Figure 3.4.1 IL-17 and IFN-γ production in whole blood peaks 1 week post-vaccination. Whole blood (WB) from vaccinated subjects was stimulated for 6 h with a pool of 66 Ag85A peptides. Phytohaemagglutinin (PHA)-treated and untreated cells were used as positive and negative controls respectively. Lymphocytes were gated for and cytokine-expressing cells quantified as described above. Percentages of IL-17$^+$ and IFN-γ$^+$IL-17$^+$ cells responding to the Ag85A peptide pool (with the percentages from unstimulated cells subtracted) are shown in (**A**) and (**B**). Differences in percentages of cells at the relevant peak time point in PBMC vs. WB is shown in (**C**). n = 7.

3.5 Discussion

Here I show that there is a relationship between ATP hydrolysis, and IFN-γ and IL-17 expression by CD4$^+$ T cells following vaccination with MVA85A, which also relates to percentages of CD39$^+$ Treg in PBMC. In healthy BCG – MVA85A-vaccinated subjects, CD39$^+$ Treg numbers decrease post-vaccination, with a maximum decrease 2 weeks post-vaccination. This is associated with a decrease in ATP hydrolysis, suggesting that ATP hydrolysis is driven at least in part by CD39$^+$ Treg. Strikingly, at 2 weeks post-vaccination, we also show an increase in the percentage of IFN-γ$^+$IL-17$^+$ cells. IFN-γ$^+$IL-17$^+$ cells have been previously been described in autoimmune diseases [163] and

ulcerative colitis [211] as well as in response to mycobacterial antigens [124]. Our data support the hypothesis that extracellular ATP may help to drive the development of these cells. This hypothesis is supported by the fact that IL-17$^+$ and IFN-γ$^+$IL-17$^+$ cells are more readily detectable in whole blood compared to PBMC; the extracellular environment of whole blood is far more complex than that of PBMC and our experiments have shown a higher concentration of ATP in whole blood compared to PBMC following stimulation. Furthermore, ATP has previously been shown to induce IL-17 production by T cells in mice [212].

The link between these observations following MVA85A vaccination is still under investigation. One mechanism that could contribute to increased cytokine production is activation of the NALP3 inflammasome. This leads to IL-1β production, which in turn acts on induction of CD4$^+$ T cells to produce IL-17 [115]. Since CD39 metabolises ATP, a vaccine-induced reduction in circulating CD39$^+$ Treg may result in increased concentrations of pro-inflammatory extracellular ATP, known to act through the P2X7 receptor to activate the inflammasome [213, 214]. Adding to this effect, a decrease in circulating CD39$^+$ Treg would also reduce the concentration of breakdown products of ATP, such as adenosine, which is known to act in an inhibitory fashion through the A2A receptor on activated T cells [159].

A further contributing factor to inflammasome activation and IL-17 induction might be the viral vector MVA, which has been found to activate the NALP3 inflammasome in THP-1 cells following its endocytosis [215].

These findings demonstrate vaccine-mediated induction of a subset of IFN-γ$^+$IL-17$^+$ CD4$^+$ T cells, whose peak corresponds with a reduction in the ability of cells from the same volunteer to hydrolyse ATP in a CD39-mediated manner. Should this cell subset prove to be protective in vaccine-induced protection against TB disease, this pathway represents a potential target for manipulation for their enhancement.

Knowledge of mechanisms through which IL-17, and IFN-γ and IL-17-producing cells can be induced is important with regard to vaccine development, with the next step being to determine their role in vaccine-induced protection or pathology.

Furthermore, it is important to investigate regulatory aspects of cellular immunity, as the overall outcome of any vaccine-induced immunity will be the result of a balance between both effector and regulatory responses. The work here helps to dissect this interaction between regulatory and effector responses following vaccination and provides potential avenues for manipulation of immune responses in order to provide improved vaccine-induced protection.

4 EVALUATING THE IMMUNOGENICITY OF A BCG PRIME – MVA85A BOOST VACCINATION REGIME IN MICE

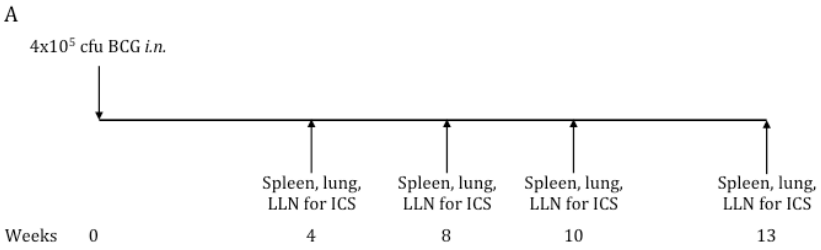
4.1 Introduction

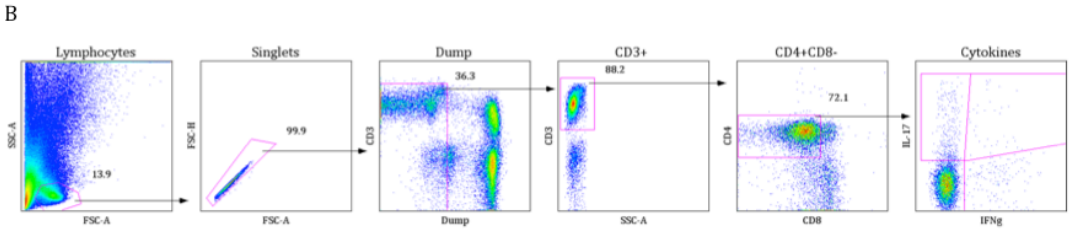
With respect to IFN-γ, the vaccination regime of BCG prime – MVA85A boost in mice, delivered both *i.d.* and *i.n.*, has previously been characterised in terms of both immunogenicity and efficacy [216]. The ability of either BCG or BCG – MVA85A vaccination to induce IL-17 in mice, however, has not been explored. Here, both Balb/c and C57BL/6 mice were vaccinated with either BCG alone or BCG followed 10 weeks later by MVA85A. The vaccines were delivered either *i.n.* or *i.d.* in the Balb/c animals, and *i.n.* in the C57BL/6 animals.

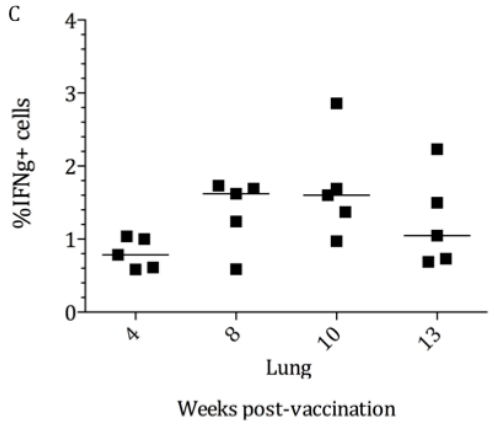
4.2 Timecourse of BCG-induced IFN-γ and IL-17 following intranasal vaccination of Balb/c mice

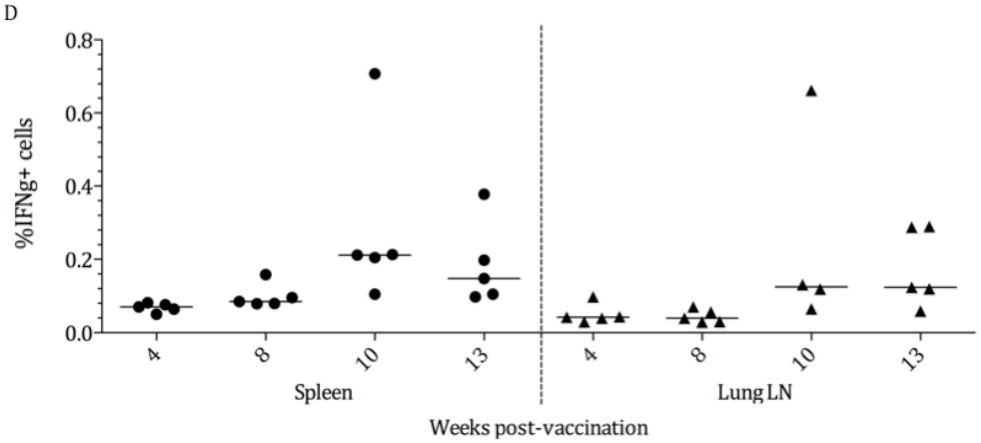
In order to determine the timecourse of IFN-γ and IL-17 induced following mucosal delivery of BCG, Balb/c mice received $4x10^5$ cfu BCG *i.n.* Lungs, spleens and lung LN from 5 mice were collected at 4, 8, 10 and 13 weeks post-vaccination as shown in figure 4.2.1A. Percentages of $CD4^+$ T cells producing IFN-γ and IL-17, both individually and simultaneously, were determined through ICS following stimulation. The gating strategy for $CD4^+$ T cells is shown in figure 4.2.1B.

As expected, intranasal vaccination induced a strong mucosal response. High levels of IFN-γ were detected in the lungs following stimulation, peaking 8-10 weeks post-vaccination and contracting at 13 weeks post-vaccination (Fig 4.2.1C). The kinetics in the spleen and lung LN were slower, peaking 10-13 weeks post-vaccination and with lower percentages of IFN-γ-producing cells (Fig 4.2.1D).

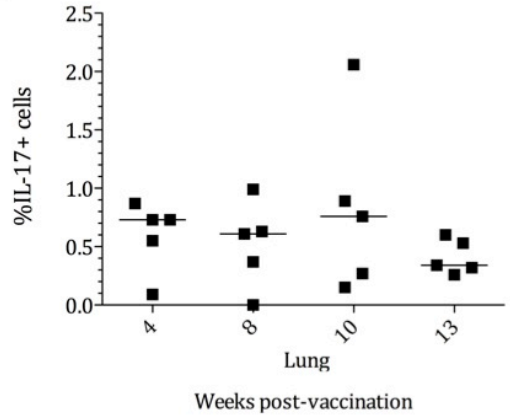

A
4x10^5 cfu BCG i.n.
Spleen, lung, LLN for ICS
Spleen, lung, LLN for ICS
Spleen, lung, LLN for ICS
Spleen, lung, LLN for ICS
Weeks 0 4 8 10 13


B
Lymphocytes
Singlets
Dump
CD3+
CD4+CD8-
Cytokines
13.9
99.9
36.3
88.2
72.1
SSC-A
FSC-A
FSC-H
CD3
Dump
SSC-A
CD4
CD8
IL-17
IFNg

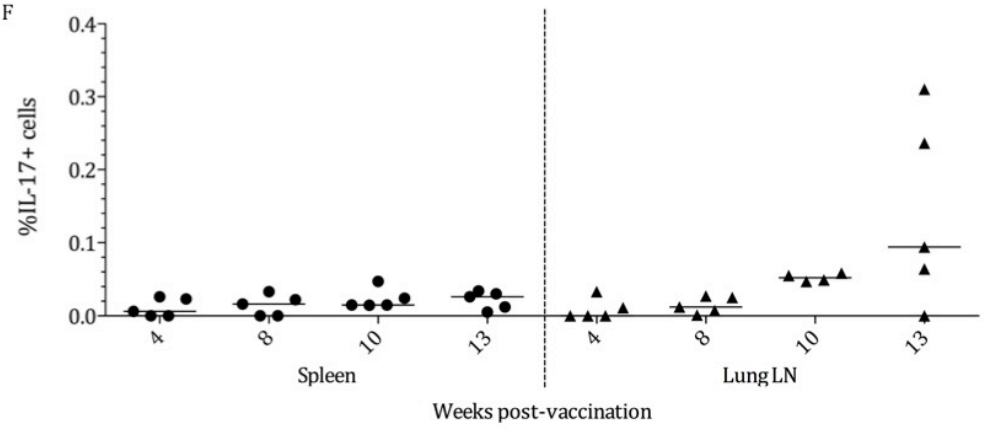

C
%IFNg+ cells
Lung
Weeks post-vaccination


D
%IFNg+ cells
Spleen
Lung LN
Weeks post-vaccination

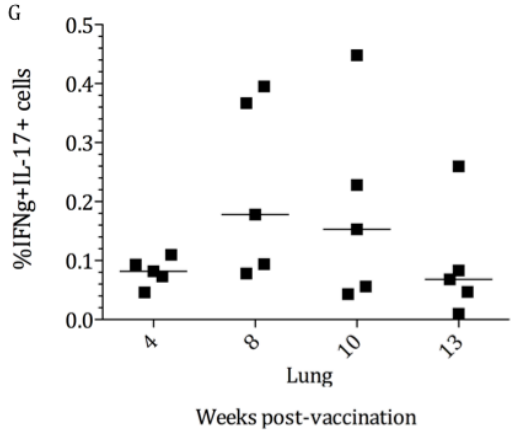
E


%IL-17+ cells
2.5
2.0
1.5
1.0
0.5
0.0
4
8
10
13
Lung
Weeks post-vaccination

F


%IL-17+ cells
0.4
0.3
0.2
0.1
0.0
4
8
10
13
Spleen
Lung LN
Weeks post-vaccination

G


%IFNg+IL-17+ cells
0.5
0.4
0.3
0.2
0.1
0.0
4
8
10
13
Lung
Weeks post-vaccination

H

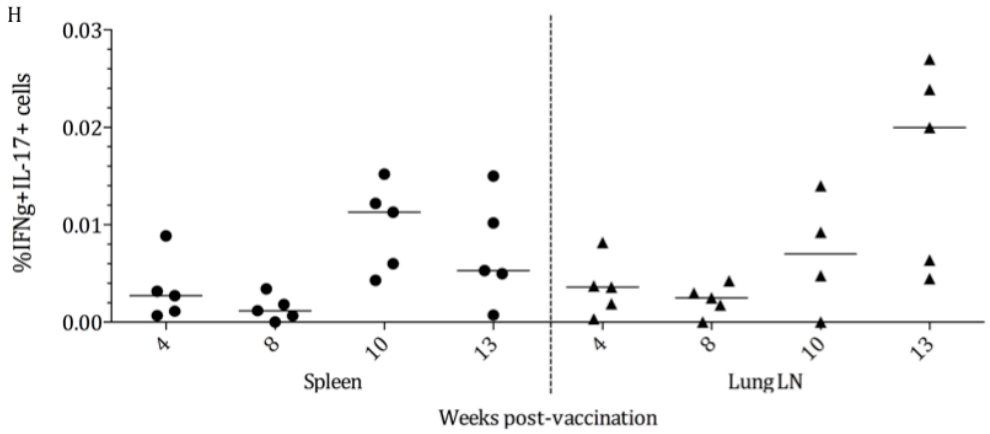

%IFNg+IL-17+ cells
0.03
0.02
0.01
0.00
4
8
10
13
Spleen
Lung LN
Weeks post-vaccination

Figure 4.2.1 Immunogenicity of BCG delivered *i.n.* Animals received 4x10^5 cfu BCG delivered *i.n.* Five animals were taken down at 4, 8, 10 and 13 weeks post-vaccination and lungs, spleen and lung-draining LN collected (**A**). Cells were stimulated with PPD in the presence of Brefeldin A and GolgiStop and cytokine expression analysed by ICS. **B** shows the gating strategy used for $CD4^+$ T cells. Boolean gating was used on the quadrants shown in the final panel for the percentages of IFN-γ, IL-17 and double-positive cells. Percentages of $CD4^+$ T cells producing IFN-γ only (**C** & **D**), IL-17 only (**E** & **F**) or both cytokines simultaneously (**G** & **H**) were calculated.

As was seen for IFN-γ, a high percentage of cells in the lungs produce IL-17 only. Percentages of these cells peaked early at 4 weeks post-vaccination and remained high throughout the first 10 weeks before contracting around 13 weeks post-vaccination (Fig 4.2.1E). Very little IL-17 was detectable at any time point in the spleen (Fig 4.2.1F), consistent with the hypothesis that this cytokine is mucosally induced and associated. Levels of IL-17 in the lung LN were low but there was a clear increase in the percentages of cells producing the cytokine at 10-13 weeks post-vaccination (Fig 4.2.1F). $CD4^+$ T cells producing both IFN-γ and IL-17 simultaneously were detectable at 4 weeks in the lungs, and these percentages increased through 8 and 10 weeks post-vaccination (Fig 4.2.1G), similar to the kinetics of IFN-γ-producing cells. The kinetics of these IFN-γ^+IL-17^+ in the spleen and lung LN were also similar to those of IFN-γ-producing cells, peaking 10 weeks post-vaccination in spleen, but continuing to rise at 10-13 weeks post-vaccination in lung LN, however percentages of these cells were very low compared to those of cells producing only IFN-γ (Fig 4.2.1H).

These results show that intranasal BCG vaccination is able to induce IL-17 production by $CD4^+$ T cells, and that the kinetics of IL-17 are more rapid than those of IFN-γ, with IL-17 peaking earlier in the lungs following vaccination before tapering off. Assuming MVA85A is able to boost IL-17 in mice as it does in humans, this high percentage of IL-17^+ cells post-prime means it should be possible to boost these cells with MVA85A to produce more IL-17 at a later timepoint.

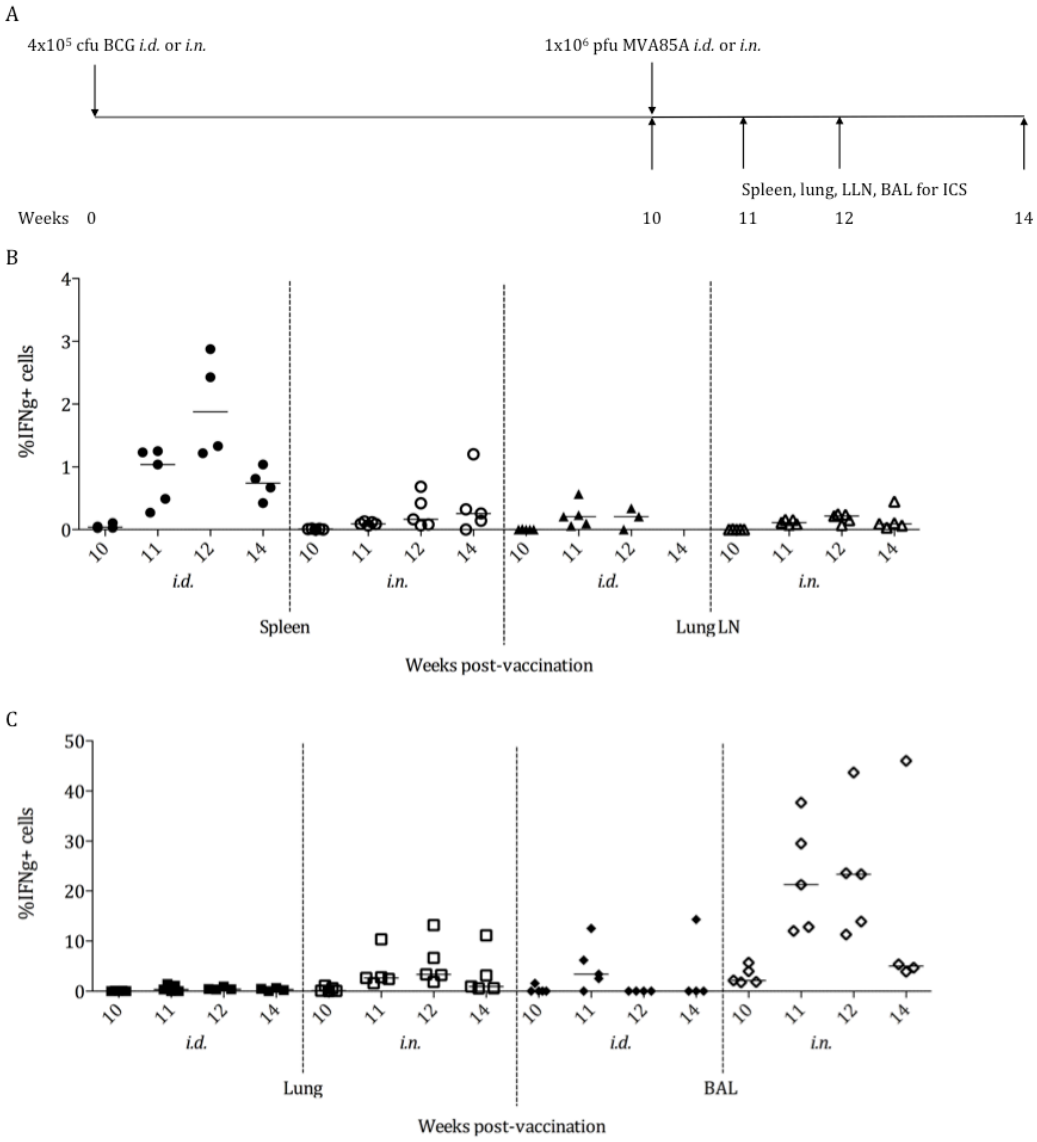
4.3 Timecourse of BCG – MVA85A-induced IFN-γ and IL-17 following *i.d.* vs. *i.n.* vaccination of Balb/c mice

Having established that IL-17-producing cells can be induced by intranasal vaccination with BCG, the ability of an MVA85A boost to further expand this population was investigated. Both intradermal and intranasal routes of vaccination were compared. Animals received BCG either *i.d.* or *i.n.* followed 10 weeks later by MVA85A, administered by the same route as the BCG prime (Fig 4.3.1A). Cytokine production by $CD4^+$ T cells was measured by ICS as described previously.

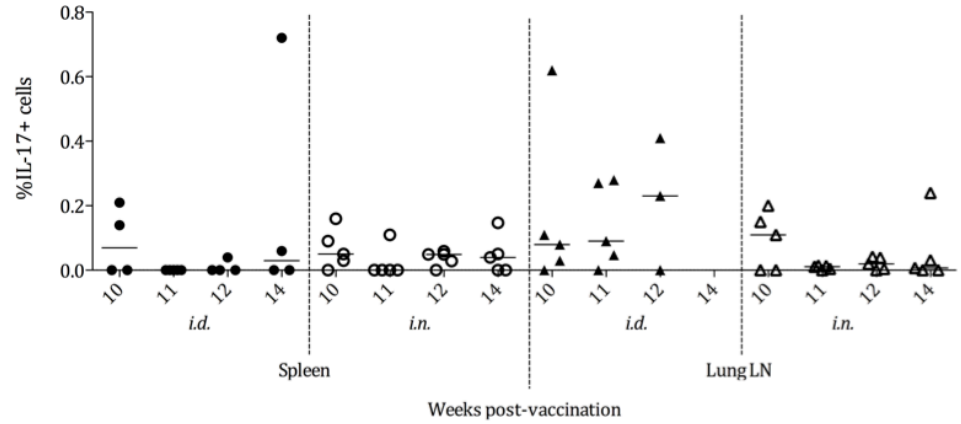
Results showed that *i.d.* vaccination induced strong IFN-γ responses in the spleen, with percentages of IFN-γ-producing cells peaking 2 weeks post-boost (Fig 4.3.1B). Intranasal vaccination induced very low responses in the spleen, and both *i.n.* and *i.d.* vaccination induced similar low responses in the lung LN.

As expected, intradermal vaccination with BCG followed by MVA85A did not induce strong responses in either the lung or the BAL (Fig 4.3.1C). In contrast, *i.n.* delivery of both BCG and MVA85A yielded high percentages of IFN-γ-producing $CD4^+$ T cells in lungs and BAL, reflecting the mucosal route of delivery.

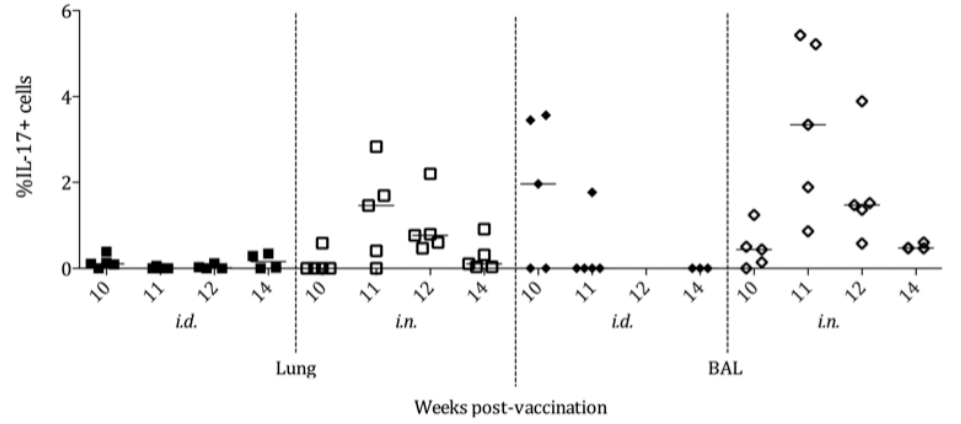
As was observed following BCG vaccination, very few or no IL-17 single-producing cells were detected in spleen following an MVA85A boost, with either *i.n.* or *i.d.* vaccination (Fig 4.3.1D). Low percentages of cells producing IL-17 only were induced in the lung LN following *i.d.* but not *i.n.* vaccination (Fig 4.3.1D).



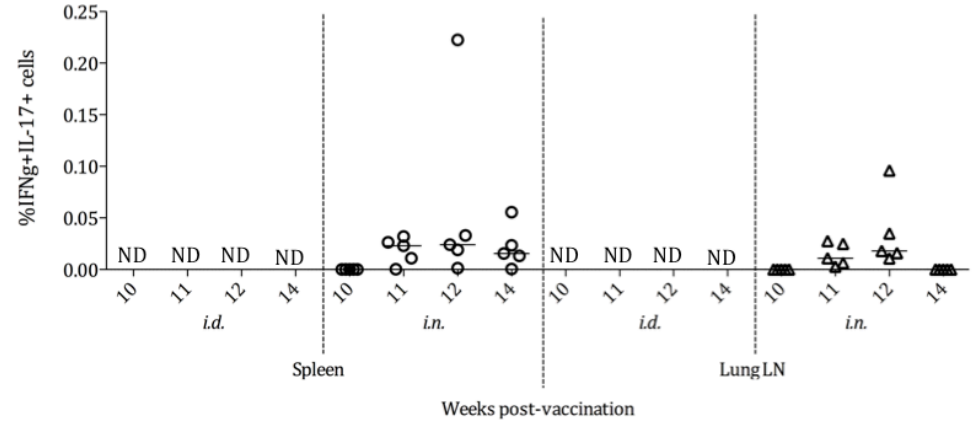
D


%IL-17+ cells
0.8
0.6
0.4
0.2
0.0
10 11 12 14 10 11 12 14 10 11 12 14 10 11 12 14
i.d. i.n. i.d. i.n.
Spleen
Lung LN
Weeks post-vaccination

E


%IL-17+ cells
6
4
2
0
10 11 12 14 10 11 12 14 10 11 12 14 10 11 12 14
i.d. i.n. i.d. i.n.
Lung
BAL
Weeks post-vaccination

F


%IFNg+IL-17+ cells
0.25
0.20
0.15
0.10
0.05
0.00
ND ND ND ND ND ND ND ND
10 11 12 14 10 11 12 14 10 11 12 14 10 11 12 14
i.d. i.n. i.d. i.n.
Spleen
Lung LN
Weeks post-vaccination

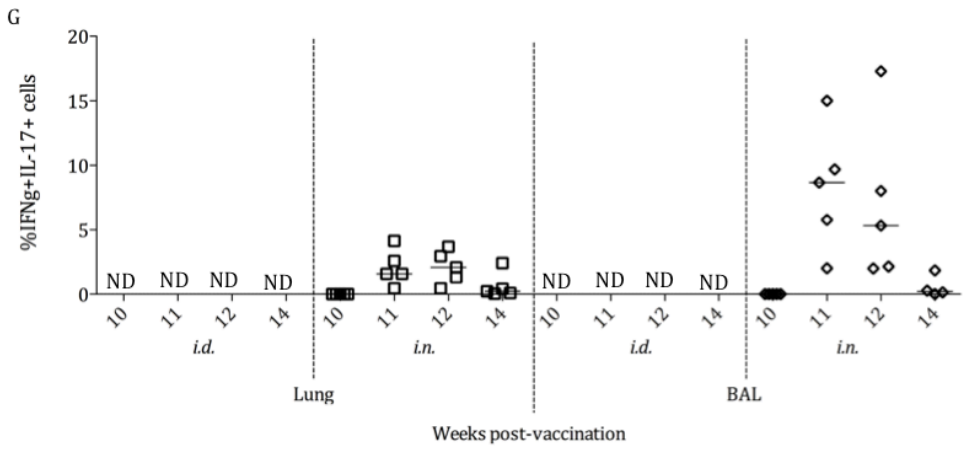


Figure 4.3.1 Immunogenicity of BCG – MVA85A by *i.d.* and *i.n.* administration. Animals received BCG either *i.n.* or *i.d.* followed by MVA85A 10 weeks later delivered by the same route. Spleen, lung LN, lungs and BAL were taken from 5 mice at each timepoint at 10, 11, 12 and 14 weeks post-BCG (**A**). Cells were stimulated with an Antigen 85A single peptide pool in the presence of Brefeldin A and GolgiStop and cytokine expression analysed by ICS. Percentages of $CD4^+$ T cells producing IFN-γ only (**B** & **C**), IL-17 only (**D** & **E**) or both cytokines simultaneously (**F** & **G**) were calculated. ND = not detected.

There were high percentages of IL-17-producing $CD4^+$ T cells detected in the lungs and BAL following *i.n.* vaccination (Fig 4.3.1E), indicating an ability of MVA85A to boost the IL-17-producing cells induced here by BCG vaccination (Fig 4.2.1C).

No IFN-γ^+IL-17^+ cells were detectable in any organ following *i.d.* vaccination. In contrast, *i.n.* vaccination induced small percentages of double-positive cells in spleen and lung LN and higher percentages in lungs and BAL (Figs 4.3.1F & G).

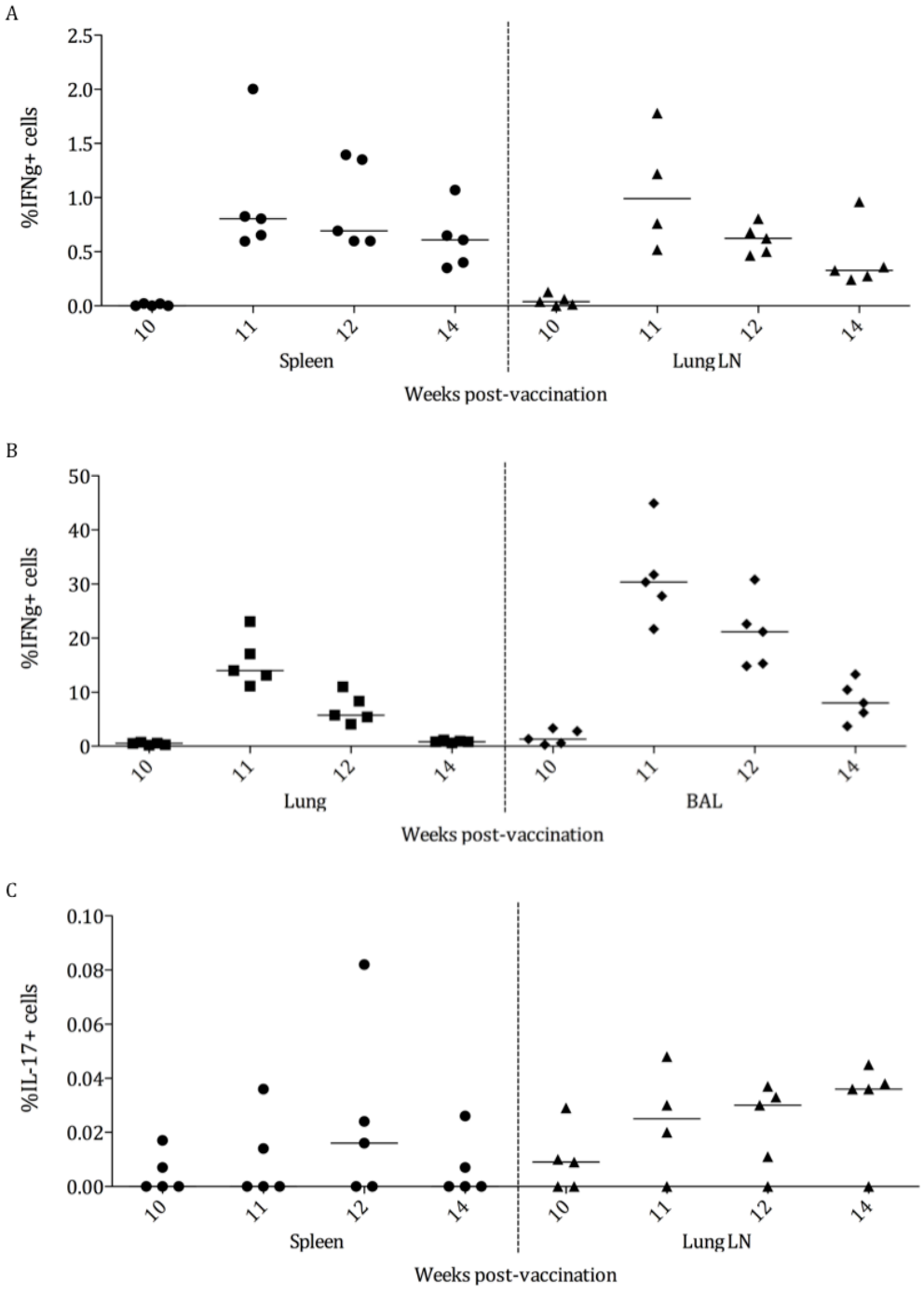
With regard to peak production post-vaccination, IFN-γ peaked later than IL-17 in all organs. IL-17 had a peak 1 week post-MVA85A, whereas IFN-γ peaked 1-2 weeks post-boost. This is consistent with reports by Gopal *et al.* [185], who observed delayed induction of IFN-γ-producing cells following vaccination compared to IL-17.

4.4 Timecourse of BCG – MVA85A-induced IFN-γ and IL-17 following intranasal vaccination in C57BL/6 mice

Previously in this laboratory, Balb/c mice have been used for *M.tb* challenge models due to their level of susceptibility to infection that allows for chronic infection without causing serious wasting disease within 4 weeks of challenge [190]. In this project,

however, I planned to use two knockout strains both on a C57BL/6 background. While susceptibility to *M.tb* in this strain is similar to that in Balb/c mice, it was important to form a picture of the immunogenicity of BCG – MVA85A in WT C57BL/6 animals. In order to do this, C57BL/6 animals were vaccinated with BCG *i.n.* followed 10 weeks later by intranasally-delivered MVA85A. Spleen, lung LN, lungs and BAL were collected at 10, 11, 12 and 14 weeks post-vaccination and cytokine expression analysed as described previously.

Compared to Balb/c mice, IFN-γ production by $CD4^+$ T cells peaked earlier in C57BL/6 mice at 1 week post-vaccination. Furthermore, higher percentages of IFN-γ-producing $CD4^+$ T cells were observed in the spleen and lung LN as well as in the lungs (Fig 4.4.1A & B). BAL responses were comparable across strains. As in Balb/c animals, IL-17 production in the spleen and lung LN was low (Fig 4.4.1C). There were comparable percentages of $CD4^+$ T cells in lungs producing IL-17 alone (Fig 4.4.1D), however in contrast to Balb/c mice, low levels of IL-17 production was detected in BAL. Also, percentages of the cells were similar in C57BL/6 mice in spleen, lung LN and lungs (Fig 4.4.1E & F). Percentages of IFN-γ^+IL-17^+ cells in BAL were similar in C57BL/6 mice compared to Balb/c mice.


A
%IFNg+ cells
2.5
2.0
1.5
1.0
0.5
0.0
10
11
12
14
Spleen
Lung LN
Weeks post-vaccination
B
%IFNg+ cells
50
40
30
20
10
0
Lung
BAL
Weeks post-vaccination
C
%IL-17+ cells
0.10
0.08
0.06
0.04
0.02
0.00
Spleen
Lung LN
Weeks post-vaccination

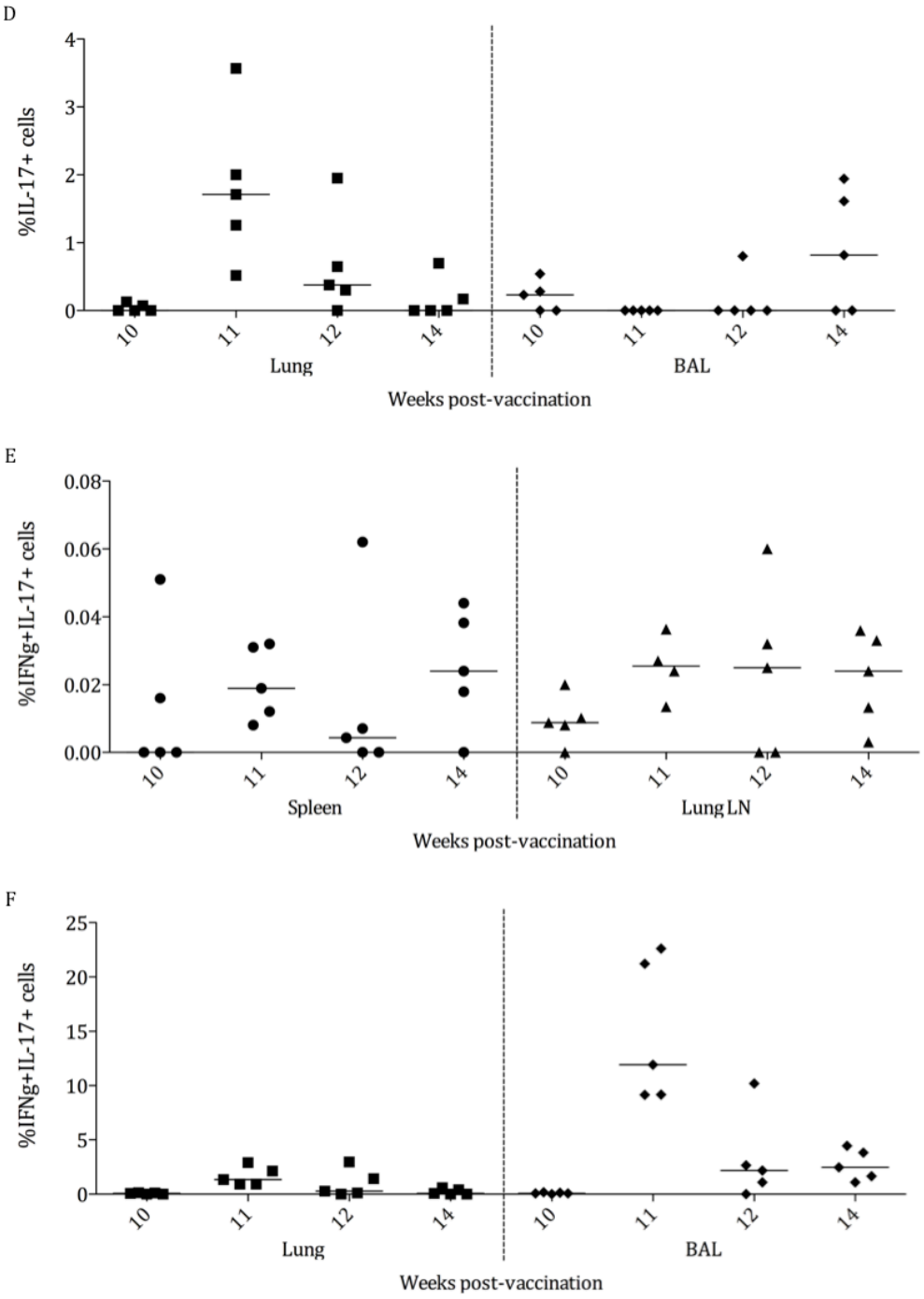


Figure 4.4.1 Immunogenicity of BCG – MVA85A delivered *i.n.* in C57BL/6 mice. C57BL/6 animals were vaccinated with BCG delivered *i.n.* followed 10 weeks later by MVA85A by the same route. Spleen, lung LN, lungs and BAL from 5 mice were taken at each timepoint at 10, 11, 12 and 14 weeks post-vaccination. Cells were stimulated with an Antigen 85A peptide pool in the presence of Brefeldin A and GolgiStop and cytokine expression analysed by ICS. Percentages of $CD4^+$ T cells producing IFN-γ only (**A** & **B**), IL-17 only (**C** & **D**) or both cytokines simultaneously (**E** & **F**) were calculated.

4.5 Induction of CD8+ T cells following BCG or BCG – MVA85A vaccination

Although there is thought to be some role for CD8+ T cells in protection against TB disease, the focus of this thesis is CD4+ T cells since *i.d.* administration of neither BCG nor BCG – MVA85A induces CD8+ T cells [216]. Intranasal administration of BCG improves CD8+ T cell induction in the lungs and the lung lymph nodes, but still does not induce numbers comparable to CD4+ T cells, and these cells can be marginally boosted [216]. Although the rest of this thesis will focus on CD4+ T cells, I briefly investigated CD8+ T cell induction by BCG delivered *i.n.* and found very low induction in spleen and lung LN, and moderate induction of IFN-γ-producing and IL-17-producing CD8+ T cells in the lungs (Fig 4.5.1A & B).

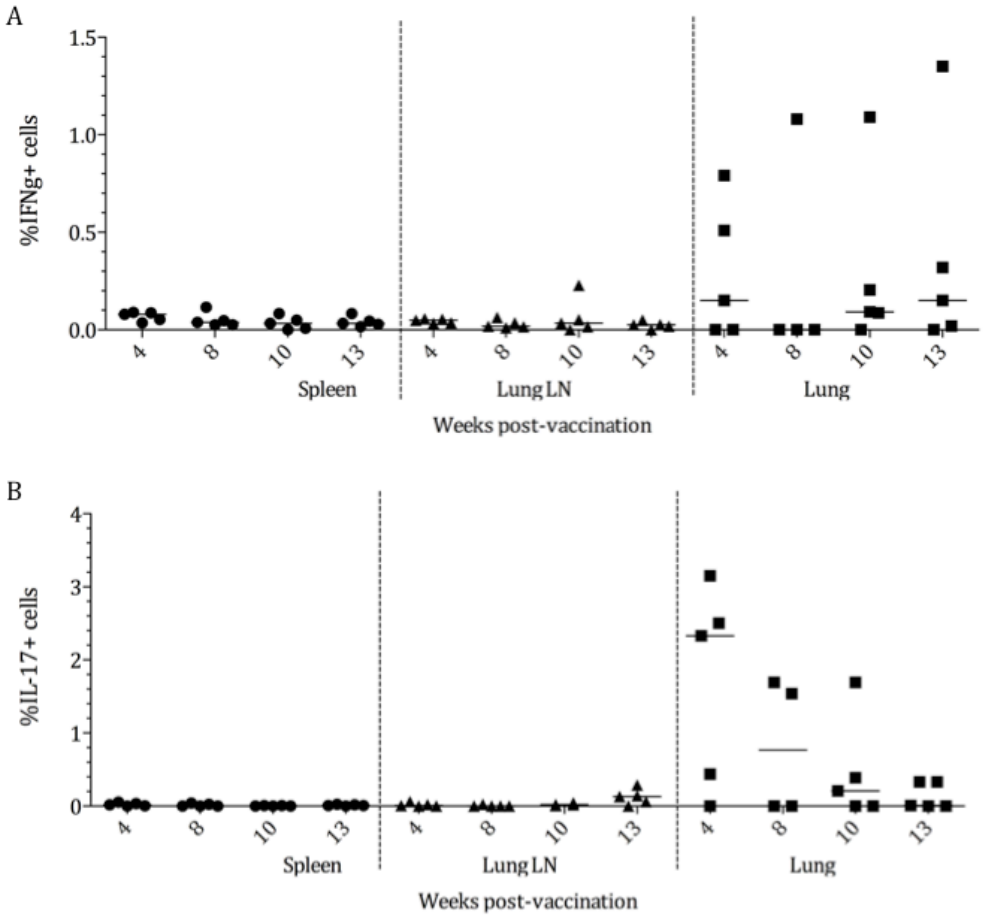


Figure 4.5.1 CD8+ T cell induction following *i.n.* BCG vaccination. Balb/c mice were vaccinated with BCG *i.n.* and 5 mice were culled at 4, 8, 10 and 13 weeks post-vaccination. Spleen, lung LN and lungs were dissected and stimulated with PPD in the presence of BfA and expression of IFN-γ (**A**) and IL-17 (**B**) evaluated by ICS.

Notably, the IL-17-producing cells peaked early at 4 weeks (possibly earlier) post-vaccination in the lungs, but contracted to very low numbers at the time at which the MVA85A boost is usually administered (10 weeks post-vaccination).

In order to see if these $CD8^+$ T cells could be boosted by administration of MVA85A, mice having received BCG either *i.d.* or *i.n.* were given MVA85A by the same route. As shown in figure 4.5.2A, *i.d.* vaccination induces a late peak of $CD8^+$ T cells 2 weeks post-MVA85A, and a similar peak is seen following *i.n.* vaccination in the lungs. No IFN-γ-producing $CD8^+$ T cells were detected in the spleen following *i.n.* vaccination or in the lung LN following either vaccine regime (Fig 4.5.2A).

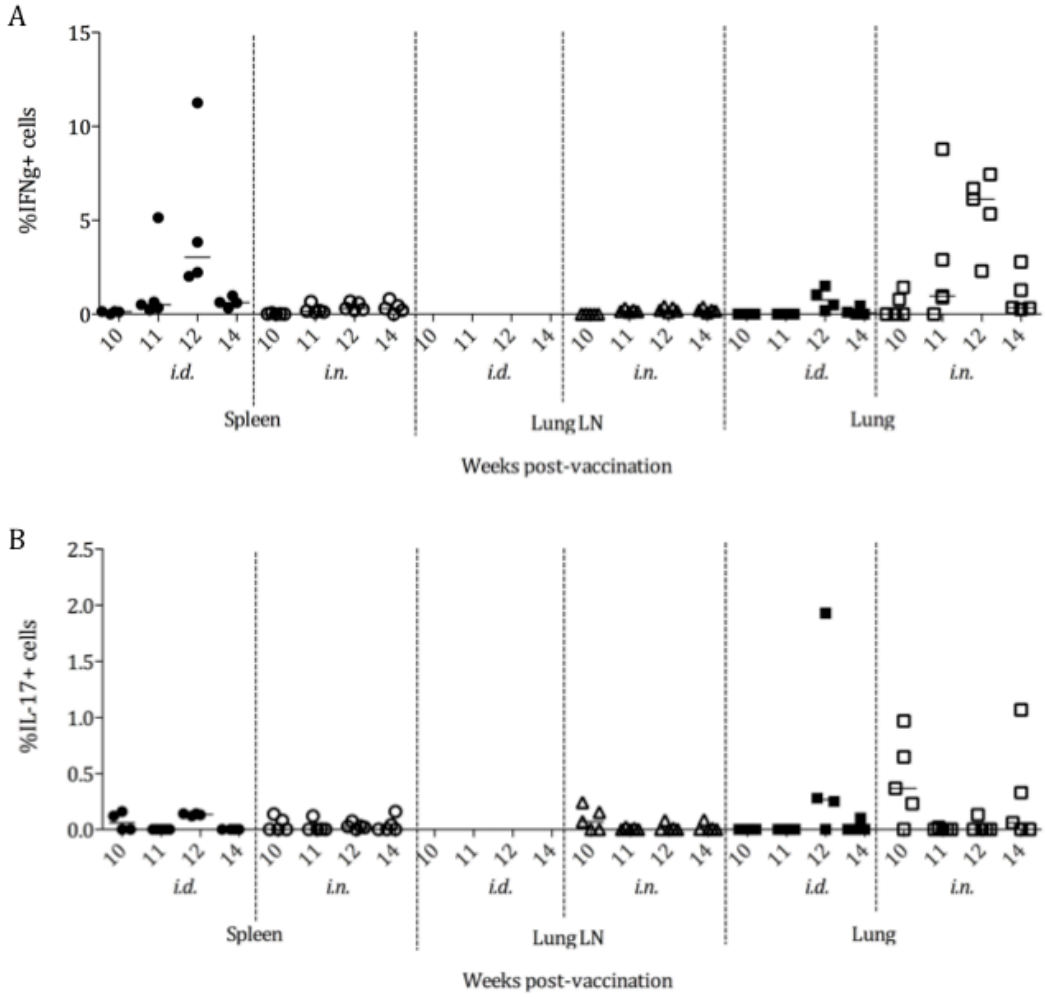


Figure 4.5.2 Boosting of BCG-induced $CD8^+$ T cell responses with MVA85A. Mice receiving BCG either *i.n.* or *i.d.* were given MVA85A by the same route at 10 weeks. 5 mice were culled at 10, 11, 12 and 14 weeks post-BCG and spleen, lung LN and lungs taken and stimulated with an Ag85A peptide pool and production of IFN-γ (**A**) and IL-17 (**B**) examined by ICS.

No IL-17 production was seen following any route, apart from a low percentage of IL-17$^+$ cells in the lungs at 10 weeks post-BCG prior to MVA85A boost (Fig 4.5.2B).

4.6 Discussion

The purpose of the experiments described in this chapter was to establish the ability of three different vaccine regimes (BCG delivered *i.n.* and BCG – MVA85A delivered either *i.n.* or *i.d.*) to induce CD4$^+$ T cells expressing two key cytokines in the control of *M.tb*: IFN-γ and IL-17. Two different strains of mouse were used, namely Balb/c and C57BL/6, in order to establish immunogenicity of the vaccine in both strains.

In Balb/c mice, BCG delivered *i.n.* was a potent inducer of both IFN-γ and IL-17 in the lungs, with IL-17 peaking earlier than IFN-γ. BCG *i.n.* followed by MVA85A *i.n.* was able to boost both IFN-γ and IL-17 in the lungs, with the peak of IL-17 occurring 1 week post-MVA85A and IFN-γ peaking a week later. Also consistent across both vaccine regimes (BCG and BCG – MVA85A) was the reduced level of IL-17 production in both spleen and lung LN. This is consistent with IL-17 being a mucosally-induced cytokine.

Cells producing both IFN-γ and IL-17 were also detected in lungs, and in the spleen and lung LN at lower levels, of animals vaccinated with either BCG or with BCG – MVA85A (both delivered *i.n.*). This subset of cells is almost certainly mucosally-induced since intradermal delivery of BCG followed by MVA85A does not induce double-positive cells at all. It should be noted that this is in contrast with observations in humans, where *i.d.* delivery of BCG – MVA85A induced only IFN-γ$^+$IL-17$^+$ cells and no CD4$^+$ T cells producing IL-17 alone. This could reflect intrinsic differences in requirements for T cell priming in mice and humans.

Comparing an intradermal regime with an intranasal regime further, the most striking difference is the lack of CD4$^+$ T cell response in the lungs following *i.d.* vaccination. Responses in the spleen and lung LN were lower following *i.n.* delivery compared to *i.d.* with respect to IFN-γ and similarly low with respect to IL-17. The impact of these differences on protection against TB disease will be investigated in later chapters.

In order to ensure that BCG – MVA85A vaccination was immunogenic in C57BL/6 animals as well as in Balb/c mice (discussed above), C57BL/6 mice were vaccinated *i.n.* with BCG – MVA85A. Cytokine production by $CD4^+$ T cells following vaccination was comparable to that in Balb/c mice. The key differences were that the peak IFN-γ response occurred 1 week post-vaccination in C57BL/6 mice in contrast to the 1-2 week peak observed in Balb/c mice.

Overall, however, the immunogenicity of the regime in both mouse strains is comparable, and the results indicate that knockout animals on a C57BL/6 background can be used with confidence as a test of the effect of genetic changes on vaccine immunogenicity and efficacy, with WT C57BL/6 animals as controls. It should be noted, however, that there is a slightly slower IL-17 response in C57BL/6 mice compared to Balb/c mice, which could have an effect on adjuvants targeting IL-17.

As expected, very low percentages of $CD8^+$ T cells were induced following either BCG alone or BCG – MVA85A vaccination. Interestingly, a small percentage of $CD8^+$ T cells producing IL-17 were observed early following BCG delivered *i.n.*, however these contracted rapidly and were not boosted further by MVA85A.

5 CHOLERA TOXIN TREATMENT

5.1 Introduction

In the previous chapter it was established that intranasal administration of both BCG and BCG – MVA85A was able to induce strong mucosal IFN-γ and IL-17 responses from $CD4^+$ T cells. Here the use of CT, known to induce IL-17, was explored as a potential adjuvant, and its effect on vaccine efficacy following *M.tb* challenge was investigated. Cholera toxin was administered either mixed with intranasal BCG or with MVA85A, which was delivered as a boost after an *i.n.* BCG prime. Since IL-17 has been implicated in vaccine-induced protection against TB disease, it was important to establish whether any increase in IL-17 production could translate to increased protection against *M.tb* challenge. Vaccine efficacy in mice can be evaluated using an aerosol challenge set up, which exposes the animals in a nose-only exposure unit to aerosolised *M.tb*. Animals are exposed to a standard dose of ~100 cfu *M.tb*, which after 4 weeks of infection in unvaccinated animals leads to a level of infection of $1x10^6$ – $1x10^7$ cfu in the lungs and usually $1x10^5$ – $1x10^6$ cfu in the spleen. BCG vaccination in Balb/c and C57BL/6 mice consistently gives an expected protection of 1 – 2 log cfu in the lungs. In the past, various routes of challenge have been used, including *i.v.*, *i.p, i.n.* and *s.c.,* however aerosol challenge is now widely used as it is thought to best represent the human route of exposure.

The role of IL-17 in both unvaccinated mice exposed to *M.tb* and in vaccine-induced protection was further investigated through the use of mice lacking the *IL17a* gene. In these experiments, mice were vaccinated with BCG *i.d.* or *i.n.* with or without CT.

5.2 The effect of cholera toxin administration with BCG ± MVA85A on immunogenicity

5.2.1 CT administered with BCG

Balb/c mice were vaccinated with BCG *i.n.*. In half the animals, CT (2μg/mouse) was co-administered with the BCG. Lungs, spleens and lung LN were taken 10 weeks post-vaccination and stimulated with PPD in the presence of Brefeldin A and GolgiStop before analysis of cytokine expression by ICS. As can be seen in figure 5.2.1A & B, production of IFN-γ by $CD4^+$ T cells was not affected by co-administration of CT with BCG. The percentages of cells producing IL-17 in both lungs and spleen (Fig 5.2.1C & D), however, were significantly increased when CT was administered along with BCG ($p = 0.0317$ and 0.0159 for lung and spleen respectively, $n = 5$). Interleukin 17 production in the lung LN was not affected. The percentages of $CD4^+$ T cells expressing both IFN-γ and IL-17 in the lungs, but not spleen or lung LN, were significantly increased following CT treatment ($p = 0.0079$, $n = 5$).

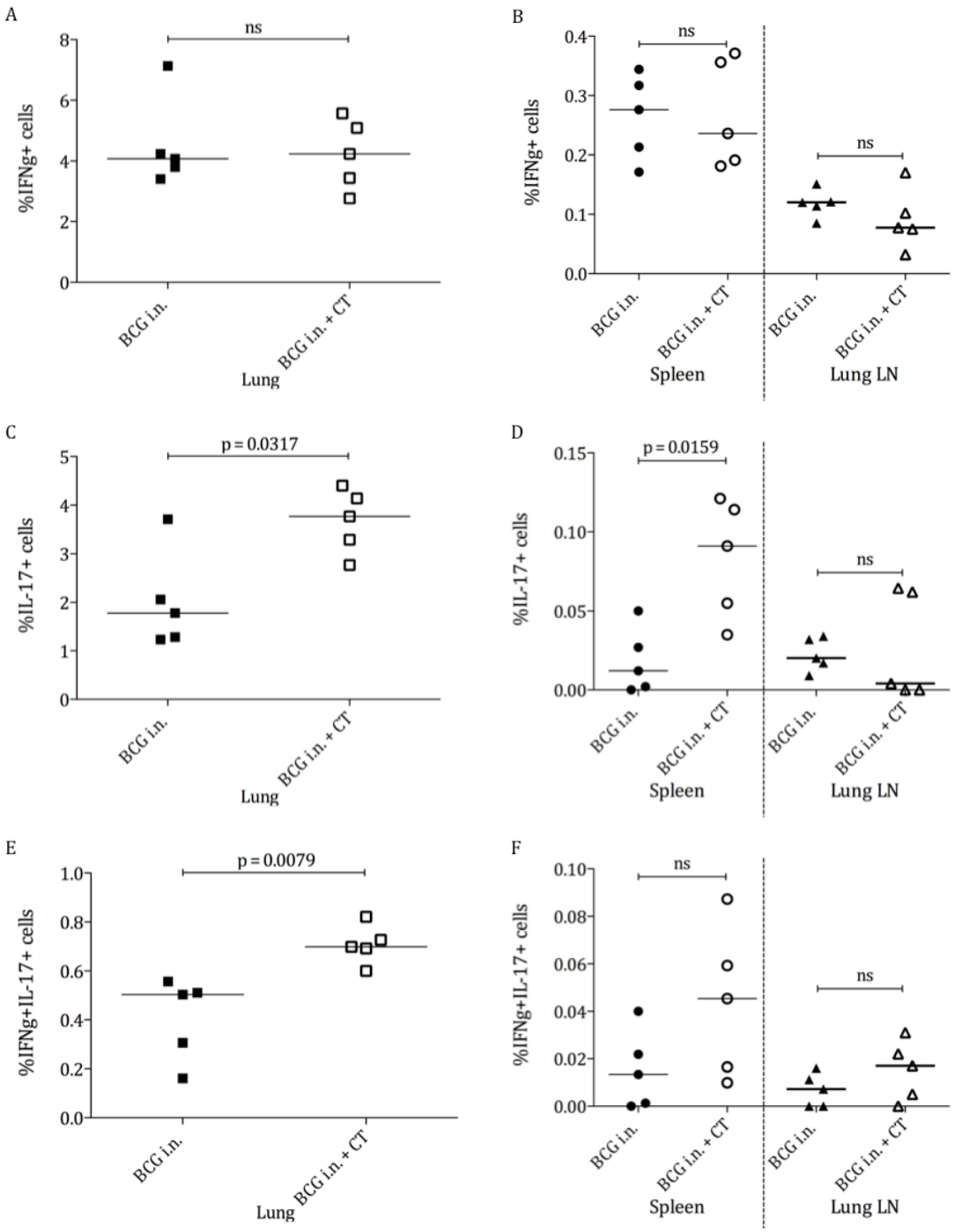
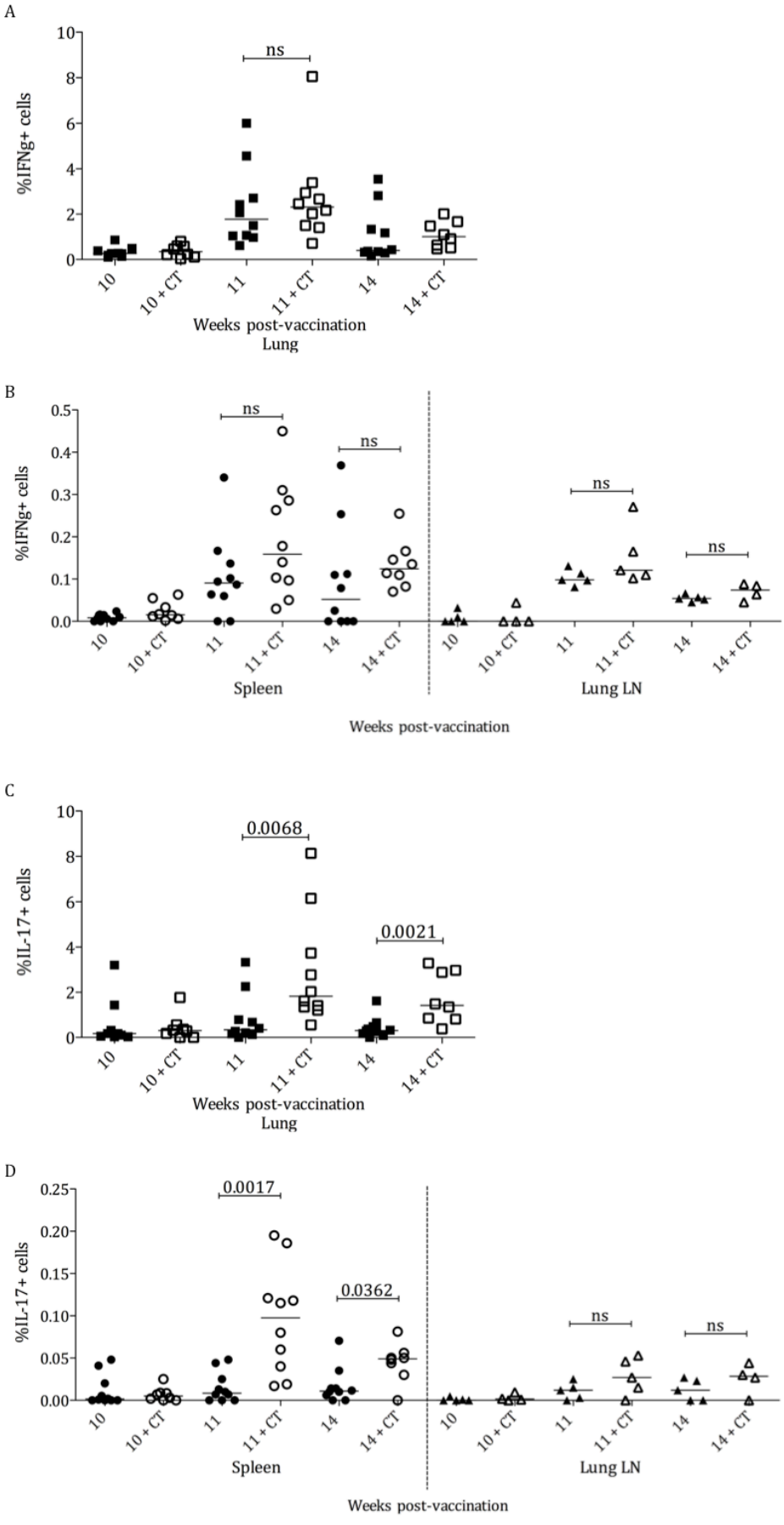


Figure 5.2.1 Effect of cholera toxin on BCG immunogenicity. Five mice received 4x10^5 cfu BCG *i.n.* and another 5 were given 4x10^5 cfu BCG + 2µg CT *i.n.* After 10 weeks, mice were culled and lungs, spleen and lung LN dissected and stimulated with PPD in the presence of Brefeldin A and GolgiStop. Percentages of CD4$^+$ T cells producing IFN-γ and IL-17 were calculated following ICS on lung cells (**A, C** & **E**), splenocytes and cells from lung LN (**B, D** & **F**). Mice receiving BCG only are plotted with closed symbols and those receiving CT have open symbols. Significance was calculated using the Mann Whitney test. For all groups n = 5.

5.2.2 CT with BCG followed by MVA85A

In the previous section (Section 5.2.1), it was established that IL-17 production by $CD4^+$ T cells following *i.n.* BCG vaccination could be enhanced using CT co-administered with BCG. Here, the aim was to investigate whether the increased IL-17 production observed following BCG + CT could be further boosted with MVA85A delivered *i.n.*

As was observed for BCG + CT alone, boosting further by MVA85A did not significantly change IFN-γ production by $CD4^+$ T cells in the lungs, spleen or lung LN (Fig 5.2.2A & B). Percentages of $CD4^+$ T cells producing IL-17, in contrast, were significantly higher in animals vaccinated with BCG + CT followed by MVA compared to those receiving BCG alone followed by MVA85A (Fig 5.2.2C & D; $p = 0.0068$ and 0.0021 at 11 and 14 weeks post-BCG respectively in lungs, and $p = 0.0017$ and 0.0362 in spleen). No difference was observed between the regimes in lung LN. For IFN-γ^+IL-17^+ cells, the difference between animals receiving CT and those not was observed at 1 week post-MVA85A only in the lungs and the spleen (Fig 5.2.2E & F; $p = 0.0068$ and 0.015 for lungs and spleen respectively). This difference was not detectable by 4 weeks post-MVA85A.


A
%IFNg+ cells
ns
10
10 + CT
11
11 + CT
14
14 + CT
Weeks post-vaccination
Lung
B
%IFNg+ cells
ns
ns
ns
ns
Spleen
Lung LN
Weeks post-vaccination
C
%IL-17+ cells
0.0068
0.0021
Weeks post-vaccination
Lung
D
%IL-17+ cells
0.0017
0.0362
ns
ns
Spleen
Lung LN
Weeks post-vaccination

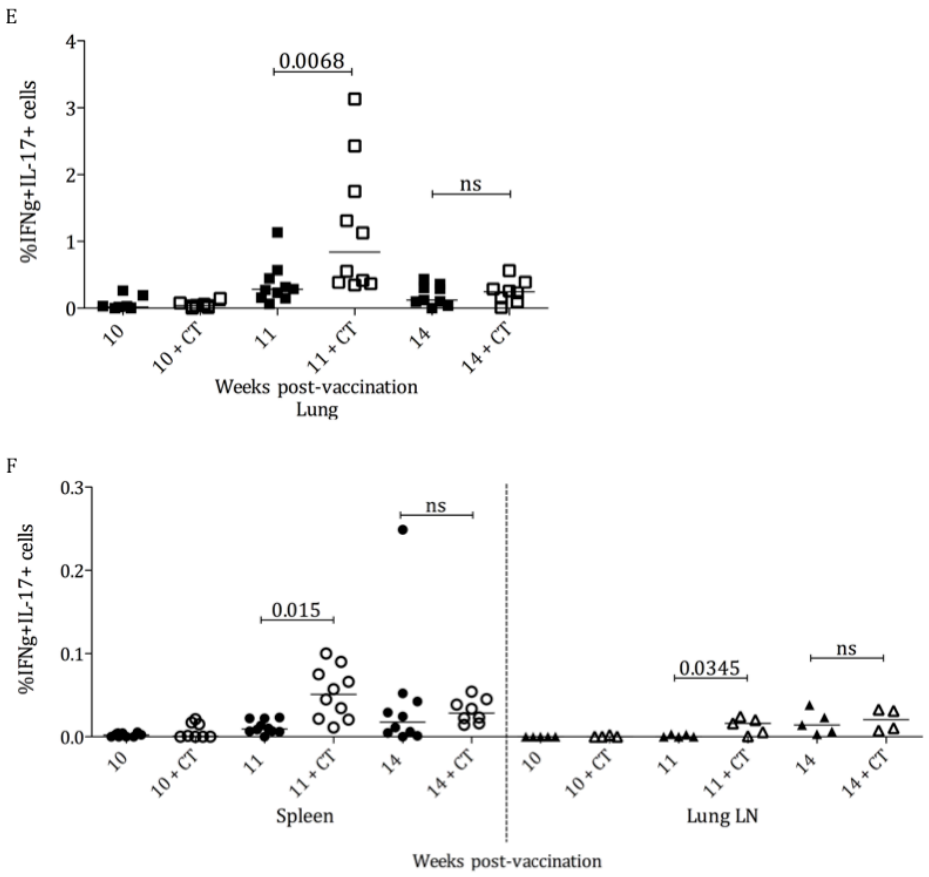
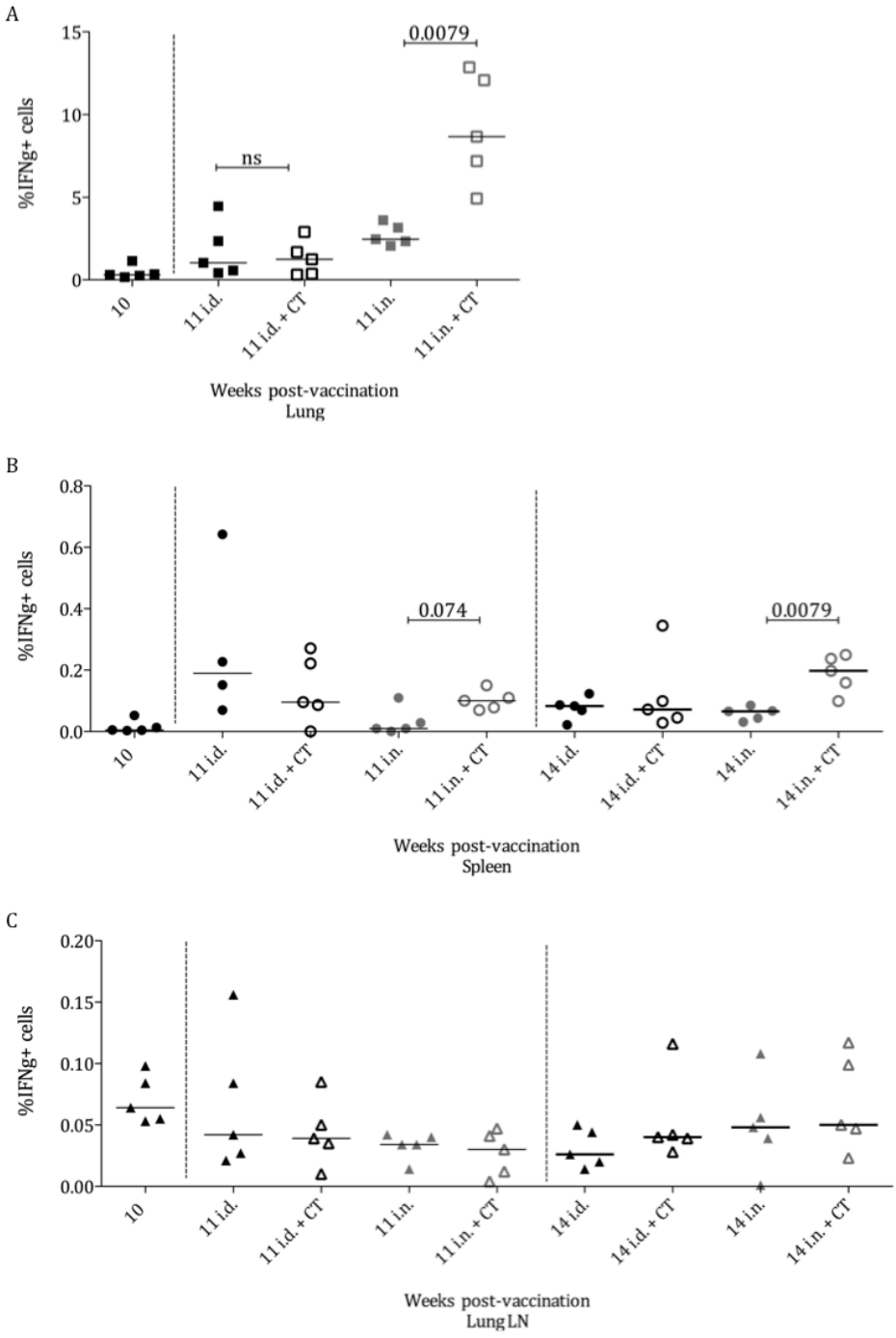


Figure 5.2.2 Immunogenicity of BCG + CT followed by MVA85A. Balb/c mice received BCG ± CT *i.n.* followed by MVA85A 10 weeks later. Lungs (**A, C** & **E**), spleen and lung LN (**B, D** & **F**) were taken at 10, 11 and 14 weeks post-BCG and cytokine-producing cells responding to an Antigen 85A peptide pool quantified using ICS. Responses from animals receiving BCG alone followed by MVA85A (closed symbols) were compared with those receiving BCG + CT followed by MVA85A (open symbols). Statistical analysis was performed using Prism and the Mann Whitney test. n = 10, 5 each from 2 experiments.

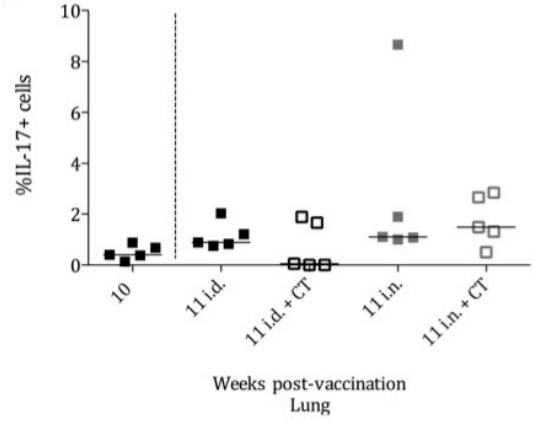
5.2.3 BCG followed by CT with MVA85A

It would be expected that CT co-administered with BCG would be most potent at inducing a 'boostable' population of $CD4^+$ T cells, however, delivery of the CT along with MVA85A following an intranasal BCG boost was also investigated. BCG was delivered *i.n.*, and 10 weeks later animals received MVA85A either *i.d.* or *i.n.* with or without CT. $CD4^+$ T cell responses to an Ag85A peptide pool were measured using ICS and compared between groups. In contrast to administering CT along with BCG, co-administration of the adjuvant with an intranasal MVA85A boost yielded an increase in the percentage of

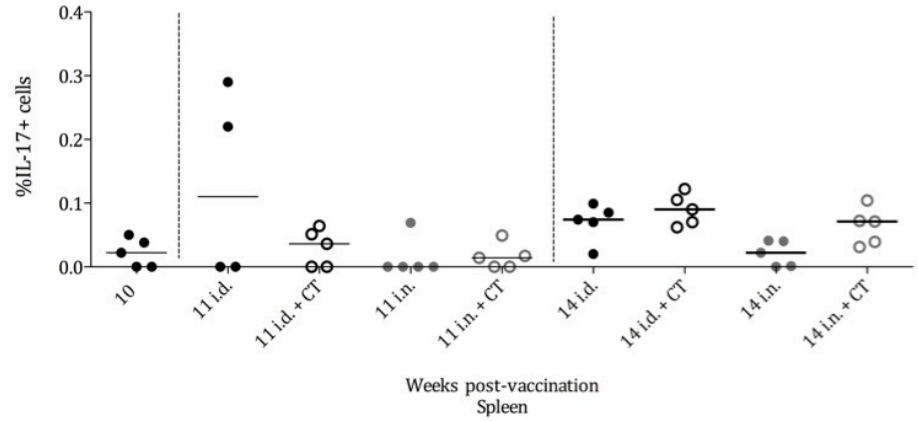
$CD4^+$ T cells producing IFN-γ in lungs 1 week post-MVA85A and in spleen 4 weeks post-MVA85A (Fig 5.2.3A & B; p = 0.0079 for both). There were no differences in cells producing IFN-γ in the lung LN or IL-17 in any organ (Fig 5.3C, D, E & F). There were no significant differences in percentages of IFN-γ^+IL-17^+ $CD4^+$ T cells in either lungs or lung LN (Fig 5.2.3G & I), however percentages of these cells were increased in the spleen following intranasal vaccination both 11 and 14 weeks post-BCG in animals receiving CT along with the MVA85A (Fig 5.2.3H; p = 0.0212 and 0.0097 respectively).


A
%IFNg+ cells
15
10
5
0
0.0079
ns
10
11 i.d.
11 i.d. + CT
11 i.n.
11 i.n. + CT
Weeks post-vaccination
Lung
B
%IFNg+ cells
0.8
0.6
0.4
0.2
0.0
0.074
0.0079
10
11 i.d.
11 i.d. + CT
11 i.n.
11 i.n. + CT
14 i.d.
14 i.d. + CT
14 i.n.
14 i.n. + CT
Weeks post-vaccination
Spleen
C
%IFNg+ cells
0.20
0.15
0.10
0.05
0.00
10
11 i.d.
11 i.d. + CT
11 i.n.
11 i.n. + CT
14 i.d.
14 i.d. + CT
14 i.n.
14 i.n. + CT
Weeks post-vaccination
Lung LN

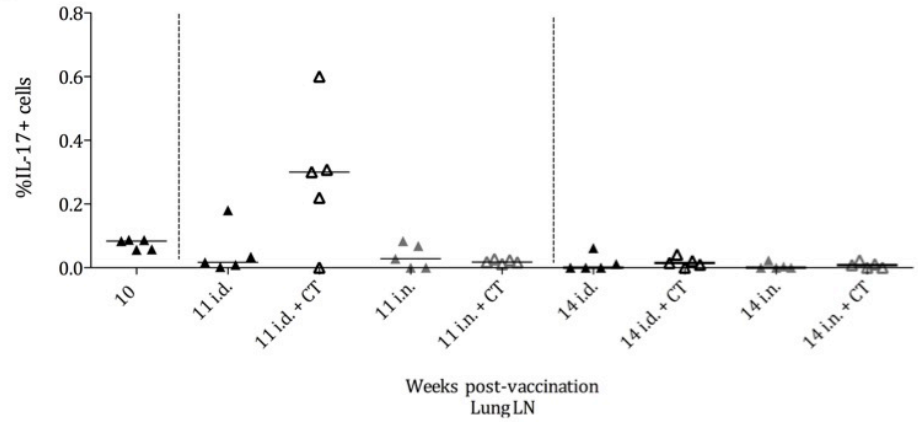
D


%IL-17+ cells
10
8
6
4
2
0
10
11 i.d.
11 i.d. + CT
11 i.n.
11 i.n. + CT
Weeks post-vaccination
Lung

E


%IL-17+ cells
0.4
0.3
0.2
0.1
0.0
10
11 i.d.
11 i.d. + CT
11 i.n.
11 i.n. + CT
14 i.d.
14 i.d. + CT
14 i.n.
14 i.n. + CT
Weeks post-vaccination
Spleen

F


%IL-17+ cells
0.8
0.6
0.4
0.2
0.0
10
11 i.d.
11 i.d. + CT
11 i.n.
11 i.n. + CT
14 i.d.
14 i.d. + CT
14 i.n.
14 i.n. + CT
Weeks post-vaccination
Lung LN

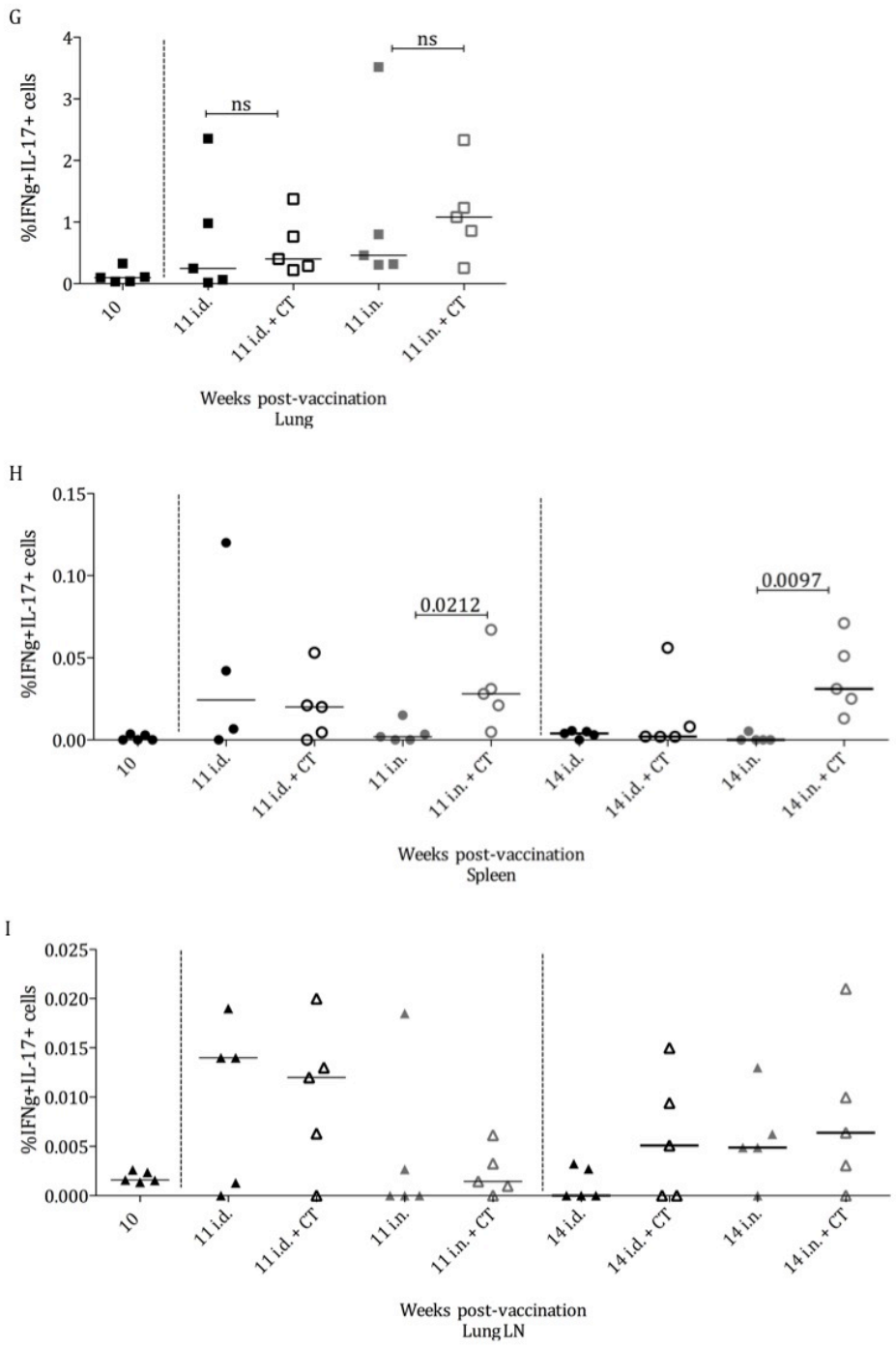


Figure 5.2.3 Administration of CT with MVA85A either *i.n.* or *i.d.* following an intranasal BCG prime. Balb/c animals received 4x10^5 cfu BCG *i.n.* followed 10 weeks later by MVA85A ± CT delivered either *i.n.* (grey symbols) or *i.d.* (black symbols). Cytokine expression by CD4$^+$ T cells was examined using ICS and CT-treated groups (open symbols) compared to groups receiving BCG + MVA85A only (closed symbols). IFN-γ-producing cells are shown in **A** – **C**, IL-17-producing cells in **D** – **F** and IFN-γ$^+$IL-17$^+$ cells in **G** – **I.** Statistical analysis was performed using Prism and the Mann Whitney test. n = 5.

5.3 The effect of cholera toxin administration with BCG on vaccine efficacy

Since the vaccine regimes in which CT was co-administered with intranasal BCG were those that yielded an increase in production of IL-17 from $CD4^+$ T cells, these were taken forward into *M.tb* challenge experiments in order to determine the effect of this on vaccine efficacy.

5.3.1 CT administered with BCG

In order to determine the vaccine efficacy of CT co-administered with intranasal BCG, Balb/c mice received either BCG or BCG + CT. Ten weeks later, animals were challenged with ~100 cfu *M.tb* via aerosol. Four weeks post-challenge, animals were culled and lungs and spleen taken and plated in order to determine bacterial load in each organ. Control groups included unvaccinated animals and animals receiving BCG *i.d.*, which is the route known to provide 1 – 2 log protection in an *M.tb* aerosol challenge.

Figure 5.3.1A shows the expected 1 – 2 log protection conferred by BCG in lungs (median = $1.37x10^7$ and $7.49x10^5$ cfu for naïve and BCG *i.d.* respectively, $p < 0.0001$).

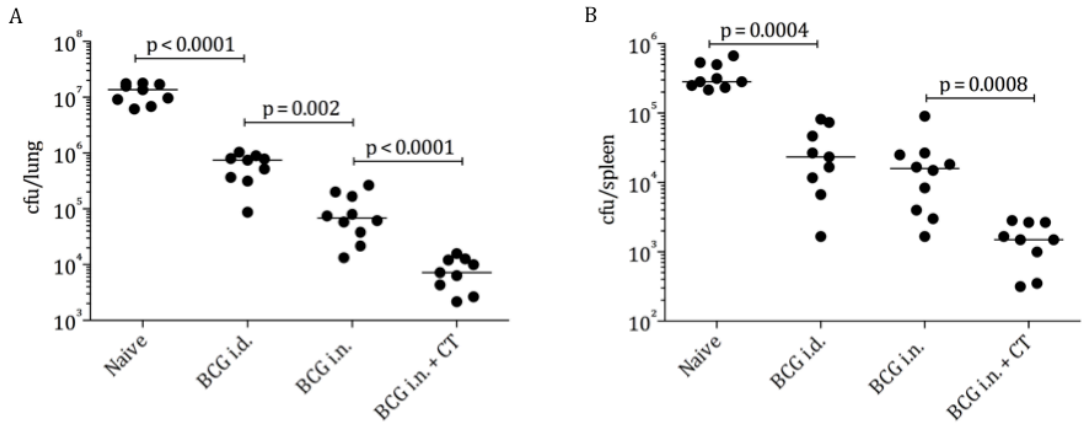


Figure 5.3.1 Vaccine efficacy of BCG *i.n.* + CT. Balb/c mice received $4x10^5$ cfu BCG *i.n.* either with or without CT. BCG control animals received $4x10^5$ cfu BCG *i.d.* Unvaccinated control animals were age-matched but received no intervention prior to challenge. Animals were divided into 9 animals/group. Animals were exposed to $5x10^6$ cfu/mL aerosolised *M.tb* for 10 min. Four weeks post-challenge, animals were culled and lungs and spleen taken and homogenised before plating in 1/10 serial dilutions in duplicate. Colonies on the plates were counted after 4 weeks and quantified as shown in **A** for lungs and **B** for spleens. Statistical analysis was performed using Prism and Mann Whitney tests after performing a Kruskall Wallis test comparing the vaccinated groups ($p < 0.0001$ and $p = 0.0005$ for lungs and spleen respectively).

Intranasal administration of the vaccine offers a further 0.6 log protection in lungs but not in spleen compared to BCG *i.d.* (median = $7.49x10^5$ and $6.825x10^4$ cfu for BCG *i.d.* and *i.n.* respectively, $p = 0.002$) as has previously been shown [216]. The addition of CT to the regime, however, further increased the vaccine efficacy by almost 1 log compared to BCG *i.n.* in both lungs and spleen (lungs: median = $6.825x10^4$ and $7.17x10^3$ cfu for BCG *i.n.* and BCG + CT respectively, $p < 0.0001$; for spleen: $1.585x10^4$ and $1.5x10^3$ cfu for BCG *i.n.* and BCG + CT respectively, $p = 0.0008$). These data suggest that co-administration of CT with BCG as a vaccine prior to *M.tb* challenge can significantly improve BCG vaccine efficacy in both spleen and lungs. It was shown previously in Section 5.2.1 that CT increases IL-17 but not IFN-γ production by $CD4^+$ T cells and while it is tempting to conclude that this increase is the cause of increased protection, further work will be required to confirm this hypothesis.

5.3.2 Cholera toxin with BCG followed by MVA85A

In Section 5.3.1, it was demonstrated that co-administration of CT with BCG improved vaccine efficacy over BCG alone, either *i.n.* or *i.d*. Pre-challenge immunology discussed in Section 5.2.1 showed increased IL-17 production by $CD4^+$ T cells in the lungs and spleen compared to animals receiving BCG alone. In Section 5.2.2, it was observed that the increased IL-17 induced following BCG + CT could be further boosted by MVA85A delivered *i.n.* 10 weeks post-BCG. Animals receiving this vaccine regime were therefore challenged with aerosolised *M.tb* 4 weeks post-MVA85A in order to investigate whether an MVA85A boost could confer improved vaccine efficacy. The following groups were challenged and 4 weeks later lungs and spleen were taken for quantitation of bacterial burden: unvaccinated control, BCG *i.d.*, BCG *i.n.*, BCG + MVA85A all *i.n.*, and BCG + CT followed by MVA85A all *i.n.*

As shown in figure 5.3.2A & B, BCG *i.d.* conferred the expected 1 – 2 log protection against TB disease in both lungs and spleen (median = 1.0565×10^6 and 7.83×10^5 cfu for naïve and BCG *i.d.* respectively, p = 0.002). BCG delivered *i.n.* conferred slightly but not statistically significantly better protection in lungs compared to BCG *i.d.* The same was observed for animals vaccinated with BCG followed by MVA85A.

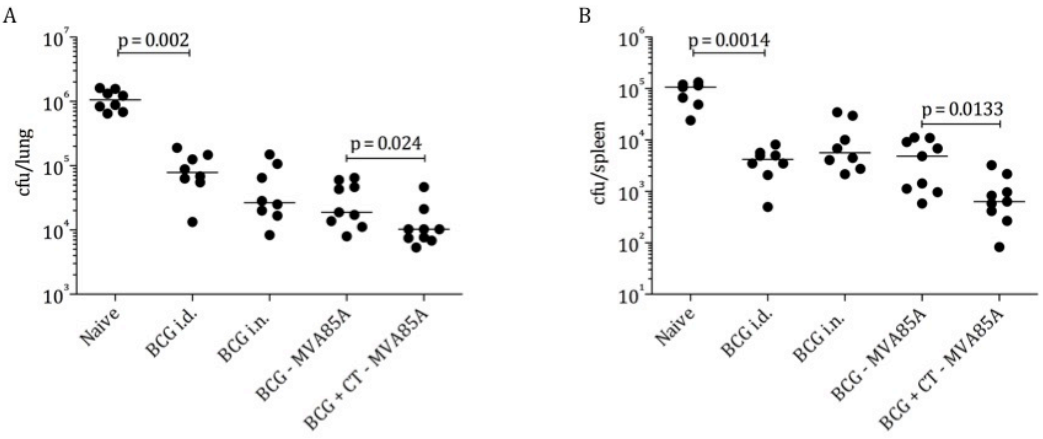


Figure 5.3.2 Effect of CT on vaccine efficacy in a BCG – MVA85A vaccine regime. Balb/c mice were vaccinated with either 4×10^5 cfu BCG or BCG + 2µg CT delivered *i.n.* Ten weeks later, animals received 1×10^6 pfu MVA85A *i.n.* Control groups included unvaccinated animals, animals receiving BCG *i.d.* A group receiving BCG *i.n.* was included in order to compare BCG + MVA85A all *i.n.* to BCG *i.n.* Animals were exposed to 5×10^6 cfu/mL *M.tb* via aerosol 4 weeks post-MVA85A to give an infection of ~100 cfu/mouse. Four weeks post-challenge, animals were culled and lungs and spleen collected and plated for cfu quantification. Colony counts were plotted as shown above for lungs (**A**) and spleen (**B**). Statistical analysis was performed using Prism. Mann Whitney tests were used following a Kruskall Wallis test comparing the vaccinated groups (p = 0.0014 and 0.0037 for lungs and spleen respectively).

When CT was administered along with BCG prior to MVA85A, however, there were significantly lower colony counts in both lungs and spleen compared to BCG alone followed by MVA85A (for lungs: median = 1.88×10^4 and 1.03×10^4 cfu for untreated and CT-treated respectively, p = 0.0024; for spleen: median = 4.83×10^3 and 6.33×10^2 cfu for untreated and CT-treated respectively, p = 0.0133). This is consistent with the results presented in Section 5.3.1 showing increased protection against TB disease in animals vaccinated *i.n.* with CT and BCG.

5.4 The effect of cholera toxin administration with BCG on lung pathology following challenge

It has been shown in previous sections that CT administration along with BCG can improve protection against TB disease, both when MVA85A is used a boost to a BCG prime, or when BCG is given alone. Pre-challenge immunological studies showed that IL-17 was increased following CT treatment and may play a role in the increased protection. Interleukin 17 is a highly inflammatory cytokine implicated as a negative factor in many inflammatory diseases such as multiple sclerosis, psoriasis and rheumatoid arthritis [217-219]. Apart from transient illness immediately after vaccination, no adverse effects were observed in animals receiving CT, however it was important to examine the lungs of the challenged animals in order to investigate the effects of the CT-induced IL-17 on lung pathology. One lung lobe was dissected from four animals in each group at the time of challenge take down and H&E staining was used to examine the inflammatory state of the lung. Section images were cropped using Adobe Photoshop so that no white space was visible surrounding the section (~30% of the image) as shown in figure 5.4.1A.

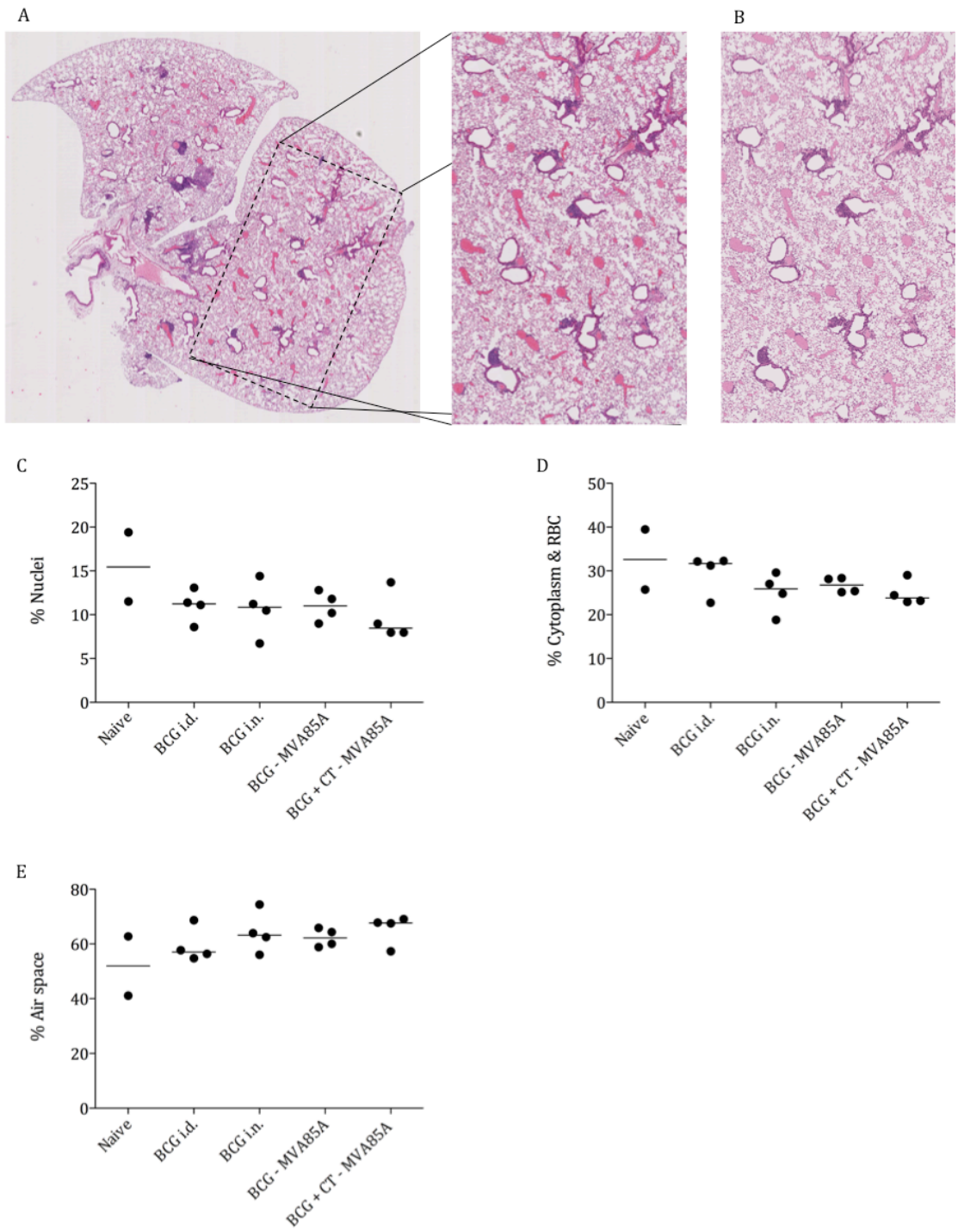


Figure 5.4.1 Histological analysis of *M.tb*-exposed lungs. One lobe from each mouse was inflated with 10% NBF and dissected. Lungs were embedded in paraffin, sectioned and mounted onto slides. Slides were stained with haematoxylin and eosin. Images were cropped so that no external white space was visible (**A**). Analysis was performed using a k-means clustering algorithm in MATLAB (**B**). Percentages of the image represented by one of three colours (purple, red or white) was calculated and plotted (**C – E**).

Cropped sections were analysed using k-means clustering in MATLAB in order to determine the percentage of the section represented by each of the following colours: purple (nuclei), pink (red blood cells and cytoplasm) and white (space for gas exchange). A sample of the resulting image in comparison to the original is shown in figure 5.4.1B. Figure 5.4.1C-E shows the percentages of each 'colour' for each of the groups. Although numbers were too low to perform statistical analysis, there is a trend towards a decrease in cell infiltrate (as measured by % nuclei, and % red blood cells and cytoplasm) with an increase in lung cfu (Fig 5.4.1C & D), and conversely an increase in airspace along with a decrease in colony count. None of these yielded a significant correlation when tested (data not shown).

One can conclude from these data that no adverse effect was observed on lung pathology following increased IL-17 production induced by CT treatment. This suggests that an adjuvant capable of inducing high levels of IL-17 in the lungs could safely be used should IL-17 prove to be protective following *M.tb* infection.

5.5 The effect of blocking IL-17 following challenge of BCG + CT – MVA85A-vaccinated animals

In the previous sections in this chapter, the effect of the administration of CT along with vaccination was studied in relation to induction of IL-17 production by $CD4^+$ T cells, and in relation to protection against *M.tb* challenge. It was observed that IL-17 at mucosal sites following *i.n.* vaccination was increased following CT co-administration with BCG. This IL-17 could be further boosted by MVA85A administered *i.n.* 10 weeks after BCG. These animals also performed significantly better in an *M.tb* aerosol challenge compared to animals receiving either BCG alone or BCG – MVA85A. Here we attempted to block the improved protection observed using an anti-IL-17A blocking antibody, administered *i.p.* every 3-4 days post-challenge for 4 weeks. This regime for antibody administration was based on previously published data ([220] and Dr. Shabaana Khader, personal communication). A series of experiments were performed to ascertain

the blocking capacity of the antibody, and are outlined in the Appendix in figure 8.3.1 on page f.

The following groups received the blocking antibody: BCG – MVA85A, and BCG + CT – MVA85A, all administered *i.n.* A group vaccinated with BCG – MVA85A received an IgG2A isotype control antibody in order to discount any non-specific effects of the antibody.

Pre-challenge immunology was performed 10 weeks post-BCG and then 1 week and 4 weeks post-MVA85A on lungs, spleen and lung LN. Results from these experiments confirmed results from the initial experiment with CT, and data were pooled with the initial experiment and shown in Fig 5.2.2 (Section 5.2.2).

Following challenge, the same 1 – 2 log protection was conferred by BCG *i.d.* (mean (log_{10}) = 6.477 and 4.958 cfu for naïve and BCG *i.d.* respectively, $p < 0.0001$) as was seen in previous experiments (Fig 5.5.1A & B).

As was observed in the first experiment, administration of CT along with the BCG prime improved protection against both lung and spleen challenge significantly (Fig 5.5.1A & B; for lungs: mean (log_{10}) 4.569 and 4.079 cfu for untreated and CT-treated respectively, $p = 0.0002$; for spleen: 3.676 and 3.077 cfu for untreated and CT-treated respectively, $p = 0.0016$). Administration of the isotype control antibody did not significantly change the lung or spleen cfu, indicating that any difference seen in the antibody-treated groups can be attributed to the antibody (for lungs: mean (log_{10}) = 4.569 and 4.738 cfu for no antibody and isotype respectively; for spleen: 3.676 and 3.820 cfu for no antibody and isotype respectively). Comparing the BCG – MVA85A group receiving antibody and the group that received the isotype control, the lung cfu is significantly higher in the anti-IL-17-treated group (mean (log_{10}) = 4.738 and 5.142 cfu for isotype and anti-IL-17 respectively, $p = 0.0147$), however this difference was not observed in spleen. In the lungs, there was significantly higher in animals vaccinated with BCG + CT – MVA85A and receiving the anti-IL-17 antibody (mean (log_{10}) = 4.079 and 4.418, $p = 0.00792$),

suggesting that the blocking antibody is having a marginal effect in reducing the vaccine efficacy.

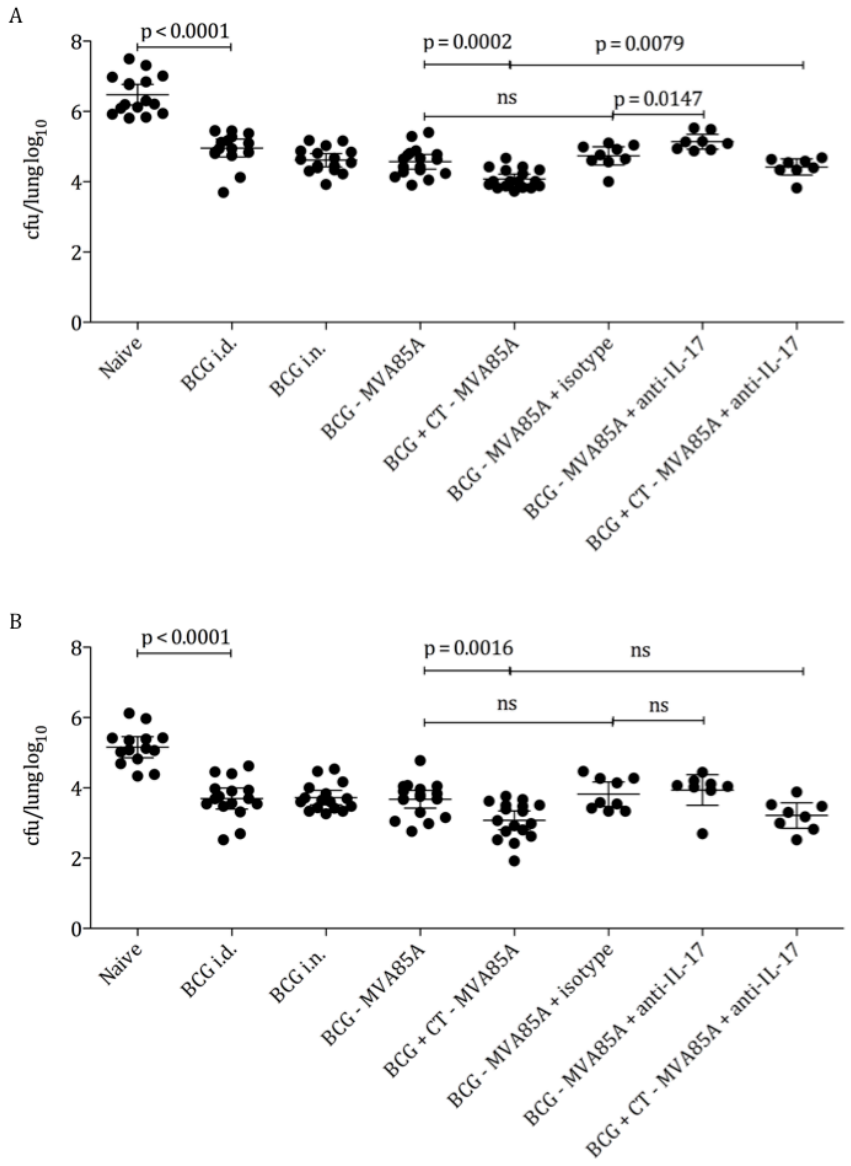


Figure 5.5.1 Effect of blocking IL-17 on vaccine efficacy following *M.tb* challenge. Balb/c mice were vaccinated and challenged as described previously in figure 5.3.2. Groups vaccinated with BCG – MVA85A, and BCG + CT – MVA85A received an anti-IL-17 blocking antibody (MAB421 from R&D Systems) administered *i.p.* every 3-4 days post-challenge. One group vaccinated with BCG – MVA85A received an IgG2a isotype control antibody (MAB006 from R&D Systems) on the same regime. Mice were culled 4 weeks post-challenge and spleens and lungs taken for cfu determination. Plates were counted 4 weeks later and cfu/lung or spleen determined and plotted as shown above. Data was logged and checked for Gaussian distribution. Statistical analysis was performed using t tests in Prism after performing a one way ANOVA on the vaccinated groups (n = 8-16).

In the spleens, the anti-IL-17 antibody appears to have no effect, either in the group receiving BCG – MVA85A or the group that received CT along with the BCG. This could reflect a high challenge dose that meant sensitivity of the vaccine in the spleen was lost. Alternatively, it could be that the improved protection observed in the spleen following CT treatment is independent of a mechanism involving IL-17.

5.6 The effect of CT administration with BCG *i.d.* on *M.tb* challenge outcome

It has been shown in Section 5.3 that BCG + CT *i.n.* or BCG + CT – MVA85A *i.n.* can reduce bacterial load in the lungs of *M.tb*-challenged mice. From pre-challenge immunogenicity studies, it is clear that CT enhances production of IL-17 by $CD4^+$ T cells, and it is likely that this enhanced IL-17 production contributes to the improved protection. These experiments were all performed following mucosal administration of the vaccine and adjuvant, so here I investigated the effect of parenteral (*i.d.*) administration of BCG + CT on vaccine efficacy. C57BL/6 mice were vaccinated *i.d.* with BCG ± CT. Due to time constraints, mice were challenged 6 weeks later, and lung cfu determined 4 weeks post-challenge. Pre-challenge immunogenicity data for this experiment is not yet available, however as shown in figure 5.6.1A, results from the *M.tb* challenge confirmed that even challenging 6 weeks post-BCG conferred a significant 0.8log protection (Naïve median = $1.65x10^6$, BCG *i.d.* median = $1.82x10^5$ cfu/lung, p = 0.0009). As was previously observed, delivery of BCG *i.n.* improved protection in the lungs compared to BCG *i.d.* (BCG *i.d.* median = $1.82x10^5$, BCG *i.n.* median = $5.92x10^4$, p = 0.0019). Furthermore, these results confirmed the improved protection offered by administration of CT together with BCG *i.n.* (BCG *i.n.* median = $5.92x10^4$, BCG *i.n.* + CT median = $3.03x10^4$ cfu/lung, p = 0.0156). Delivery of CT with BCG delivered *i.d.*, however, did not improve protection offered by BCG *i.d.* alone (BCG *i.d.* median = $1.82x10^5$, BCG *i.d.* + CT median = $1.79x10^5$, p = 0.9078), suggesting that CT must be delivered mucosally for a protective effect to be observed.

Similar results were observed in the spleen (Fig 5.6.1B), with no effect of CT on BCG delivered *i.d.* (spleen cfu median = 7.35×10^3 and $1.33x10^4$ for BCG *i.d.* and BCG *i.d.* + CT,

respectively). In contrast to observations in previous experiments, there was no significant difference in spleen cfu between mice vaccinated with BCG *i.n.* and BCG *i.n.* + CT (BCG *i.n.* median = $6.60x10^3$, BCG *i.n.* + CT median = $3.22x10^3$ cfu/spleen, p = 0.083). This could be due to the shortened time between BCG vaccination and challenge in this experiment compared to previous experiments.

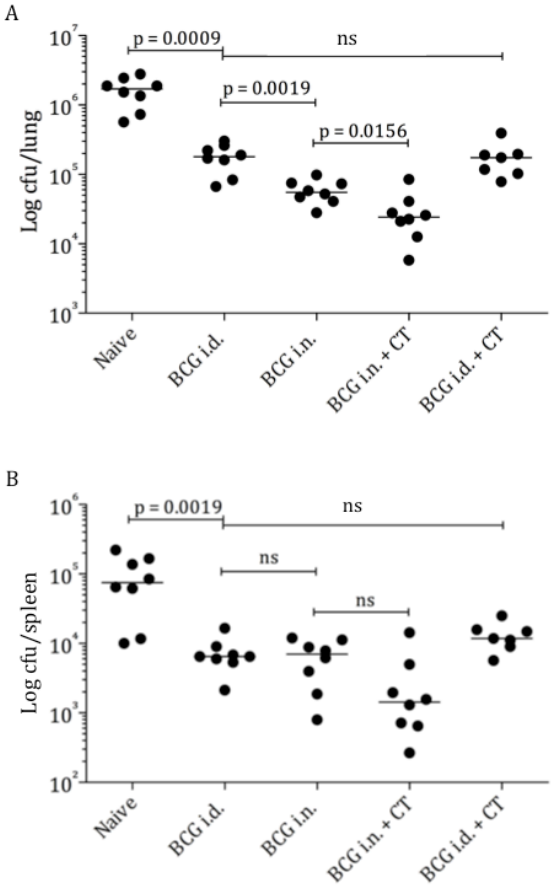


Figure 5.6.1 Effect of BCG *i.d.* + CT on *M.tb* challenge outcome. C57BL/6 mice were vaccinated with $4x10^5$ cfu BCG ± 2µg CT *i.d.* or *i.n.* Six weeks post-vaccination, animals were challenged with ~100 cfu *M.tb* via aerosol. Lungs (**A**) and spleens (**B**) were taken 4 weeks post-challenge and cfu quantified. n = 7 – 8 animals/group. A Kruskall-Wallis test was performed to account for multiple comparisons; p < 0.0001.

Pre-challenge immunology will provide insight into the differences in cytokines induced by this regime compared to BCG *i.n.* ± CT.

5.7 The effect of cholera toxin administration with BCG in animals lacking IL-17A

It has already been established that vaccination of IL-23p19$^{-/-}$ mice with BCG offers less protection than WT mice [185], whilst there is no difference in the bacterial load in the naïve animals. Since BCG + CT vaccination induced an increase in production of IL-17 and conferred improved protection against *M.tb* challenge, which could be partially reversed by IL-17 blocking, I investigated the direct contribution of IL-17 to vaccine-induced protection using IL-17$^{-/-}$ mice. These animals and their WT counterparts were vaccinated with BCG ± CT *i.n.* A group of IL-17$^{-/-}$ animals was also vaccinated with BCG *i.d.* in order to determine if mucosal delivery of BCG in IL-17$^{-/-}$ could improve on parenteral vaccination, as is observed in WT animals. Due to restrictions in numbers, there were not enough animals to perform pre-challenge immunogenicity. Results showed that IL-17$^{-/-}$ animals had significantly higher lung cfu than their WT controls (Fig 5.7.1A; WT = $1.65x10^6$, KO = $2.6x10^7$ cfu/lung, p = 0.0168), however the bacterial loads in the spleens were no different (Fig 5.7.1B; medians for WT = $9.49x10^4$, KO = $1.16x10^5$).

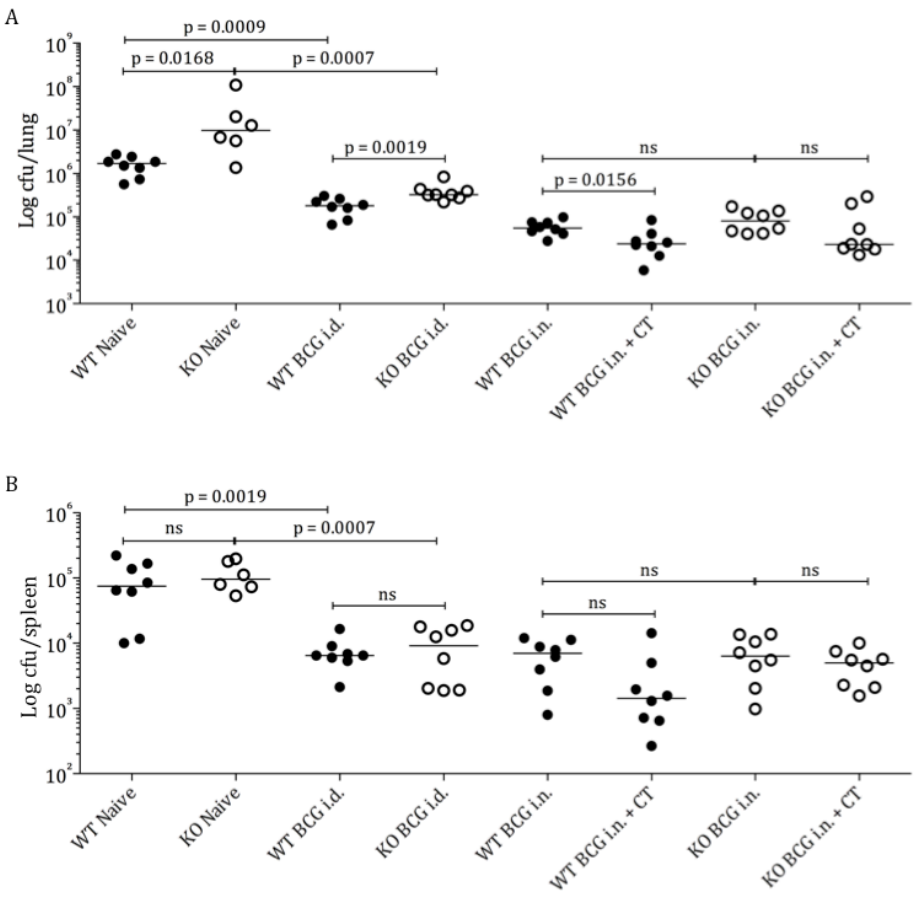


Figure 5.7.1 Effect of BCG ± CT in IL-17$^{-/-}$ mice following *M.tb* challenge. C57BL/6 mice or IL-17$^{-/-}$ mice on a C57BL/6 background were vaccinated with BCG *i.d.* or *i.n.* BCG *i.n.* was delivered ± CT. Six weeks post- vaccination, animals were challenged with ~100 cfu *M.tb* via aerosol and 4 weeks post-challenge were sacrificed and lungs and spleen taken for quantitation of bacterial load as shown for lungs (**A**) and spleens (**B**). WT animals are represented by closed circles and KO animals by open circles. n = 6 – 8 animals /group. A Kruskall Wallis test was performed on all groups, p < 0.0001.

This trend was also observed following vaccination with BCG *i.d.*, with WT mice having significantly lower lung cfu than IL-17$^{-/-}$ animals, but similar spleen cfu (medians for WT lung BCG *i.d.* = 1.82x10^5, KO lung BCG *i.d.* = 3.9x10^5 cfu/lung, p = 0.0019; medians for WT spleen BCG *i.d.* = 7.35x10^3, KO spleen BCG *i.d.* = 9.56x10^3 cfu/spleen), however BCG vaccination still conferred protection in KO animals compared to WT animals (p = 0.0009 and 0.0007 for WT and KO respectively). This difference between WT and KO animals was not observed following intransal vaccination, however, suggesting that the mucosal route of delivery is effective even in the absence of IL-17 (median lung cfu =

$5.92x10^4$ and $9.05x10^4$ for BCG *i.n.* in WT and KO, respectively; median spleen cfu = $6.60x10^3$, $7.24x10^3$ for WT and KO BCG *i.n.*, respectively). Interestingly, however, the improved protection conferred by BCG *i.n.* + CT in WT animals (discussed in Section 5.6) was not observed in KO animals (median lung cfu = $9.05x10^4$ and $8.07x10^4$ for BCG *i.n.* and BCG + CT *i.n.* respectively), indicating that IL-17 may play a role in the improved protection conferred by CT.

5.8 Discussion

Experiments described in this chapter aimed to explore the use of CT as an adjuvant in both BCG and BCG – MVA85A vaccine regimes with the aim of boosting levels of IL-17 produced. Vaccine-induced immunogenicity showed that CT, when administered together with the BCG prime, was able to induce high levels of IL-17 both post-BCG and post-MVA85A in lungs and spleen when the vaccines were delivered *i.n.* When CT was administered with the MVA85A boost following an intranasal BCG prime, however, IFN-γ but not IL-17 was boosted. This suggests that, in the case of a mucosal adjuvant such as CT, administration is important at the time of prime in order to induce an increased pool of cells producing the cytokine of interest that can later be boosted. Interestingly, no increase in IL-17 was seen in the lung LN with any of the vaccine regimes.

When Balb/c mice were vaccinated with BCG ± CT, either alone or followed by an MVA85A boost, those animals receiving CT had lower lung and spleen cfu compared to the animals receiving non-adjuvanted BCG. The effect in the lungs could be partially blocked by administration of an anti-IL-17 antibody, supporting the already-published theory of a role for IL-17 in vaccine-mediated protection against TB disease. Although not investigated here, other cytokines involved in the IL-17 pathway, such as IL-23, IL-21 and IL-22 are likely also upregulated by CT treatment and it is probable that these also play a role in protection following *M.tb* infection. Further work should define comprehensively the cytokine profile induced by CT.

Interestingly, in contrast to mucosal vaccination, when CT was administered along with a non-mucosal vaccine (BCG *i.d.*), no adjuvanting effect compared to BCG *i.d.* alone was observed following *M.tb* challenge. Unfortunately, no pre-challenge immunology data is available at this stage, however one could speculate that there are only low levels of cytokine production in the lungs, and that IL-17 is not upregulated in the spleens.

It should be noted that these latter experiments were performed in C57BL/6 mice, whereas the former used Balb/c mice. As observed in the immunogenicity studies described in Chapter 4, C57BL/6 animals have a slightly slower IL-17 kinetic, which could affect the impact of CT administration on the immunogenicity of the vaccine. Furthermore, in the experiments performed in C57BL/6 mice, the *M.tb* challenge was performed 6 weeks post-vaccination, in contrast to 10 weeks post-vaccination, which could also impact on the development of a memory population prior to challenge.

In experiments using mice lacking IL-17, both unvaccinated IL-17$^{-/-}$ mice and those vaccinated with BCG *i.d.* had significantly higher lung cfu compared to the WT controls, suggesting IL-17 plays some role in protection following *M.tb* challenge. In contrast to these findings, however, vaccination of IL-17$^{-/-}$ mice with BCG *i.n.* offered the same level of protection as WT controls, suggesting that IL-17 alone is not instrumental in the improved protection conferred by mucosal over parenteral vaccination.

When these same animals were vaccinated with BCG + CT *i.n.* and challenged with *M.tb*, however, CT had no effect on challenge outcome, in contrast to the effect observed in WT animals. Therefore, although IL-17 may be redundant in protection offered following mucosal vaccination alone, it could have a more central role in CT-induced protection.

The action of CT on cell types other than CD4^{+} T cells should also be investigated. For example, γδ T cells are known to be potent producers of both IL-17 and IL-22 and have also been implicated in mediating protection against TB disease, providing a link between the innate and the adaptive response. Experiments have shown, however, that

γδ T cells are more important in *M.tb* infection of unvaccinated animals, and that IL-17-producing $CD4^+$ T cells are more important in vaccine-induced protection.

Although CT is not an adjuvant suitable for use in humans due to its strong inflammatory effects and side effects, including diarrhoea and possible neurological symptoms [208], its use in animal models is a valuable tool for studying a) the outcomes of such a potent adjuvant, and b) mechanisms that could be targeted to achieve a similar results.

I have shown here that CT given at the time of a BCG prime is an adjuvant capable of improving vaccine-induced protection against murine *M.tb* challenge. Since CT acts through the cAMP pathway, this implicates the cAMP pathway as a potential target for adjuvants designed to be given with BCG either as a vaccine on its own or as a prime for a boosting vaccine such as MVA85A. Alternatively, pathways downstream of simply increasing intracellular cAMP concentrations could be targeted, however since cAMP acts relatively high up the cascade, it is difficult to know exactly which elements to target and furthermore, there maybe several factors that are involved in protection against TB disease, so targeting just one may not be as effective as targeting cAMP itself.

Factors that may increase cAMP levels include molecules that bind GPCR, such as PGE_2 or extracellular ATP, thus increasing activation of the pathway externally. There is also potential for the non-toxic B subunit of CT to be used as an adjuvant, however there is conflicting data regarding its ability to induce Th17 cells [205] [207]. This is worth exploring, however, as it could be that the antigen for which CT is being used as an adjuvant influences the mechanism through which it acts.

It has already been shown that IL-17 production by PBMC from MVA85A-vaccinated volunteers can be enhanced when the PBMC are treated with extracellular ATP. The mechanism proposed in this case was activation of the NALP3 inflammasome through binding to the P2X7 receptor, however another possible mechanism is the binding of extracellular ATP to the P2Y2 receptor, a GPCR. This leads to activation of the cAMP

pathway as described in Yu *et al.* [221]. It is possible that both pathways are involved as there is some evidence that the two pathways can be linked by PKA-mediated activation of caspase-1, the enzyme in the NALP3 inflammasome required for cleaving pro-IL-1 to IL-1β, which in turn is a cytokine implicated in the induction of Th17 cells [222]. Given these two potential interactions of ATP and IL-17 as well as the existence of non-hydrolysable ATP analogues, ATP is a strong candidate for further investigation as an adjuvant for TB vaccines.

6 VACCINATION AND CHALLENGE OF $CD39^{-/-}$ ANIMALS

6.1 Introduction

In Chapter 3, I demonstrated that MVA85A administered to human volunteers could induce IL-17 production by $CD4^+$ T cells in PBMC. The production of IL-17 was inversely related to the level of ATP hydrolysis by these cells. It was hypothesised that this hydrolysis may be mediated by the ectonucleosidase CD39 expressed on the cell surface of lymphocytes. One way to examine this system further and determine the relevance to protection against TB disease would be to explore it in the murine *M.tb* challenge model. In order to do this, I set up a collaboration with Dr Simon Robson at the Beth Israel Deaconess Medical Centre at Harvard University to obtain $CD39^{-/-}$ animals. The hypothesis was that vaccinated animals lacking CD39 would perform better following *M.tb* challenge due to a more inflammatory environment. Since ATP triggers the IL-17 pathway, it wasn't expected that naïve animals would control *M.tb* infection better than their WT counterparts, since IL-17 has been shown to be important only in vaccine-induced protection against TB disease, not during exposure of unvaccinated animals to *M.tb* infection [128]. The animals were vaccinated with BCG *i.n.* or BCG – MVA85A, all *i.n.* Appropriate C57BL/6 WT controls were included. Lungs, spleen and lung LN were taken at 10, 11 (1 week post-MVA85A) and 14 weeks post-BCG and remaining animals were challenged at 14 weeks. Lungs and spleen were taken for cfu quantification 4 weeks post-challenge and a sample of the lung homogenate was stored in RLT buffer for mRNA extraction and quantification of gene expression by qPCR.

6.2 Immunogenicity of BCG – MVA85A in CD39$^{-/-}$ mice

Due to technical difficulties, results are not available for the spleens at 11 weeks, and double positive cytokine expression could not be quantified at any timepoint.

Since the CD39$^{-/-}$ animals should not be expressing CD39, regulatory T cells expressing CD25 and CD39 were stained for in both WT and KO animals. As expected, there were no CD39^{+} cells in the KO animals (Fig 6.2.1A).

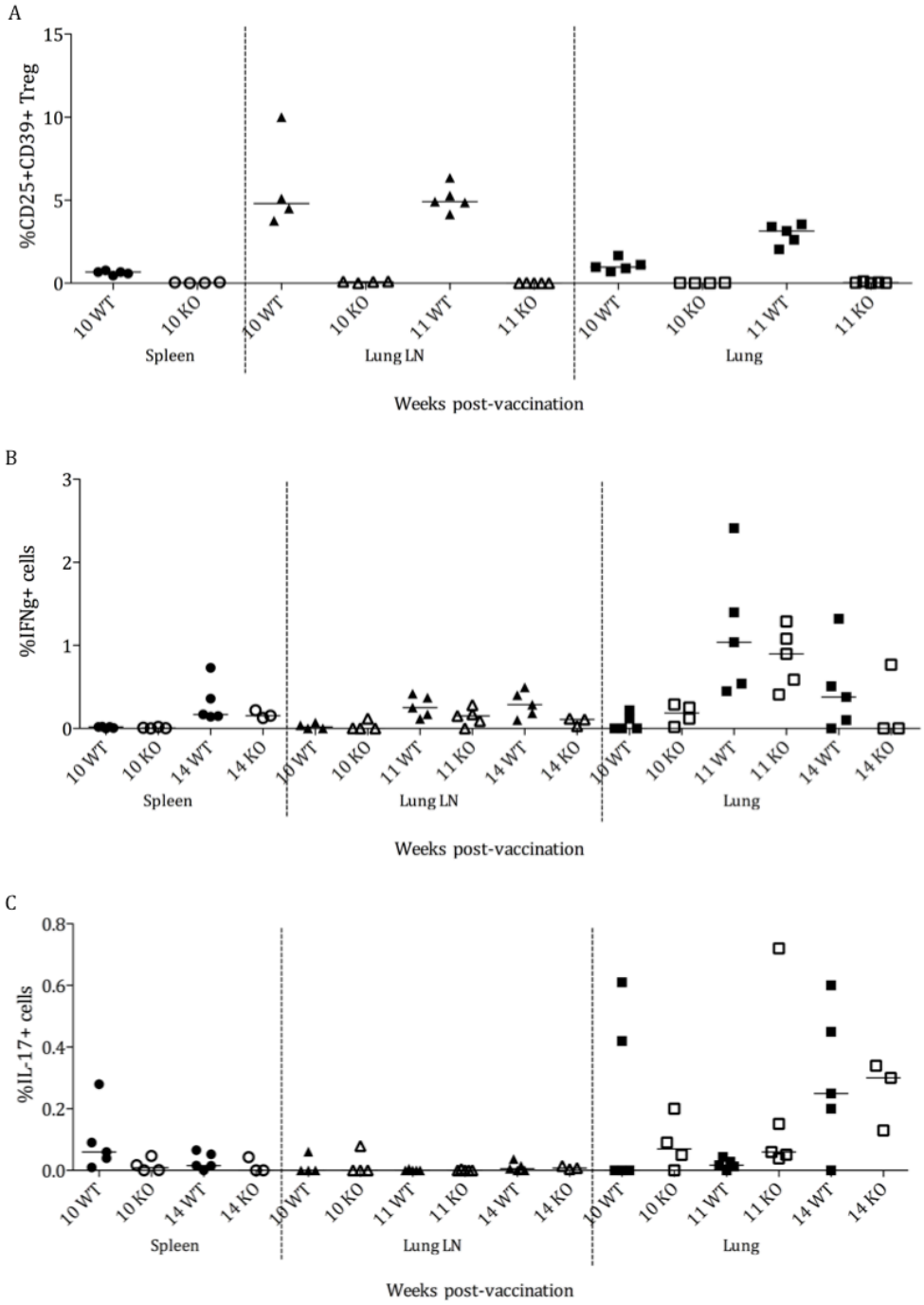


Figure 6.2.1 Immunogenicity of BCG – MVA85A in CD39$^{-/-}$ mice. Animals received either 4 x 10^5 cfu BCG *i.n.* followed 10 weeks later by 1 x 10^6 cfu MVA85A, or BCG *i.n.* alone. Five animals/group were culled at 10 weeks, 11 week and 14 weeks post-BCG. Percentages of cells expressing CD25 and CD39 in spleen (circles), lung LN (triangles) and lungs (squares) were calculated in **A**. Solid symbols represent WT animals and open symbols represent KO animals. Cytokine production by $CD4^+$ T cells was quantified and shown in **B** & **C**.

Levels of IFN-γ expression in WT vs. KO mice were similar, with a trend to lower expression in the KO animals in both lung LN and lungs (Fig 6.2.1B). In contrast, percentages of IL-17 single positive cells were trending towards higher percentages in the lungs of KO animals (Fig 6.2.1C). As has been observed previously, percentages of IL-17 single positive cells in spleen and lung LN were very low. These results could suggest that the lack of CD39 in the KO animals is driving a more IL-17-biased response to vaccination, although none of the differences are significant.

6.3 Vaccinated CD39$^{-/-}$ animals are better protected against *M.tb* challenge compared to WT animals

The vaccinated animals were challenged as described previously with ~100 cfu *M.tb* via aerosol, and cfu in lungs and spleen quantified 4 weeks post-challenge. As shown in figure 6.3.1A & B, BCG delivered *i.d.* conferred the expected 1 – 2 log protection in both lungs and spleen (medians = 6.67 x 10^6 and 6.17 x 10^5 for WT naïve and WT BCG *i.d.* respectively, p = 0.0004). Vaccination (both BCG *i.n.* and BCG – MVA85A) afforded protection in the KO animals (medians = 5.00 x 10^6, 1.83 x 10^5 and 1.25 x 10^5 for KO naïve, KO BCG *i.n.* and KO BCG – MVA85A respectively. p = 0.0007 for KO naïve vs. KO BCG *i.n.* and p = 0.0004 for KO naïve vs. BCG – MVA85A).

Comparing the WT and KO animals, no significant differences were observed between any of the individual groups, however if the vaccinated groups are pooled (BCG *i.n.* and BCG – MVA85A), the KO animals were better protected than the WT animals in the lung

(medians = 3.25 x 10^5 and 1.77 x 10^5 for WT and KO respectively, p = 0.029). This protection was not observed in spleen.

These data suggest that the slight differences in cytokine production observed between the two groups in Section 6.2 may account for slightly improved protection following vaccination in CD39$^{-/-}$ animals compared to WT C57BL/6 animals.

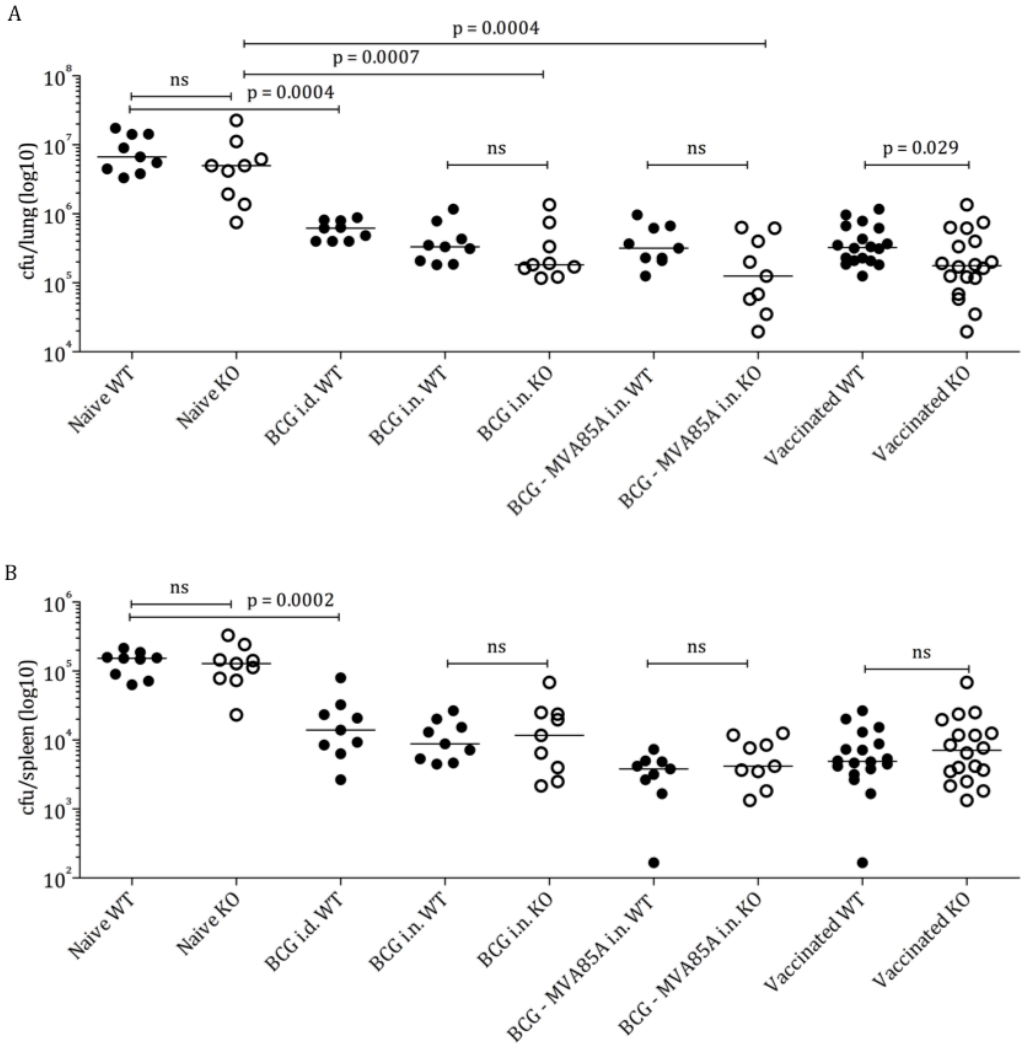


Figure 6.3.1 Challenge of CD39$^{-/-}$ animals with *M.tb*. Animals vaccinated as described above were challenged with ~100 cfu *M.tb* and were culled 4 weeks later. Lungs (**A**) and spleen (**B**) were taken for cfu determination. Closed circles represent WT animals and open circles represent KO animals. A Kruskall Wallis test was performed for all groups ($p < 0.0001$ for lungs and spleen) followed by Mann-Whitney tests for comparing individual groups. n = 9 for all groups.

6.4 Pathology

Since it was expected that the CD39$^{-/-}$ animals would produce higher levels of IL-17 following both vaccination and challenge, the level of pathology in the lungs was examined post-challenge. Previously (Section 5.4), it was observed that animals with higher lung cfu had a greater percentage of their lungs made up of nuclei, and cytoplasm and RBC, and a lower percentage of their lungs made up of air space. I therefore expected to see a similar scenario here, with the KO animals having more airspace and lower percentages of nuclei, and cytoplasm and RBC compared to the WT animals. Figure 6.4.1, however, shows that vaccinated KO animals, in spite of having lower cfu compared to the WT animals, had a lower percentage of their lungs made up of airspace ($p = 0.0007$), and a higher percentage made up of infiltrating cells (nuclei, and cytoplasm and RBC; $p = 0.0379$ and 0.0207 respectively).

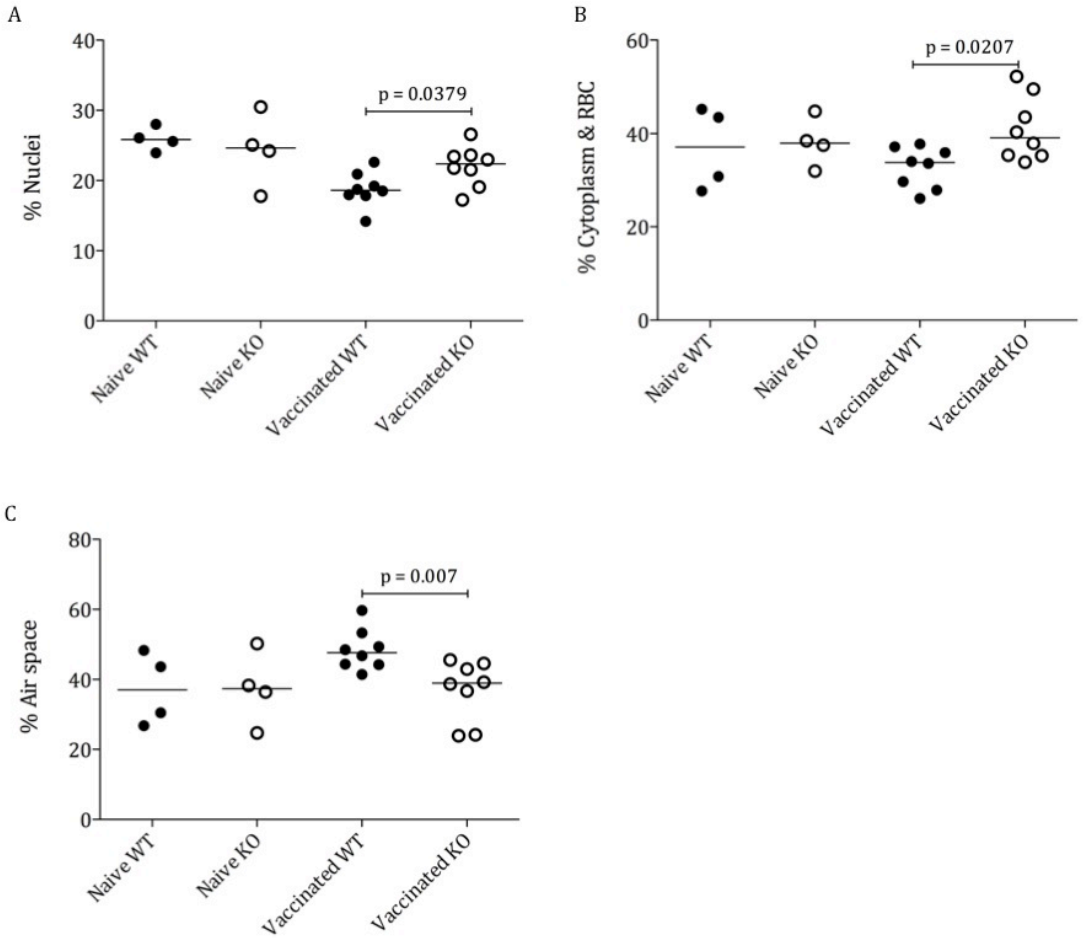


Figure 6.4.1 Histological analysis of lung sections from WT and CD39$^{-/-}$ animals challenged with *M.tb*. Lungs from animals challenged in Section 6.3 were fixed in 10% NBF, embedded in paraffin, and sectioned and stained with H&E by HistoPathOx. Stained slides were scanned by OCHRe and analysed using k-means clustering in MATLAB. Percentages of each section represented by purple (nuclei, **A**), pink (cytoplasm and RBC, **B**) and white (air space, **C**) was plotted above. WT animals are represented by closed circles and KO animals by open circles. Mann-Whitney tests were used to calculate differences between groups in Prism.

These results could reflect the fact that CD39 plays a role in negatively regulating inflammation, so removing this regulatory function from an inflammatory environment such as an *M.tb* infection could therefore mean that greater pathology is caused by the inflammatory cytokines such as IFN-γ, TNF-α and IL-17, even if the bacterial burden is reduced.

6.5 Post-challenge gene expression

Following challenge with *M.tb*, homogenised lungs were placed in RLT buffer and RNA extracted using a Qiagen fibrous tissue kit. Expression of *IL-17A, IL-17F, IFN-γ, TNF-α, IL-10, Rorc, Foxp3, IL-23R, IL-23p19, CXCL10* and *CXCL9* was investigated using qPCR. No significant differences in gene expression across the groups were found for *IL-17A, IL-17F, TNF-α, Rorc, Foxp3, IL-23R, IL-23p19* or *CXCL9* (data not shown). Expression of *IFN-γ*, however, was significantly different between naïve and vaccinated WT animals, with higher expression in naïve animals ($p = 0.0146$), and overall a positive correlation between *IFN-γ* gene expression and lung cfu was observed (Fig 6.5.1A & B). In contrast, as shown in figure 6.5.1C, the gene encoding the regulatory cytokine IL-10 was differentially expressed between naïve and vaccinated WT animals ($p = 0.0013$), and between naïve and vaccinated KO animals, with vaccinated animals expressing higher levels of *IL-10.* There was also a difference in *IL-10* expression in WT and KO naïve animals ($p = 0.0142$), with the KO animals having higher expression, and overall, *IL-10* expression correlated negatively with lung cfu (Fig 6.5.1D), suggesting a contribution of this regulatory cytokine to prevention of lung pathology.

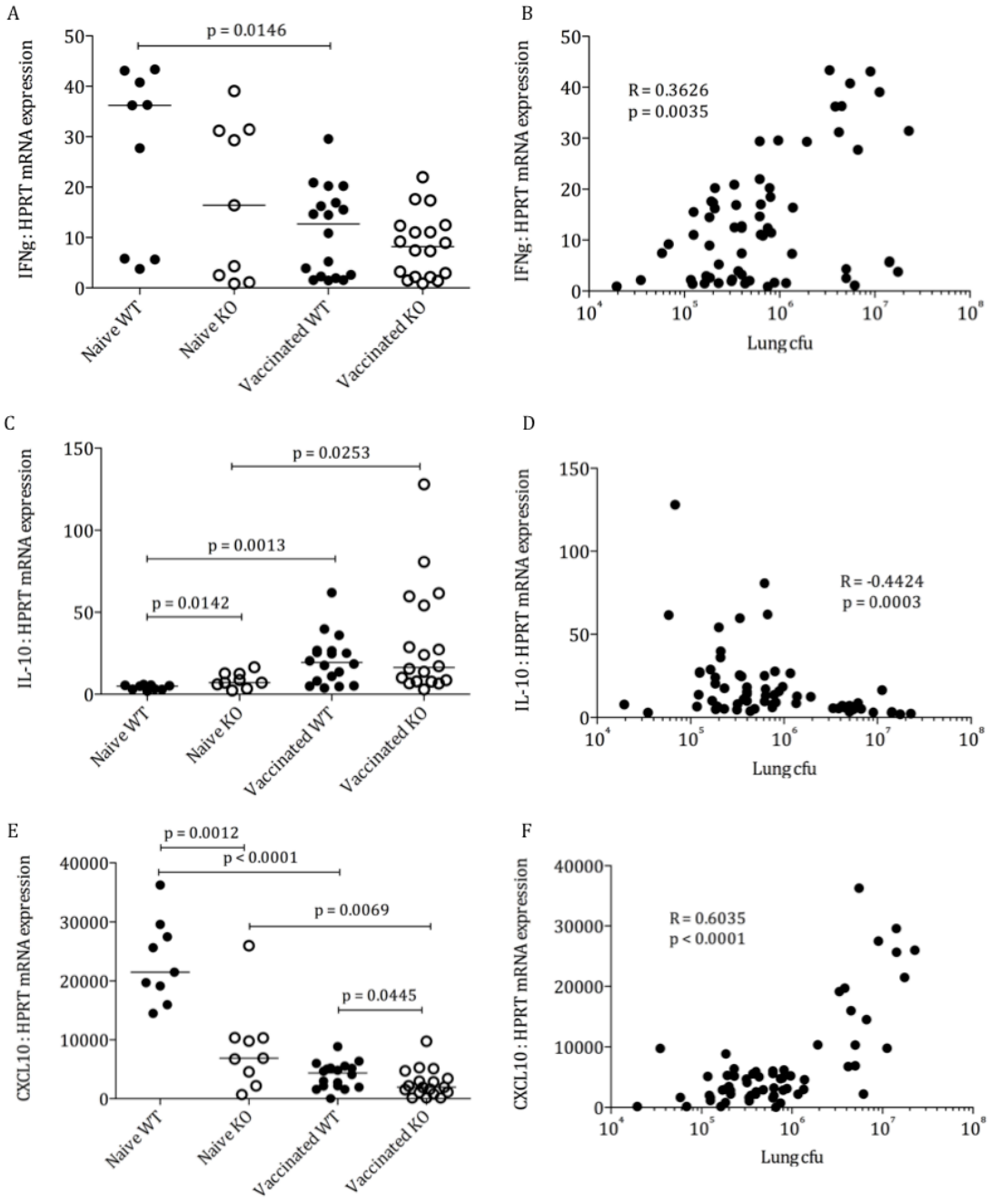


Figure 6.5.1 Gene expression in lungs of *M.tb*-challenged WT and CD39$^{-/-}$ mice. Homogenised lungs from vaccinated and challenged mice were stored in RLT buffer prior to mRNA extraction. Gene expression analysis for IFN-γ (**A**), IL-10 (**C**) and CXCL10 (**E**) was performed using qPCR and was expressed as the ratio of the gene to the housekeeping gene HPRT. Correlations with lung cfu were performed for IFN-γ, IL-10 and CXCL10 (**B**, **D** and **F** respectively). WT animals are represented by solid circles and KO animals by open circles. Mann-Witney tests were performed in Prism.

CXCL9 and CXCL10 have been shown to be upregulated by IL-17 following *M.tb* challenge of vaccinated mice and are believed to have a role in both recruiting Th1 cells to the lungs following infection [128] as well as inducing IFN-γ production by CD4^{+} T

cells [223]. Here we show that although there were no differences in *CXCL9* expression (data not shown), *CXCL10* was downregulated in vaccinated compared to naïve animals for both WT and KO ($p < 0.0001$ and $p = 0.0069$ for WT and KO respectively). It was also downregulated in KO animals compared to WT animals, both naïve and vaccinated ($p = 0.0012$ and 0.0445 for naïve and vaccinated respectively). There was also a positive correlation between *CXCL10* expression and bacterial burden. These results suggest that expression of *CXCL10* is driven by inflammation and could reflect the relationship between CXCL10 and IFN-γ-secreting cells in the lungs.

It is important to note that in these experiments, the mice had been infected with *M.tb* for 4 weeks at the time of analysis, so it is likely that cytokine and chemokine expression are a reflection of a state of heightened chronic inflammation, rather than an active immune response with protective efficacy. Ideally, for analysis of the effect of cytokine expression post-challenge on disease outcome, gene expression analysis would be done 1 – 2 weeks post-challenge, especially since factors such as IL-17 and CXCL10 are known to be expressed early following challenge in order to initiate an effective IFN-γ-based response.

6.6 Discussion

As discussed previously, CD39 is an ectonucleosidase expressed on the surface of lymphocytes with the role of hydrolysing extracellular ATP to ADP. Along with CD73, it works to a) rid the extracellular environment of pro-inflammatory ATP, as well as b) increase levels of adenosine, the anti-inflammatory product of hydrolysed AMP. ATP can help to activate the NALP3 inflammasome, promoting the cleavage and release of IL-1β [224], a cytokine that can, along with IL-6 and TGF-β, induce Th17 cells [116]. I have previously shown that IL-17 production by $CD4^+$ T cells *ex vivo* could be enhanced through blocking the function of CD39 using the apyrase inhibitor ARL67156. It was therefore hypothesised that mice lacking CD39 would be more prone to a Th17-skewed

T cell response following vaccination and that this might lead to improved protection against *M.tb* challenge.

Following vaccination, $CD39^{-/-}$ animals did indeed show slightly reduced IFN-γ production and increased IL-17 production compared to the C57BL/6 controls, however none of these were statistically significant. Unfortunately, technical errors mean that immunogenicity data for $IFN\text{-}\gamma^{+}IL\text{-}17^{+}$ cells is not available, however one would expect that there would be a trend towards a greater percentage of double positive cells in the KO animals compared to WT.

After challenge, there was no difference in the bacterial burdens of either the lungs or the spleens of unvaccinated KO and WT animals, suggesting that CD39 has no impact on infection of naïve animals. The same was observed with respect to the pathology of the lungs, with no difference between KO and WT.

In the vaccinated groups, on the other hand, although there was no difference between the individual groups, when the BCG *i.n.* was pooled with the BCG – MVA85A, KO animals had a significantly lower bacterial burden in the lungs, but not the spleens. This would imply that regulatory factors such as CD39 are important in vaccine-induced immunity, perhaps through mechanisms such as controlling the response post-vaccination, which would have an impact on the size and phenotype of the pool of memory cells available to respond on challenge.

IFN-γ expression (along with *CXCL10*) correlated positively with lung cfu. Pre-infection, IFN-γ is known to be a correlate of protection for developing active TB, however it has been shown previously that high levels of IFN-γ post-infection correlate with lung pathology and poor bacterial control in cattle [225]. This could be a reflection of the chronic inflammatory state induced during active TB, which is supported by the observation that *IL-10* expression correlated negatively with lung cfu. This indicates that a more regulatory environment in late stages of infection reflects better control of

the disease. This is evident in the fact that loss of the regulatory CD39, although it improves bacterial control overall, likely leads to worsened pathology.

It was also interesting to note that *IL-10* expression was not significantly lower in $CD39^{-/-}$ animals, which would suggest that either the IL-10-producing capacity of $CD39^{+}$ Treg is not impaired by loss of this enzyme, or that these cells do not produce IL-10.

In terms of approaches to vaccination, it would appear that the CD39-mediated pathway has potential for targeting in order to improve vaccine efficacy, however, given that although the KO animals had improved bacterial burdens in the lungs, they also had worsened pathology, it will be important to target the correct aspect of the pathway. For example, if it can be shown that increased ATP can improve activation of the NALP3 inflammasome, this would be a valid target, but it would also be important to keep in place the regulatory aspects, for example the potential for generation of the anti-inflammatory adenosine.

CONCLUSIONS & FUTURE WORK

7 CONCLUSIONS & FUTURE WORK

Based on initial findings of IL-17 induced following MVA85A vaccination of human volunteers with a history of BCG vaccination, this thesis has aimed to

a) Expand on these findings by relating IL-17 production to regulatory factors in the blood microenvironment
b) Investigate the capacity of BCG – MVA85A vaccination to induce IL-17 in mice following both mucosal and parenteral delivery
c) Investigate the enhancement of IL-17 by administration of BCG or MVA85A with CT
d) Investigate the effect of enhancement of IL-17 on the efficacy of *M.tb* challenge; and
e) Link the murine model findings back to the findings in humans by investigating the effect of a lack of regulatory factors described in a) on vaccine efficacy.

It is becoming increasingly evident from the literature that IL-17, produced largely by $CD4^+$ T cells following vaccination, is an important cytokine in vaccine-induced protection against TB disease in both mice and cattle, and that it likely has a dual role both at the time of priming of the immune response and at the time of encounter with the pathogen.

It was therefore interesting to identify IL-17-producing cells in PBMC and whole blood from MVA85A-vaccinated volunteers [76, 77]. Upon further analysis by flow cytometry, I found that the $IL\text{-}17^+$ cells identified in the PBMC, originally identified by ELISpot, produced IFN-γ as well as IL-17, and cytokine production by these cells could be increased *in vitro* following the addition of the apyrase inhibitor ARL67156. The apyrase CD39 is expressed on the surface of lymphocytes, in particular Treg cells, and addition of the same inhibitor to an assay measuring hydrolysis of ATP in solution reduced the hydrolysing capacity of the PBMC. The peak percentage of $IFN\text{-}\gamma^+IL\text{-}17^+$ cells occurred 2

weeks post-MVA85A, a timepoint that coincided with a drop in ATP hydrolysis by PBMC. This suggested that if the capacity to hydrolyse ATP is reduced at this timepoint, then the microenvironment is more pro-inflammatory, either due to an increase in the concentration of extracellular ATP, or to a decrease in anti-inflammatory adenosine. In a vaccine context, it would be advantageous to be able to make use of this phenomenon and artificially enhance the proinflammatory environment in order to increase the pool of responding cells. Ideally this would be done at the time of priming and via a route that would induce the cell type required at the location required. In the case of a TB vaccine, T cell responses are needed in the lungs and lung LN, and it is likely that both Th1 and Th17 responses are required for an effective vaccine. In mice, I found that as in humans, BCG – MVA85A vaccination induces both Th1 and Th17 cells, as well as IFN-γ^+IL-17^+ cells. In humans, data from an as yet unblinded trial delivering MVA85A either via aerosol or *i.d.* shows detection of IL-17 in BAL and whole blood of most vaccinated volunteers, suggesting that IL-17-producing $CD4^+$ T cells are detectable both at the site of vaccination and peripherally regardless of the route of vaccination. This is in contrast to my findings in mice, which suggest that IL-17-producing cells were only detectable following mucosal delivery of the vaccine. Intranasal delivery was therefore chosen for further study of the role of IL-17 in protection against TB disease in mice. Indeed, mucosal BCG – MVA85A delivery has already been shown to improve vaccine-induced protection in mice following *M.tb* challenge [216]. This was confirmed in my experiments, and this improved protective effect of BCG alone or BCG – MVA85A delivered *i.n.* was further enhanced when CT was administered along with BCG. This effect was at least partially due to enhanced IL-17, as shown by the use of anti-IL-17 blocking antibodies following challenge. Studies in IL-$17^{-/-}$ animals showed that CT lost its adjuvanting effect in the absence of IL-17 production, further implicating the IL-17 pathway in protection against TB disease. Furthermore, administration of CT along with

BCG *i.d.* did not improve protection, again suggesting that, at least in mice, the mucosal route is important for vaccine-induced protection following *M.tb* challenge.

Interestingly, although an increase in IL-17 production by $CD4^+$ T cells is observed following *i.n.* vaccination compared to *i.d.*, when IL-$17^{-/-}$ animals were vaccinated with BCG *i.n.*, their lung cfu were identical to the WT controls, suggesting that although CT may act directly through IL-17, other cytokines likely make IL-17 redundant following mucosal administration of a vaccine in the absence of CT. This warrants further exploration as it could highlight other cytokines whose induction pathways could be targeted. These may include TNF-α, whose protective effects in TB disease are well-established, or interleukins 21 and 22, which are important mucosal cytokines.

In terms of a mechanism of action of IL-17 on improved protection, the early induction of IL-17 compared to IFN-γ following BCG *i.n.* in these studies confirms the theory put forward by Gopal *et al.* [185] that IL-17 induced by BCG is able to overcome the suppressive effects of IL-10 on IL-12 production by infected APCs.

The observation in humans that parenteral delivery of MVA85A to BCG-vaccinated volunteers is likely to induce IL-17 in the lungs raises the question of whether mucosal vaccination is indeed necessary for improved site-directed immunogenicity of the vaccine. This is heartening to know, as it narrows the focus down to needing only to identify an adjuvant that could be delivered along with BCG that is able to enhance an IL-17-inducing pathway such as the ATP/inflammasome/cAMP pathways without having to consider safe mucosal administration of a prime.

As mentioned previously, CT cannot be used in humans, however an ATP-related pathway has been identified that could be targeted in the development of a vaccine. Although exploring the mechanism of action of ATP has not been in the remit of this thesis, it is possible that it could target similar pathways to CT as proposed in figure 7.1.1. Cholera toxin acts by inducing constitutive activation of the cAMP pathway, which drives expression of the cytokines IL-1β and IL-6 [205]. ATP has been shown to activate

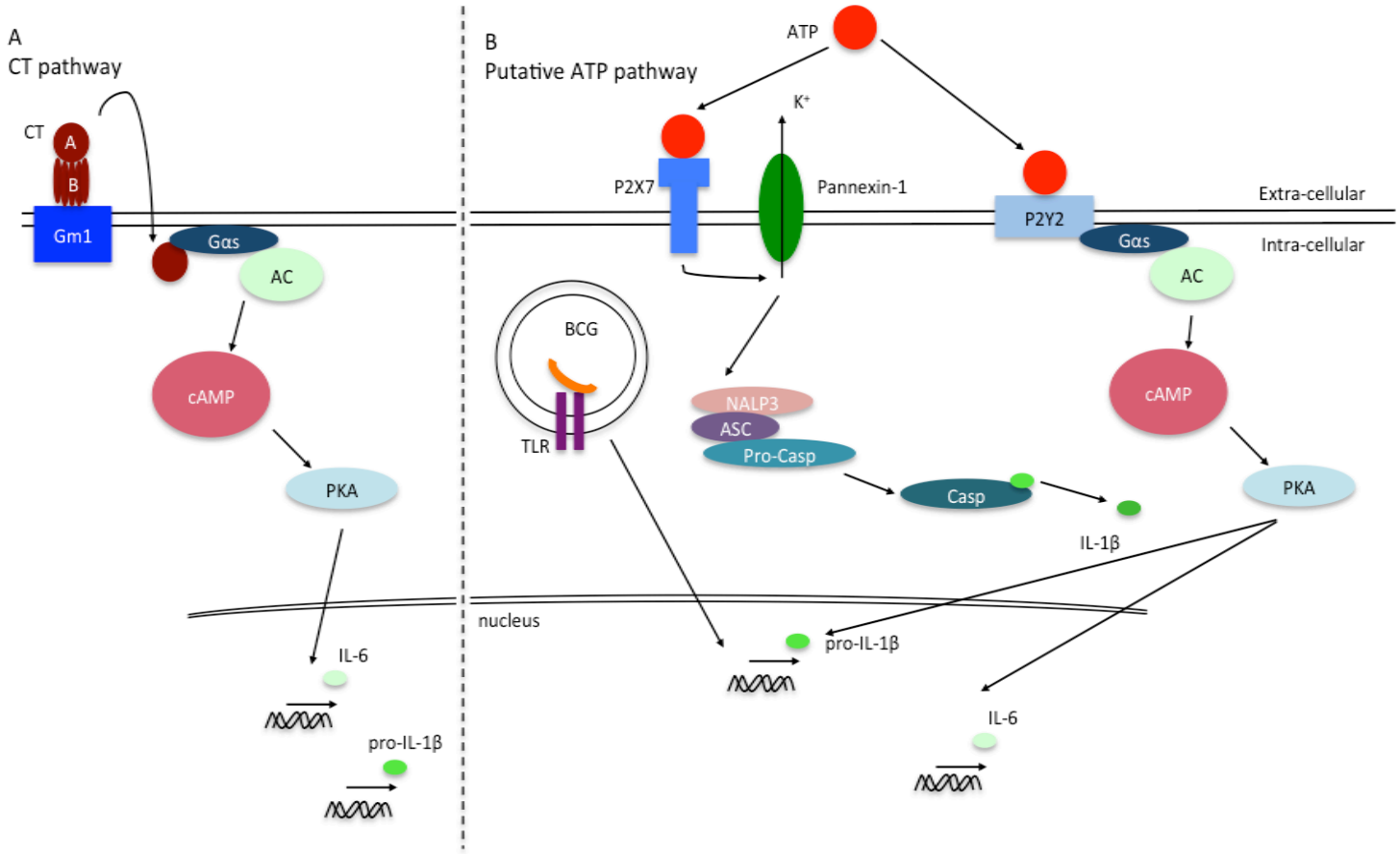


Figure 7.1.1. Comparison of CT and ATP adjuvanting pathways. (**A**) CT acts by binding to Gαs and constitutively activating AC to activate the cAMP pathway, inducing production of Th17-related cytokines IL-6 and IL-1β. (**B**) ATP can bind to the purinergic receptors P2X7 and P2Y2 to promote production of Th17-inducing cytokines IL-1β and IL-6, as well as inducing the assembly of the NALP3 inflammasome to promote cleavage of pro-IL-1β to active IL-1β.

the NALP3 inflammasome [115] and can also signal through the P2Y2 receptor and activate the cAMP pathway [221], thereby further enhancing production of IL-17-inducing cytokines IL-1β and IL-6. This suggests some similarities in the mechanisms of action of CT and ATP, and an ATP-related adjuvant could be investigated as a safer alternative to CT in humans.

Another important finding in this thesis was the link between lung cfu and lung pathology. A concern that accompanied the use of a potent adjuvant such as CT was increased recruitment of neutrophils to the lungs by IL-17 and therefore worsened pathology mediated by these cells. In the experiments in which CT was used, however, healthier-looking lungs, primarily indicated by more 'white space', were related to lungs from which a lower cfu was recovered. This suggests that although higher levels of IL-17 were detected pre-challenge in the lungs, this had no deleterious effect on lung pathology, possibly due to the fact that many of these cells may also produce IFN-γ, which could have had a *cis*-regulating effect on IL-17 production over time. In these mice, there was a presence of a population of functional regulatory cells that was able to modulate the inflammatory environment. In contrast, results from challenge of $CD39^{-/-}$ animals suggest that although these animals had lower lung cfu compared to WT controls, there was a significantly lower percentage of the lung made up of 'white space' in the $CD39^{-/-}$ animals. This indicates that a functional regulatory environment is important for keeping inflammation in check even if bacterial load is under control.

In the context of human disease, it is important to consider these differences in the relationship of lung pathology to either IL-17 or Treg cells, since it suggests that while enhanced IL-17 may be an effective way of improving vaccine-induced protection against TB disease in healthy individuals without the risk of worsened lung pathology, in immunocompromised individuals, such as HIV^{+} patients, the lack of an effective regulatory response may lead to worsened pathology and therefore worsened disease.

Interestingly, throughout my experiments, little or no change in either IFN-γ^+ or IL-17^+ cells was observed in the lung LN and overall, low percentages of cytokine-producing cells were recovered. Although in these experiments the type of memory cell induced was not investigated, a lack of boosting occurring in the lung LN could suggest induction and boosting of largely T_{em} cells, as reflected by high percentages of cytokine-producing antigen-specific cells detected in both BAL and lungs of vaccinated animals. It would be interesting to track these cells for a longer time post-boost in order to investigate their potential to convert to T_{cm} cells.

The readout of *M.tb* challenges in mice is lung cfu. This reflects the ability of the host to control *M.tb* replication in the lungs. Ideally, a protected mouse would show no lung cfu, reflecting the ability of the adaptive immune response to completely clear the infection, however sterilising immunity in TB has not been consistently demonstrated, and given the ability of *M.tb* to delay the onset of the adaptive immune response, sterilising immunity would likely depend on a highly-efficient innate response. While some people most likely do mount an efficient innate response that clears *M.tb* infection, it is not yet possible to control or improve innate immunity by vaccination. Therefore, it might be reasonable to conclude that what we can hope to achieve with a novel TB vaccine is to improve the ability of the host to respond rapidly with an effective adaptive response, and aim if not for complete clearance of the *M.tb*, then at least control to a level of bacteraemia manageable in the long term, and low enough to still be manageable should the host become immunocompromised in any way. Since latent *M.tb* infection is an asymptomatic disease in a healthy immunocompetent individual and, importantly, not transmissible, this is a reasonable goal. Over time, one could expect that although prevalence of *M.tb* infection may not decrease, incidence of active TB, and therefore transmission, will. Bringing this back to measuring the outcome of challenges in animal models, although TB disease progression in mice may not exactly reflect that in humans,

it is agreed that cytokines produced by $CD4^+$ T cells are equally important in both species. Therefore, the downstream effects of these cytokines, measurable by lung cfu and lung pathology in mice, are relevant. Furthermore, one could expect that a reduction in lung cfu in mice vaccinated by different regimes would reflect a similar result in humans.

From the results of my thesis, it would seem that the next challenge is to further explore the pathway through which CT operates in order to identify elements translatable to a human system. It would appear that for optimal IL-17 induction, any adjuvanting factor should be administered at the time of prime, which means introduction of either an improved BCG or an adjuvant that could be administered along with BCG.
Although the mucosal route was the focus of this thesis, it would also be relevant to further investigate BCG administered *i.d.*, although the mouse model is perhaps not the ideal one for this. Indeed, a model such as cattle may be more suitable, since IL-17 has already been shown to be induced in cattle vaccinated with BCG – MVA85A *i.d.*

Tuberculosis remains an important and devastating disease, and it is clear that improved diagnostic tests, treatments and preventative means are needed. As mentioned previously, in the long term, vaccination is the most sustainable, both economically and by means of implementation. There are several approaches to novel TB vaccines, and MVA85A administered as a boost to BCG is the one that has progressed furthest in development. It is already known that MVA85A induces unprecedented levels of IFN-γ from $CD4^+$ T cells, and it is also clear that it can induce IL-17 production from the same in both humans and animal models. This thesis has provided evidence that this combination of cytokine production is important in the efficacy of the vaccine, and that there are mechanisms available for further enhancing production of both cytokines simultaneously.

APPENDIX

8 APPENDIX

8.1 Table of reagents

Reagent	Supplier	Product code
10% Neutral Buffered Formalin	Sigma Aldrich Company Ltd.	HT5011
7H9 Broth Base	Beckton Dickinson Ltd.	271310
ADC growth supplement	Beckton Dickinson Ltd.	212352
Adenosine triphosphate (ATP)	Millipore	20-306
anti-mouse interleukin 17A monoclonal antibody	R&D Systems	MAB421
Anti-sedan	Oxford University Veterinary Services	
APC anti-human CD25	eBioscience	17-0259
APC anti-mouse CD25	eBioscience	17-0251
APC-eFluor780 anti-human CD8	eBioscience	47-0088
APC-eFluor780 anti-mouse CD25	eBioscience	47-0251
APC-eFluor780 anti-mouse CD8	eBioscience	47-0081
Aquatex aqueous mountant	Merck Biosciences Ltd.	1085620050
ARL67156 trisodium salt	Tocris Bioscience	1238
Benzonase	Merck Biosciences Ltd.	70664-3
Biotinylated anti-mouse interleukin 17A	Mabtech AB	3521-6-250
Bovine Serum Albumin	Sigma Aldrich Company Ltd.	A3059
Brefeldin A	Sigma Aldrich Company Ltd.	B7651
Brilliant Violet 421 anti-mouse interferon γ	BioLegend	505829
CD4 MicroBeads, mouse	Miltenyi Biotech Ltd.	130-049-201
CellTiter-Glow cell viability assay	Promega	G7570
Cholera toxin	Quadratech	100B
CK28R reinforced 2mL tubes containing 2.8mm ceramic beads	Stretton Scientific	03961-1-007
Collagenase	Sigma Aldrich Company Ltd.	C7657
Cytofix/Cytoperm	Beckton Dickinson Ltd.	554714
Cytomation Target Retrieval Solution pH 6	Dako	R1669
DAB peroxidase substrate kit 3,3'-diaminobenzidene	Vector Laboratories	SK-4100

Dimethylsulphoxide (DMSO)	Sigma Aldrich Company Ltd.	D2650-100ML
DNAse	Sigma Aldrich Company Ltd.	D5025
Dormitor	Oxford University Veterinary Services	
Dulbecco's Modified Eagle's Medium (DMEM)	Sigma Aldrich Company Ltd.	D5546
eFluor 650NC anti-mouse CD4	eBioscience	95-0041
ExtrAvidin Alkaline Phosphatase	Sigma Aldrich Company Ltd.	E2636
FITC anti-human interferon γ	eBioscience	11-7319
FITC anti-mouse CD4	eBioscience	11-0041
FITC anti-mouse interferon γ	eBioscience	11-7311
Foetal Bovine Serum	BioSera Ltd.	S08670S1810/500
Foetal Calf Serum	Sigma Aldrich Company Ltd.	F2442
FrameStar PCR plates	4titude	4ti-0952
Glycerol	Sigma Aldrich Company Ltd.	49767
GolgiStop	Beckton Dickinson Ltd.	554724
Haematoxylin Solution Gill No.3	Sigma Aldrich Company Ltd.	GHS316
Histo-Clear	National Diagnostics	HS-200
Horse serum 2.5%	Vector Laboratories	S-2012
Ionomycin	Sigma Aldrich Company Ltd.	I0634
IsoFlo	Oxford University Veterinary Services	
Ketaset	Oxford University Veterinary Services	3530736
L-Glutamine	Sigma Aldrich Company Ltd.	G7513
Live/Dead Fixable red dead cell stain	Invitrogen	L23102
Live/Dead fixable yellow dead cell stain	Invitrogen	L34955
LS Columns	Miltenyi Biotech Ltd.	130-042-401
Maxisorp 96 well plate	Fisher Scientific Ltd.	DIS-976-200D
Middlebrook 7H10 Agar Base	Sigma Aldrich Company Ltd.	M0303
Mycobacterium tuberculosis	BEI Resources	NR-15404
OADC enrichment	Beckton Dickinson Ltd.	212240

Omniscript RT kit	Qiagen	205111
p-Nitrophenyl Phosphate Substrate disodium salt hexahydrate tablets	Sigma Aldrich Company Ltd.	N2765
PE anti-human interleukin 17A	eBioscience	12-7179
PE anti-mouse interleukin 17A	eBioscience	12-7177
PE-Cy5 anti-human CD3	eBioscience	15-0038
PE-Cy5 anti-mouse CD3	eBioscience	15-0031
PE-Cy5 anti-mouse Gr-1	eBioscience	15-5931
PE-Cy7 anti-human CD39	eBioscience	25-0399
PE-Cy7 anti-mouse CD11b	eBioscience	25-0112
PE-Cy7 anti-mouse CD39	eBioscience	25-0391
Penicillin/Streptomycin	Sigma Aldrich Company Ltd.	P0781
PFTE Tubing 0.3mm x 0.6mm	Sigma Aldrich Company Ltd.	Z609692
Phorbol 12-myristate 13-acetate	Sigma Aldrich Company Ltd.	P8139
Phosphate buffered saline (PBS)	Sigma Aldrich Company Ltd.	D8537
Purified Protein Derivative	Statens Serum Institut	2390
Qdot605 anti-mouse CD4	Invitrogen	Q10092
Qdot655 anti-human CD4	Invitrogen	Q10007
QuantiTect SYBR Green PCR	Qiagen	204143
Rabbit polyclonal anti-mouse CD3	AbCam	ab5690
Rat IgG2A Isotype control antibody	R&D Systems	MAB006
Rat monoclonal anti-mouse B220	Beckton Dickinson Ltd.	550539
Rat monoclonal anti-mouse F4/80	AbD Serotec	MCA497G
Recombinant mouse interleukin 17A	R&D Systems	421-ML-25
RNeasy Fibrous Tissue mini kit	Qiagen	74704
RPMI 1640	Sigma Aldrich Company Ltd.	R0883-500ML
Simple Stain Mouse MAX PO (Rabbit) Universal Immuno-peroxidase Polymer for tissue samples	Histofine	414341F
Simple Stain Mouse MAX PO (Rat) Universal Immuno-peroxidase Polymer for tissue samples	Histofine	414311F
Tween80	Beckton Dickinson Ltd.	231181

8.2 Table of solutions

Solution	Recipe
ACK	8.29g NaCl (0.15M) + 1g $KHCO_3$ (1mM) + 37.2g Na_2EDTA in 800mL dH_2O. pH adjusted to 7.2-7.4 with 1M HCl then made up to 1L with dH_2O
FACS buffer	PBS + 1% FCS
Freezing mix	50% FBS + 40% RPMI 1640 + 10% DMSO
Ketamine/medetomidine solution	1.4mL Ketaset + 2mL Dormitor in 16.6mL water
MACS buffer	PBS + 0.5% BSA
Middlebrook agar	900mL dH_2O + 19.7g Middlebrook agar base + 5mL Glycerol (+ 100mL OADC added after autoclaving)
R0 Medium	RPMI 1640 + 2mM L-Glutamine + 100U/mL Penicillin + 100µg/mL Streptomycin sulphate
R10 Medium	RPMI 1640 + 10% FBS + 2mM L-Glutamine + 100U/mL Penicillin + 100µg/mL Streptomycin sulphate

8.3 Testing the blocking activity of the anti-IL-17 antibody MAB421 from R&D Systems

The MAB421 anti-IL-17 blocking antibody has been widely used in the literature [128, 188, 226]. Nonetheless, I considered it important to demonstrate its blocking capacity prior to administration in my experiments.

In a first attempt, I set up an anti-IL-17 ELISA using MAB421 as the capture antibody. Mice were vaccinated with BCG followed by MVA85A *i.n.* One week post-MVA85A, mice received either 100µg MAB421 or an equivalent volume PBS *i.p.* Mice were culled 2 days later and IL-17 in serum was measured. As shown in figure 8.3.1A, a modest drop in IL-17 was observed in neat serum but this was not carried through the dilutions.

As an alternative approach, I investigated the down stream effects of IL-17 by measuring granulocyte (classed as $Gr\text{-}1^+CD11b^+$) following CT treatment of animals that had received either MAB421 or PBS *i.p.* 24 hrs previously. Preliminary results from this experiment showed that anti-IL-17 treatment induced an increase of granulocytes into the lungs, contrary to expectations (Fig 8.3.1B). A second experiment was performed in which control groups of animals not receiving CT were included, and again, the blocking

antibody appeared to induce the recruitment of granulocytes to the lungs in the absence of CT. This induction was not increased by CT treatment (Fig 8.3.1C).

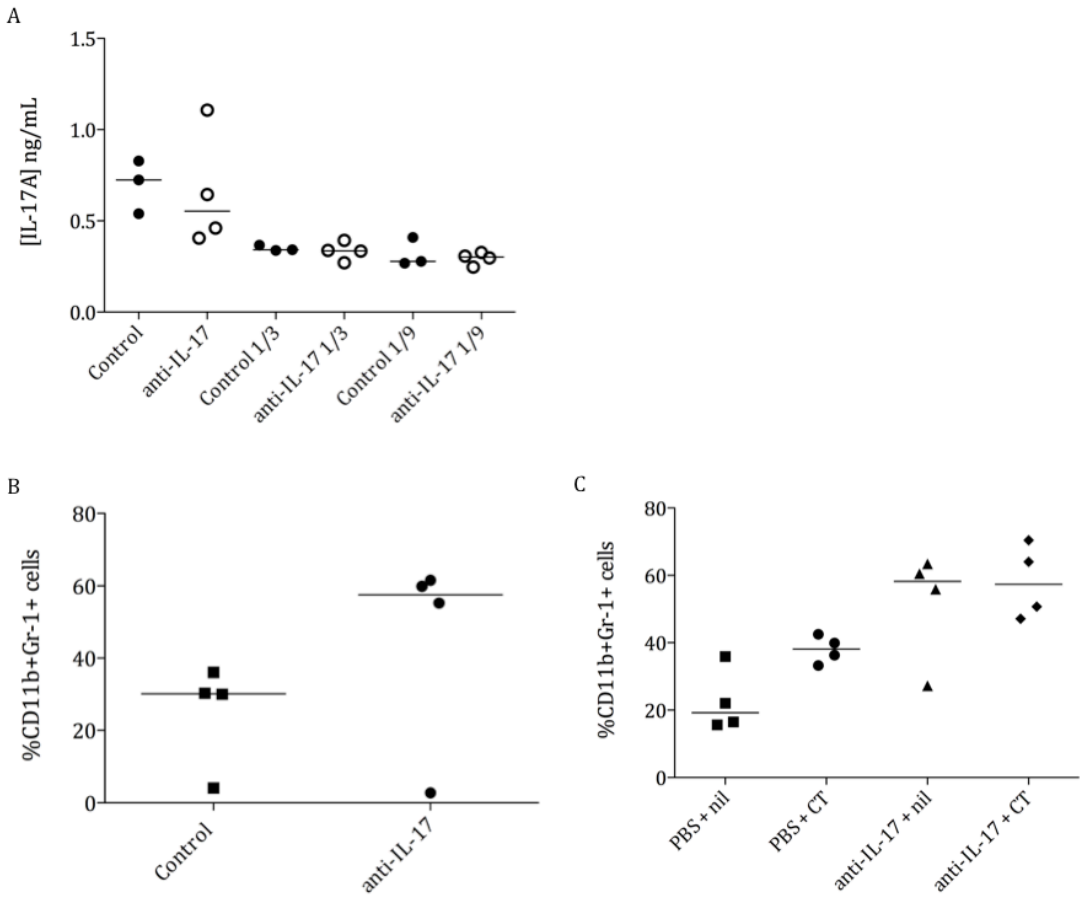


Figure 8.3.1 Effect of the anti-IL-17 blocking antibody MAB421. In (**A**), mice received 4x10^5 cfu BCG followed 10 weeks later by 1x10^6 pfu MVA85A. One week post-MVA85A, mice received 100µg anti-IL-17 or an equivalent volume of PBS *i.p.* In (**B**), mice received 100µg anti-IL-17 or equivalent volume PBS *i.p.* followed 24 hrs later by 2µg CT *i.n.* 24 hrs later, mice were culled and lungs taken and stained for CD11b and Gr-1. In (**C**), mice were treated as for (**B**), except that a group receive PBS only or anti-IL-17 only were included.

Although the blocking ability of anti-IL-17 (MAB421) could not be established, I decided to go ahead and use the antibody due to time-constraints. Other studies have already confirmed its blocking capacity, however it is something that would be useful to follow up in the future.

9 REFERENCES

1. Madison, B.M., *Application of stains in clinical microbiology.* Biotech Histochem, 2001. **76**(3): p. 119-25.
2. Dye, C., et al., *Consensus statement. Global burden of tuberculosis: estimated incidence, prevalence, and mortality by country. WHO Global Surveillance and Monitoring Project.* JAMA, 1999. **282**(7): p. 677-86.
3. WHO, *Global Tuberculosis Control 2011*, 2011, World Health Organisation.
4. Cegielski, J.P. and D.N. McMurray, *The relationship between malnutrition and tuberculosis: evidence from studies in humans and experimental animals.* Int J Tuberc Lung Dis, 2004. **8**(3): p. 286-98.
5. WHO. *Tuberculosis*. 2012 2010 [cited 2010 19/07/2010]; Available from: http://www.who.int/mediacentre/factsheets/fs104/en/index.html.
6. Steele, J.H., *Mycobacterium bovis infection in animals and humans in Regional and Country Status Report*, 1995. p. 169-172.
7. Hewinson, R.G., H.M. Vordermeier, and B.M. Buddle, *Use of the bovine model of tuberculosis for the development of improved vaccines and diagnostics.* Tuberculosis (Edinb), 2003. **83**(1-3): p. 119-30.
8. Xu, J., et al., *A unique Mycobacterium ESX-1 protein co-secretes with CFP-10/ESAT-6 and is necessary for inhibiting phagosome maturation.* Mol Microbiol, 2007. **66**(3): p. 787-800.
9. Shingadia, D., *The diagnosis of tuberculosis.* Pediatr Infect Dis J, 2012. **31**(3): p. 302-5.
10. Metcalfe, J.Z., et al., *Interferon-gamma release assays for active pulmonary tuberculosis diagnosis in adults in low- and middle-income countries: systematic review and meta-analysis.* J Infect Dis, 2011. **204 Suppl 4**: p. S1120-9.
11. Zuniga, J., et al., *Cellular and humoral mechanisms involved in the control of tuberculosis.* Clin Dev Immunol, 2012. **2012**: p. 193923.
12. van Crevel, R., T.H. Ottenhoff, and J.W. van der Meer, *Innate immunity to Mycobacterium tuberculosis.* Clin Microbiol Rev, 2002. **15**(2): p. 294-309.
13. Diaz-Silvestre, H., et al., *The 19-kDa antigen of Mycobacterium tuberculosis is a major adhesin that binds the mannose receptor of THP-1 monocytic cells and promotes phagocytosis of mycobacteria.* Microb Pathog, 2005. **39**(3): p. 97-107.
14. Ishikawa, E., et al., *Direct recognition of the mycobacterial glycolipid, trehalose dimycolate, by C-type lectin Mincle.* J Exp Med, 2009. **206**(13): p. 2879-88.

15. Schlesinger, L.S., et al., *Phagocytosis of Mycobacterium tuberculosis is mediated by human monocyte complement receptors and complement component C3.* J Immunol, 1990. **144**(7): p. 2771-80.
16. Hirsch, C.S., et al., *Complement receptor-mediated uptake and tumor necrosis factor-alpha-mediated growth inhibition of Mycobacterium tuberculosis by human alveolar macrophages.* J Immunol, 1994. **152**(2): p. 743-53.
17. Velasco-Velazquez, M.A., et al., *Macrophage--Mycobacterium tuberculosis interactions: role of complement receptor 3.* Microb Pathog, 2003. **35**(3): p. 125-31.
18. Bonar, A., et al., *Mannose-binding lectin enhances the attachment and phagocytosis of mycobacteria in vitro.* Arch Immunol Ther Exp (Warsz), 2005. **53**(5): p. 437-41.
19. Hickman, S.P., J. Chan, and P. Salgame, *Mycobacterium tuberculosis induces differential cytokine production from dendritic cells and macrophages with divergent effects on naive T cell polarization.* J Immunol, 2002. **168**(9): p. 4636-42.
20. Garcia-Romo, G.S., et al., *Mycobacterium tuberculosis manipulates pulmonary APCs subverting early immune responses.* Immunobiology, 2012.
21. Sturgill-Koszycki, S., et al., *Lack of acidification in Mycobacterium phagosomes produced by exclusion of the vesicular proton-ATPase.* Science, 1994. **263**(5147): p. 678-81.
22. Mishra, A.K., et al., *Lipoarabinomannan and related glycoconjugates: structure, biogenesis and role in Mycobacterium tuberculosis physiology and host-pathogen interaction.* FEMS Microbiol Rev, 2011. **35**(6): p. 1126-57.
23. Alonso, S., et al., *Lysosomal killing of Mycobacterium mediated by ubiquitin-derived peptides is enhanced by autophagy.* Proc Natl Acad Sci U S A, 2007. **104**(14): p. 6031-6.
24. Ponpuak, M. and V. Deretic, *Autophagy and p62/sequestosome 1 generate neo-antimicrobial peptides (cryptides) from cytosolic proteins.* Autophagy, 2011. **7**(3): p. 336-7.
25. Keane, J., H.G. Remold, and H. Kornfeld, *Virulent Mycobacterium tuberculosis strains evade apoptosis of infected alveolar macrophages.* J Immunol, 2000. **164**(4): p. 2016-20.
26. Kleinnijenhuis, J., et al., *Innate immune recognition of Mycobacterium tuberculosis.* Clin Dev Immunol, 2011. **2011**: p. 405310.

27. Schoenen, H., et al., *Cutting edge: Mincle is essential for recognition and adjuvanticity of the mycobacterial cord factor and its synthetic analog trehalose-dibehenate.* J Immunol, 2010. **184**(6): p. 2756-60.
28. Clay, H., H.E. Volkman, and L. Ramakrishnan, *Tumor necrosis factor signaling mediates resistance to mycobacteria by inhibiting bacterial growth and macrophage death.* Immunity, 2008. **29**(2): p. 283-94.
29. Churchyard, G.J., et al., *Mycobacterial disease in South African gold miners in the era of HIV infection.* Int J Tuberc Lung Dis, 1999. **3**(9): p. 791-8.
30. Pasman, L., *The complication of coinfection.* Yale J Biol Med, 2012. **85**(1): p. 127-32.
31. Cooper, A.M., et al., *Disseminated tuberculosis in interferon gamma gene-disrupted mice.* J Exp Med, 1993. **178**(6): p. 2243-7.
32. Newport, M.J., et al., *A mutation in the interferon-gamma-receptor gene and susceptibility to mycobacterial infection.* N Engl J Med, 1996. **335**(26): p. 1941-9.
33. Fang, F.C., *Antimicrobial reactive oxygen and nitrogen species: concepts and controversies.* Nat Rev Microbiol, 2004. **2**(10): p. 820-32.
34. Flannagan, R.S., G. Cosio, and S. Grinstein, *Antimicrobial mechanisms of phagocytes and bacterial evasion strategies.* Nat Rev Microbiol, 2009. **7**(5): p. 355-66.
35. Islam, N., et al., *Role of cellular activation and tumor necrosis factor-alpha in the early expression of Mycobacterium tuberculosis 85B mRNA in human alveolar macrophages.* J Infect Dis, 2004. **190**(2): p. 341-51.
36. Iles, K.E. and H.J. Forman, *Macrophage signaling and respiratory burst.* Immunol Res, 2002. **26**(1-3): p. 95-105.
37. Botha, T. and B. Ryffel, *Reactivation of latent tuberculosis infection in TNF-deficient mice.* J Immunol, 2003. **171**(6): p. 3110-8.
38. Thalayasingam, N. and J.D. Isaacs, *Anti-TNF therapy.* Best Pract Res Clin Rheumatol, 2011. **25**(4): p. 549-67.
39. WHO, *Treatment of Tuberculosis Guidelines*, 2010.
40. Dover, L.G. and G.D. Coxon, *Current status and research strategies in tuberculosis drug development.* J Med Chem, 2011. **54**(18): p. 6157-65.
41. Streicher, E.M., et al., *Emergence and treatment of multidrug resistant (MDR) and extensively drug-resistant (XDR) tuberculosis in South Africa.* Infect Genet Evol, 2012. **12**(4): p. 686-94.
42. Sharma, S.K., A. Mohan, and T. Kadhiravan, *HIV-TB co-infection: epidemiology, diagnosis & management.* Indian J Med Res, 2005. **121**(4): p. 550-67.

43. Global tuberculosis control, W., *The Global Plan to Stop TB 2011-2015*, 2010.
44. Hesseling, A.C., et al., *BCG vaccination in South African HIV-exposed infants--risks and benefits.* S Afr Med J, 2009. **99**(2): p. 88-91.
45. Rook, G.A. and R. Hernandez-Pando, *The pathogenesis of tuberculosis.* Annu Rev Microbiol, 1996. **50**: p. 259-84.
46. WHO, *BCG vaccine.* Weekly Epidemiological Record, 2004. **79**: p. 25-40.
47. Roche, P.W., J.A. Triccas, and N. Winter, *BCG vaccination against tuberculosis: past disappointments and future hopes.* Trends Microbiol, 1995. **3**(10): p. 397-401.
48. Colditz, G.A., et al., *Efficacy of BCG vaccine in the prevention of tuberculosis. Meta-analysis of the published literature.* JAMA, 1994. **271**(9): p. 698-702.
49. Roth, A.E., et al., *Beneficial non-targeted effects of BCG--ethical implications for the coming introduction of new TB vaccines.* Tuberculosis (Edinb), 2006. **86**(6): p. 397-403.
50. Roth, A., et al., *Bacillus Calmette-Guerin vaccination and infant mortality.* Expert Rev Vaccines, 2006. **5**(2): p. 277-93.
51. Hoft, D.F., et al., *A new recombinant bacille Calmette-Guerin vaccine safely induces significantly enhanced tuberculosis-specific immunity in human volunteers.* J Infect Dis, 2008. **198**(10): p. 1491-501.
52. Sun, R., et al., *Novel recombinant BCG expressing perfringolysin O and the over-expression of key immunodominant antigens; pre-clinical characterization, safety and protection against challenge with Mycobacterium tuberculosis.* Vaccine, 2009. **27**(33): p. 4412-23.
53. Kupferschmidt, K., *Infectious disease. Taking a new shot at a TB vaccine.* Science, 2011. **334**(6062): p. 1488-90.
54. Grode, L., et al., *Increased vaccine efficacy against tuberculosis of recombinant Mycobacterium bovis bacille Calmette-Guerin mutants that secrete listeriolysin.* J Clin Invest, 2005. **115**(9): p. 2472-9.
55. Sweeney, K.A., et al., *A recombinant Mycobacterium smegmatis induces potent bactericidal immunity against Mycobacterium tuberculosis.* Nat Med, 2011. **17**(10): p. 1261-8.
56. Nambiar, J.K., et al., *Protective immunity afforded by attenuated, PhoP-deficient Mycobacterium tuberculosis is associated with sustained generation of CD4+ T-cell memory.* Eur J Immunol, 2012. **42**(2): p. 385-92.
57. Von Eschen, K., et al., *The candidate tuberculosis vaccine Mtb72F/AS02A: Tolerability and immunogenicity in humans.* Hum Vaccin, 2009. **5**(7): p. 475-82.

58. Leroux-Roels, I., et al., *Improved CD4(+) T cell responses to Mycobacterium tuberculosis in PPD-negative adults by M72/AS01 as compared to the M72/AS02 and Mtb72F/AS02 tuberculosis candidate vaccine formulations: A randomized trial.* Vaccine, 2012.

59. Skeiky, Y.A., et al., *Cloning, expression, and immunological evaluation of two putative secreted serine protease antigens of Mycobacterium tuberculosis.* Infect Immun, 1999. **67**(8): p. 3998-4007.

60. Dillon, D.C., et al., *Molecular characterization and human T-cell responses to a member of a novel Mycobacterium tuberculosis mtb39 gene family.* Infect Immun, 1999. **67**(6): p. 2941-50.

61. van Dissel, J.T., et al., *Ag85B-ESAT-6 adjuvanted with IC31 promotes strong and long-lived Mycobacterium tuberculosis specific T cell responses in naive human volunteers.* Vaccine, 2010. **28**(20): p. 3571-81.

62. van Dissel, J.T., et al., *Ag85B-ESAT-6 adjuvanted with IC31(R) promotes strong and long-lived Mycobacterium tuberculosis specific T cell responses in volunteers with previous BCG vaccination or tuberculosis infection.* Vaccine, 2011. **29**(11): p. 2100-9.

63. Skeiky, Y.A., et al., *Non-clinical efficacy and safety of HyVac4:IC31 vaccine administered in a BCG prime-boost regimen.* Vaccine, 2010. **28**(4): p. 1084-93.

64. Billeskov, R., et al., *The HyVac4 Subunit Vaccine Efficiently Boosts BCG-Primed Anti-Mycobacterial Protective Immunity.* PLoS One, 2012. **7**(6): p. e39909.

65. Aagaard, C., et al., *A multistage tuberculosis vaccine that confers efficient protection before and after exposure.* Nat Med, 2011. **17**(2): p. 189-94.

66. Davidsen, J., et al., *Characterization of cationic liposomes based on dimethyldioctadecylammonium and synthetic cord factor from M. tuberculosis (trehalose 6,6'-dibehenate)-a novel adjuvant inducing both strong CMI and antibody responses.* Biochim Biophys Acta, 2005. **1718**(1-2): p. 22-31.

67. Abel, B., et al., *The novel tuberculosis vaccine, AERAS-402, induces robust and polyfunctional CD4+ and CD8+ T cells in adults.* Am J Respir Crit Care Med, 2010. **181**(12): p. 1407-17.

68. Hoft, D.F., et al., *A recombinant adenovirus expressing immunodominant TB antigens can significantly enhance BCG-induced human immunity.* Vaccine, 2012. **30**(12): p. 2098-108.

69. McShane, H., et al., *Enhanced immunogenicity of CD4(+) t-cell responses and protective efficacy of a DNA-modified vaccinia virus Ankara prime-boost vaccination regimen for murine tuberculosis.* Infect Immun, 2001. **69**(2): p. 681-6.

70. Williams, A., et al., *Boosting with poxviruses enhances Mycobacterium bovis BCG efficacy against tuberculosis in guinea pigs.* Infect Immun, 2005. **73**(6): p. 3814-6.
71. Williams, A., et al., *Evaluation of vaccines in the EU TB Vaccine Cluster using a guinea pig aerosol infection model of tuberculosis.* Tuberculosis (Edinb), 2005. **85**(1-2): p. 29-38.
72. Sharpe, S.A., et al., *Establishment of an aerosol challenge model of tuberculosis in rhesus macaques and an evaluation of endpoints for vaccine testing.* Clin Vaccine Immunol, 2010. **17**(8): p. 1170-82.
73. Vordermeier, H.M., et al., *Viral booster vaccines improve Mycobacterium bovis BCG-induced protection against bovine tuberculosis.* Infect Immun, 2009. **77**(8): p. 3364-73.
74. Scriba, T.J., et al., *A phase IIa trial of the new tuberculosis vaccine, MVA85A, in HIV- and/or Mycobacterium tuberculosis-infected adults.* Am J Respir Crit Care Med, 2012. **185**(7): p. 769-78.
75. Scriba, T.J., et al., *Dose-finding study of the novel tuberculosis vaccine, MVA85A, in healthy BCG-vaccinated infants.* J Infect Dis, 2011. **203**(12): p. 1832-43.
76. Scriba, T.J., et al., *Modified vaccinia Ankara-expressing Ag85A, a novel tuberculosis vaccine, is safe in adolescents and children, and induces polyfunctional CD4+ T cells.* Eur J Immunol, 2010. **40**(1): p. 279-90.
77. De Cassan, S., et al., *Investigating the induction of vaccine induced Th17 and regulatory T cells in healthy, BCG immunised adults vaccinated with a new tuberculosis vaccine, MVA85A.* Clin Vaccine Immunol, 2010. **17**(7): p. 1066-1073.
78. Griffiths, K.L., et al., *Th1/Th17 cell induction and corresponding reduction in ATP consumption following vaccination with the novel Mycobacterium tuberculosis vaccine MVA85A.* PLoS One, 2011. **6**(8): p. e23463.
79. Beveridge, N.E., et al., *A comparison of IFNgamma detection methods used in tuberculosis vaccine trials.* Tuberculosis (Edinb), 2008. **88**(6): p. 631-40.
80. Chackerian, A.A. and S.M. Behar, *Susceptibility to Mycobacterium tuberculosis: lessons from inbred strains of mice.* Tuberculosis (Edinb), 2003. **83**(5): p. 279-85.
81. Rhoades, E.R., A.A. Frank, and I.M. Orme, *Progression of chronic pulmonary tuberculosis in mice aerogenically infected with virulent Mycobacterium tuberculosis.* Tuber Lung Dis, 1997. **78**(1): p. 57-66.
82. Gupta, U.D. and V.M. Katoch, *Animal models of tuberculosis.* Tuberculosis (Edinb), 2005. **85**(5-6): p. 277-93.
83. Apt, A. and I. Kramnik, *Man and mouse TB: contradictions and solutions.* Tuberculosis (Edinb), 2009. **89**(3): p. 195-8.

84. Dannenberg, A.M., Jr. and F.M. Collins, *Progressive pulmonary tuberculosis is not due to increasing numbers of viable bacilli in rabbits, mice and guinea pigs, but is due to a continuous host response to mycobacterial products.* Tuberculosis (Edinb), 2001. **81**(3): p. 229-42.

85. Lin, P.L., et al., *Early events in Mycobacterium tuberculosis infection in cynomolgus macaques.* Infect Immun, 2006. **74**(7): p. 3790-803.

86. Capuano, S.V., 3rd, et al., *Experimental Mycobacterium tuberculosis infection of cynomolgus macaques closely resembles the various manifestations of human M. tuberculosis infection.* Infect Immun, 2003. **71**(10): p. 5831-44.

87. Neill, S.D., et al., *Pathogenesis of Mycobacterium bovis infection in cattle.* Vet Microbiol, 1994. **40**(1-2): p. 41-52.

88. Van Rhijn, I., et al., *Bovine tuberculosis as a model for human tuberculosis: advantages over small animal models.* Microbes Infect, 2008. **10**(7): p. 711-5.

89. Waters, W.R., et al., *Tuberculosis immunity: opportunities from studies with cattle.* Clin Dev Immunol, 2011. **2011**: p. 768542.

90. Palmer, M.V., W.R. Waters, and D.L. Whipple, *Aerosol delivery of virulent Mycobacterium bovis to cattle.* Tuberculosis (Edinb), 2002. **82**(6): p. 275-82.

91. Mosmann, T.R., et al., *Two types of murine helper T cell clone. I. Definition according to profiles of lymphokine activities and secreted proteins.* J Immunol, 1986. **136**(7): p. 2348-57.

92. Heinzel, F.P., et al., *Reciprocal expression of interferon gamma or interleukin 4 during the resolution or progression of murine leishmaniasis. Evidence for expansion of distinct helper T cell subsets.* J Exp Med, 1989. **169**(1): p. 59-72.

93. Hsieh, C.S., et al., *Development of TH1 CD4+ T cells through IL-12 produced by Listeria-induced macrophages.* Science, 1993. **260**(5107): p. 547-9.

94. Cassell, D. and J. Forman, *Linked recognition of helper and cytotoxic antigenic determinants for the generation of cytotoxic T lymphocytes.* Ann N Y Acad Sci, 1988. **532**: p. 51-60.

95. Nakanishi, Y., et al., *CD8(+) T lymphocyte mobilization to virus-infected tissue requires CD4(+) T-cell help.* Nature, 2009. **462**(7272): p. 510-3.

96. Jennings, S.R., et al., *CD4-positive T lymphocytes are required for the generation of the primary but not the secondary CD8-positive cytolytic T lymphocyte response to herpes simplex virus in C57BL/6 mice.* Cell Immunol, 1991. **133**(1): p. 234-52.

97. Szabo, S.J., et al., *A novel transcription factor, T-bet, directs Th1 lineage commitment.* Cell, 2000. **100**(6): p. 655-69.

98. Kaplan, M.H., et al., *Impaired IL-12 responses and enhanced development of Th2 cells in Stat4-deficient mice.* Nature, 1996. **382**(6587): p. 174-7.
99. Thierfelder, W.E., et al., *Requirement for Stat4 in interleukin-12-mediated responses of natural killer and T cells.* Nature, 1996. **382**(6587): p. 171-4.
100. Hou, J., et al., *An interleukin-4-induced transcription factor: IL-4 Stat.* Science, 1994. **265**(5179): p. 1701-6.
101. Zhang, D.H., et al., *Transcription factor GATA-3 is differentially expressed in murine Th1 and Th2 cells and controls Th2-specific expression of the interleukin-5 gene.* J Biol Chem, 1997. **272**(34): p. 21597-603.
102. Zheng, W. and R.A. Flavell, *The transcription factor GATA-3 is necessary and sufficient for Th2 cytokine gene expression in CD4 T cells.* Cell, 1997. **89**(4): p. 587-96.
103. Kopf, M., et al., *Disruption of the murine IL-4 gene blocks Th2 cytokine responses.* Nature, 1993. **362**(6417): p. 245-8.
104. Coffman, R.L., et al., *Antibody to interleukin-5 inhibits helminth-induced eosinophilia in mice.* Science, 1989. **245**(4915): p. 308-10.
105. Pulendran, B. and D. Artis, *New paradigms in type 2 immunity.* Science, 2012. **337**(6093): p. 431-5.
106. Ferber, I.A., et al., *Mice with a disrupted IFN-gamma gene are susceptible to the induction of experimental autoimmune encephalomyelitis (EAE).* J Immunol, 1996. **156**(1): p. 5-7.
107. Billiau, A., et al., *Enhancement of experimental allergic encephalomyelitis in mice by antibodies against IFN-gamma.* J Immunol, 1988. **140**(5): p. 1506-10.
108. Willenborg, D.O., et al., *IFN-gamma plays a critical down-regulatory role in the induction and effector phase of myelin oligodendrocyte glycoprotein-induced autoimmune encephalomyelitis.* J Immunol, 1996. **157**(8): p. 3223-7.
109. Leonard, J.P., K.E. Waldburger, and S.J. Goldman, *Prevention of experimental autoimmune encephalomyelitis by antibodies against interleukin 12.* J Exp Med, 1995. **181**(1): p. 381-6.
110. Oppmann, B., et al., *Novel p19 protein engages IL-12p40 to form a cytokine, IL-23, with biological activities similar as well as distinct from IL-12.* Immunity, 2000. **13**(5): p. 715-25.
111. Cua, D.J., et al., *Interleukin-23 rather than interleukin-12 is the critical cytokine for autoimmune inflammation of the brain.* Nature, 2003. **421**(6924): p. 744-8.
112. Rook, G.A., et al., *IL-4 in tuberculosis: implications for vaccine design.* Trends in immunology, 2004. **25**(9): p. 483-8.

113. Aggarwal, S., et al., *Interleukin-23 promotes a distinct CD4 T cell activation state characterized by the production of interleukin-17.* J Biol Chem, 2003. **278**(3): p. 1910-4.

114. Liang, S.C., et al., *Interleukin (IL)-22 and IL-17 are coexpressed by Th17 cells and cooperatively enhance expression of antimicrobial peptides.* J Exp Med, 2006. **203**(10): p. 2271-9.

115. Acosta-Rodriguez, E.V., et al., *Interleukins 1beta and 6 but not transforming growth factor-beta are essential for the differentiation of interleukin 17-producing human T helper cells.* Nat Immunol, 2007. **8**(9): p. 942-9.

116. Benwell, R.K. and D.R. Lee, *Essential and synergistic roles of IL1 and IL6 in human Th17 differentiation directed by TLR ligand-activated dendritic cells.* Clin Immunol, 2010. **134**(2): p. 178-87.

117. Zhou, L., et al., *IL-6 programs T(H)-17 cell differentiation by promoting sequential engagement of the IL-21 and IL-23 pathways.* Nat Immunol, 2007. **8**(9): p. 967-74.

118. Huang, W., et al., *Requirement of interleukin-17A for systemic anti-Candida albicans host defense in mice.* J Infect Dis, 2004. **190**(3): p. 624-31.

119. Markel, G., et al., *The involvement of IL-17A in the murine response to sub-lethal inhalational infection with Francisella tularensis.* PLoS One, 2010. **5**(6): p. e11176.

120. Higgins, S.C., et al., *TLR4 mediates vaccine-induced protective cellular immunity to Bordetella pertussis: role of IL-17-producing T cells.* J Immunol, 2006. **177**(11): p. 7980-9.

121. Happel, K.I., et al., *Divergent roles of IL-23 and IL-12 in host defense against Klebsiella pneumoniae.* J Exp Med, 2005. **202**(6): p. 761-9.

122. Nishihara, M., et al., *IL-6-gp130-STAT3 in T cells directs the development of IL-17+ Th with a minimum effect on that of Treg in the steady state.* Int Immunol, 2007. **19**(6): p. 695-702.

123. Ivanov, II, et al., *The orphan nuclear receptor RORgammat directs the differentiation program of proinflammatory IL-17+ T helper cells.* Cell, 2006. **126**(6): p. 1121-33.

124. Acosta-Rodriguez, E.V., et al., *Surface phenotype and antigenic specificity of human interleukin 17-producing T helper memory cells.* Nat Immunol, 2007. **8**(6): p. 639-46.

125. Liao, F., et al., *CC-chemokine receptor 6 is expressed on diverse memory subsets of T cells and determines responsiveness to macrophage inflammatory protein 3 alpha.* J Immunol, 1999. **162**(1): p. 186-94.

126. Griffin, G.K., et al., *IL-17 and TNF-alpha sustain neutrophil recruitment during inflammation through synergistic effects on endothelial activation.* J Immunol, 2012. **188**(12): p. 6287-99.

127. Roussel, L., et al., *IL-17 promotes p38 MAPK-dependent endothelial activation enhancing neutrophil recruitment to sites of inflammation.* J Immunol, 2010. **184**(8): p. 4531-7.

128. Khader, S.A., et al., *IL-23 and IL-17 in the establishment of protective pulmonary CD4+ T cell responses after vaccination and during Mycobacterium tuberculosis challenge.* Nat Immunol, 2007. **8**(4): p. 369-77.

129. Okamoto Yoshida, Y., et al., *Essential role of IL-17A in the formation of a mycobacterial infection-induced granuloma in the lung.* J Immunol, 2010. **184**(8): p. 4414-22.

130. Jovanovic, D.V., et al., *IL-17 stimulates the production and expression of proinflammatory cytokines, IL-beta and TNF-alpha, by human macrophages.* J Immunol, 1998. **160**(7): p. 3513-21.

131. Bai, H., et al., *IL-17/Th17 promotes type 1 T cell immunity against pulmonary intracellular bacterial infection through modulating dendritic cell function.* J Immunol, 2009. **183**(9): p. 5886-95.

132. Lin, Y., et al., *Interleukin-17 is required for T helper 1 cell immunity and host resistance to the intracellular pathogen Francisella tularensis.* Immunity, 2009. **31**(5): p. 799-810.

133. Yang, X.O., et al., *Regulation of inflammatory responses by IL-17F.* J Exp Med, 2008. **205**(5): p. 1063-75.

134. Korn, T., et al., *IL-21 initiates an alternative pathway to induce proinflammatory T(H)17 cells.* Nature, 2007. **448**(7152): p. 484-7.

135. Nurieva, R., et al., *Essential autocrine regulation by IL-21 in the generation of inflammatory T cells.* Nature, 2007. **448**(7152): p. 480-3.

136. Wei, L., et al., *IL-21 is produced by Th17 cells and drives IL-17 production in a STAT3-dependent manner.* J Biol Chem, 2007. **282**(48): p. 34605-10.

137. Fina, D., et al., *Regulation of gut inflammation and th17 cell response by interleukin-21.* Gastroenterology, 2008. **134**(4): p. 1038-48.

138. Trifari, S., et al., *Identification of a human helper T cell population that has abundant production of interleukin 22 and is distinct from T(H)-17, T(H)1 and T(H)2 cells.* Nat Immunol, 2009. **10**(8): p. 864-71.

139. Duhen, T., et al., *Production of interleukin 22 but not interleukin 17 by a subset of human skin-homing memory T cells.* Nat Immunol, 2009. **10**(8): p. 857-63.

140. Andoh, A., et al., *Interleukin-22, a member of the IL-10 subfamily, induces inflammatory responses in colonic subepithelial myofibroblasts.* Gastroenterology, 2005. **129**(3): p. 969-84.

141. Manel, N., D. Unutmaz, and D.R. Littman, *The differentiation of human T(H)-17 cells requires transforming growth factor-beta and induction of the nuclear receptor RORgammat.* Nat Immunol, 2008. **9**(6): p. 641-9.

142. Volpe, E., et al., *A critical function for transforming growth factor-beta, interleukin 23 and proinflammatory cytokines in driving and modulating human T(H)-17 responses.* Nat Immunol, 2008. **9**(6): p. 650-7.

143. Annunziato, F., L. Cosmi, and S. Romagnani, *Human and murine Th17.* Curr Opin HIV AIDS, 2010. **5**(2): p. 114-9.

144. Lee, Y.K., et al., *Late developmental plasticity in the T helper 17 lineage.* Immunity, 2009. **30**(1): p. 92-107.

145. Lexberg, M.H., et al., *IFN-gamma and IL-12 synergize to convert in vivo generated Th17 into Th1/Th17 cells.* Eur J Immunol, 2010. **40**(11): p. 3017-27.

146. O'Shea, J.J. and W.E. Paul, *Mechanisms underlying lineage commitment and plasticity of helper CD4+ T cells.* Science, 2010. **327**(5969): p. 1098-102.

147. Lanzavecchia, A. and F. Sallusto, *Dynamics of T lymphocyte responses: intermediates, effectors, and memory cells.* Science, 2000. **290**(5489): p. 92-7.

148. Sallusto, F., et al., *Two subsets of memory T lymphocytes with distinct homing potentials and effector functions.* Nature, 1999. **401**(6754): p. 708-12.

149. Pepper, M., et al., *Different routes of bacterial infection induce long-lived TH1 memory cells and short-lived TH17 cells.* Nat Immunol, 2010. **11**(1): p. 83-9.

150. Fontenot, J.D., M.A. Gavin, and A.Y. Rudensky, *Foxp3 programs the development and function of CD4+CD25+ regulatory T cells.* Nat Immunol, 2003. **4**(4): p. 330-6.

151. Asseman, C., et al., *An essential role for interleukin 10 in the function of regulatory T cells that inhibit intestinal inflammation.* J Exp Med, 1999. **190**(7): p. 995-1004.

152. Rubtsov, Y.P., et al., *Regulatory T cell-derived interleukin-10 limits inflammation at environmental interfaces.* Immunity, 2008. **28**(4): p. 546-58.

153. Wing, K., et al., *CTLA-4 control over Foxp3+ regulatory T cell function.* Science, 2008. **322**(5899): p. 271-5.

154. Koch, M.A., et al., *The transcription factor T-bet controls regulatory T cell homeostasis and function during type 1 inflammation.* Nat Immunol, 2009. **10**(6): p. 595-602.

155. Chaudhry, A., et al., *CD4+ regulatory T cells control TH17 responses in a Stat3-dependent manner.* Science, 2009. **326**(5955): p. 986-91.

156. Bettelli, E., et al., *Reciprocal developmental pathways for the generation of pathogenic effector TH17 and regulatory T cells.* Nature, 2006. **441**(7090): p. 235-8.

157. Lathrop, S.K., et al., *Antigen-specific peripheral shaping of the natural regulatory T cell population.* J Exp Med, 2008. **205**(13): p. 3105-17.

158. Naganuma, M., et al., *Cutting edge: Critical role for A2A adenosine receptors in the T cell-mediated regulation of colitis.* J Immunol, 2006. **177**(5): p. 2765-9.

159. Deaglio, S., et al., *Adenosine generation catalyzed by CD39 and CD73 expressed on regulatory T cells mediates immune suppression.* J Exp Med, 2007. **204**(6): p. 1257-65.

160. Borsellino, G., et al., *Expression of ectonucleotidase CD39 by Foxp3+ Treg cells: hydrolysis of extracellular ATP and immune suppression.* Blood, 2007. **110**(4): p. 1225-32.

161. Dwyer, K.M., et al., *Expression of CD39 by human peripheral blood CD4+ CD25+ T cells denotes a regulatory memory phenotype.* Am J Transplant, 2010. **10**(11): p. 2410-20.

162. Ferrari, D., et al., *Purinergic modulation of interleukin-1 beta release from microglial cells stimulated with bacterial endotoxin.* J Exp Med, 1997. **185**(3): p. 579-82.

163. Fletcher, J.M., et al., *CD39+Foxp3+ regulatory T Cells suppress pathogenic Th17 cells and are impaired in multiple sclerosis.* J Immunol, 2009. **183**(11): p. 7602-10.

164. Fletcher, H.A., et al., *Boosting BCG vaccination with MVA85A down-regulates the immunoregulatory cytokine TGF-beta1.* Vaccine, 2008. **26**(41): p. 5269-75.

165. Urdahl, K.B., S. Shafiani, and J.D. Ernst, *Initiation and regulation of T-cell responses in tuberculosis.* Mucosal immunology, 2011. **4**(3): p. 288-93.

166. Zinkernagel, R.M. and P.C. Doherty, *Restriction of in vitro T cell-mediated cytotoxicity in lymphocytic choriomeningitis within a syngeneic or semiallogeneic system.* Nature, 1974. **248**(450): p. 701-2.

167. Zinkernagel, R.M. and P.C. Doherty, *H-2 compatability requirement for T-cell-mediated lysis of target cells infected with lymphocytic choriomeningitis virus.*

Different cytotoxic T-cell specificities are associated with structures coded for in H-2K or H-2D. J Exp Med, 1975. **141**(6): p. 1427-36.

168. Berke, G., *The binding and lysis of target cells by cytotoxic lymphocytes: molecular and cellular aspects.* Annu Rev Immunol, 1994. **12**: p. 735-73.
169. Andersen, M.H., et al., *Cytotoxic T cells.* The Journal of investigative dermatology, 2006. **126**(1): p. 32-41.
170. Flynn, J.L., et al., *Major histocompatibility complex class I-restricted T cells are required for resistance to Mycobacterium tuberculosis infection.* Proc Natl Acad Sci U S A, 1992. **89**(24): p. 12013-7.
171. van Pinxteren, L.A., et al., *Control of latent Mycobacterium tuberculosis infection is dependent on CD8 T cells.* Eur J Immunol, 2000. **30**(12): p. 3689-98.
172. Lockhart, E., A.M. Green, and J.L. Flynn, *IL-17 production is dominated by gammadelta T cells rather than CD4 T cells during Mycobacterium tuberculosis infection.* J Immunol, 2006. **177**(7): p. 4662-9.
173. Cheng, P., et al., *Role of gamma-delta T cells in host response against Staphylococcus aureus-induced pneumonia.* BMC Immunol, 2012. **13**(1): p. 38.
174. Dejima, T., et al., *Protective role of naturally occurring interleukin-17A-producing gammadelta T cells in the lung at the early stage of systemic candidiasis in mice.* Infect Immun, 2011. **79**(11): p. 4503-10.
175. Hamada, S., et al., *IL-17A produced by gammadelta T cells plays a critical role in innate immunity against listeria monocytogenes infection in the liver.* J Immunol, 2008. **181**(5): p. 3456-63.
176. Korn, T. and F. Petermann, *Development and function of interleukin 17-producing gammadelta T cells.* Ann N Y Acad Sci, 2012. **1247**: p. 34-45.
177. Haas, J.D., et al., *CCR6 and NK1.1 distinguish between IL-17A and IFN-gamma-producing gammadelta effector T cells.* Eur J Immunol, 2009. **39**(12): p. 3488-97.
178. Ribot, J.C., et al., *CD27 is a thymic determinant of the balance between interferon-gamma- and interleukin 17-producing gammadelta T cell subsets.* Nat Immunol, 2009. **10**(4): p. 427-36.
179. Weintraub, B.C., M.R. Jackson, and S.M. Hedrick, *Gamma delta T cells can recognize nonclassical MHC in the absence of conventional antigenic peptides.* J Immunol, 1994. **153**(7): p. 3051-8.
180. Porcelli, S., et al., *Recognition of cluster of differentiation 1 antigens by human CD4-CD8-cytolytic T lymphocytes.* Nature, 1989. **341**(6241): p. 447-50.
181. Spada, F.M., et al., *Self-recognition of CD1 by gamma/delta T cells: implications for innate immunity.* J Exp Med, 2000. **191**(6): p. 937-48.

182. Martin, B., et al., *Interleukin-17-producing gammadelta T cells selectively expand in response to pathogen products and environmental signals.* Immunity, 2009. **31**(2): p. 321-30.

183. Ladel, C.H., et al., *Contribution of alpha/beta and gamma/delta T lymphocytes to immunity against Mycobacterium bovis bacillus Calmette Guerin: studies with T cell receptor-deficient mutant mice.* Eur J Immunol, 1995. **25**(3): p. 838-46.

184. Ueta, C., et al., *Increase of gamma/delta T cells in hospital workers who are in close contact with tuberculosis patients.* Infect Immun, 1994. **62**(12): p. 5434-41.

185. Gopal, R., et al., *IL-23-dependent IL-17 drives Th1-cell responses following Mycobacterium bovis BCG vaccination.* Eur J Immunol, 2012. **42**(2): p. 364-73.

186. Pitt, J.M., et al., *Blockade of IL-10 Signaling during Bacillus Calmette-Guerin Vaccination Enhances and Sustains Th1, Th17, and Innate Lymphoid IFN-gamma and IL-17 Responses and Increases Protection to Mycobacterium tuberculosis Infection.* J Immunol, 2012.

187. Umemura, M., et al., *IL-17-mediated regulation of innate and acquired immune response against pulmonary Mycobacterium bovis bacille Calmette-Guerin infection.* J Immunol, 2007. **178**(6): p. 3786-96.

188. Cruz, A., et al., *Pathological role of interleukin 17 in mice subjected to repeated BCG vaccination after infection with Mycobacterium tuberculosis.* J Exp Med, 2010. **207**(2): p. 1609-16.

189. Eruslanov, E.B., et al., *Neutrophil responses to Mycobacterium tuberculosis infection in genetically susceptible and resistant mice.* Infect Immun, 2005. **73**(3): p. 1744-53.

190. Keller, C., et al., *Genetically determined susceptibility to tuberculosis in mice causally involves accelerated and enhanced recruitment of granulocytes.* Infect Immun, 2006. **74**(7): p. 4295-309.

191. Cruz, A., et al., *Cutting edge: IFN-gamma regulates the induction and expansion of IL-17-producing CD4 T cells during mycobacterial infection.* J Immunol, 2006. **177**(3): p. 1416-20.

192. Hirota, K., et al., *Fate mapping of IL-17-producing T cells in inflammatory responses.* Nat Immunol, 2011. **12**(3): p. 255-63.

193. Aranday-Cortes, E., et al., *Upregulation of IL-17A, CXCL9 and CXCL10 in Early-Stage Granulomas Induced by Mycobacterium bovis in Cattle.* Transbound Emerg Dis, 2012.

194. Blanco, F.C., et al., *Increased IL-17 expression is associated with pathology in a bovine model of tuberculosis.* Tuberculosis (Edinb), 2011. **91**(1): p. 57-63.

195. Qiao, D., et al., *ESAT-6- and CFP-10-specific Th1, Th22 and Th17 cells in tuberculous pleurisy may contribute to the local immune response against Mycobacterium tuberculosis infection.* Scand J Immunol, 2011.

196. Matthews, K., et al., *Predominance of interleukin-22 over interleukin-17 at the site of disease in human tuberculosis.* Tuberculosis, 2011.

197. Wang, T., et al., *Increased frequencies of T helper type 17 cells in tuberculous pleural effusion.* Tuberculosis (Edinb), 2011. **91**(3): p. 231-7.

198. Ye, Z.J., et al., *Imbalance of Th17 cells and regulatory T cells in tuberculous pleural effusion.* Clin Vaccine Immunol, 2011. **18**(10): p. 1608-15.

199. Scriba, T.J., et al., *Distinct, specific IL-17- and IL-22-producing CD4+ T cell subsets contribute to the human anti-mycobacterial immune response.* J Immunol, 2008. **180**(3): p. 1962-70.

200. Cowan, J., et al., *Comparison of interferon-gamma-, interleukin (IL)-17- and IL-22-expressing CD4 T cells, IL-22-expressing granulocytes and proinflammatory cytokines during latent and active tuberculosis infection.* Clin Exp Immunol, 2012. **167**(2): p. 317-29.

201. Jurado, J.O., et al., *IL-17 and IFN-gamma expression in lymphocytes from patients with active tuberculosis correlates with the severity of the disease.* J Leukoc Biol, 2012. **91**(6): p. 991-1002.

202. Serezani, C.H., et al., *Cyclic AMP: master regulator of innate immune cell function.* Am J Respir Cell Mol Biol, 2008. **39**(2): p. 127-32.

203. Cubillos, S., J. Norgauer, and K. Lehmann, *Toxins-useful biochemical tools for leukocyte research.* Toxins (Basel), 2010. **2**(4): p. 428-52.

204. la Sala, A., et al., *Cholera toxin inhibits IL-12 production and CD8alpha+ dendritic cell differentiation by cAMP-mediated inhibition of IRF8 function.* J Exp Med, 2009. **206**(6): p. 1227-35.

205. Datta, S.K., et al., *Mucosal adjuvant activity of cholera toxin requires Th17 cells and protects against inhalation anthrax.* Proc Natl Acad Sci U S A, 2010.

206. Veglia, F., et al., *Cholera toxin impairs the differentiation of monocytes into dendritic cells, inducing professional antigen-presenting myeloid cells.* Infect Immun, 2011. **79**(3): p. 1300-10.

207. Lee, J.B., et al., *Intranasal delivery of cholera toxin induces th17-dominated T-cell response to bystander antigens.* PLoS One, 2009. **4**(4): p. e5190.

208. Lewis, D.J., et al., *Transient facial nerve paralysis (Bell's palsy) following intranasal delivery of a genetically detoxified mutant of Escherichia coli heat labile toxin.* PLoS One, 2009. **4**(9): p. e6999.

209. MacQueen, J.B., *Some methods for classification and analysis of multivariate obeservations*. Proceedings of the Fifth Berkeley Symposium on Mathematics, Statistics and Probability. Vol. 1. 1967: University of California Press.

210. Shoelson, B., *Interactively segment RGB image into n user-defined clusters*, Accessed 2012.

211. Rovedatti, L., et al., *Differential regulation of interleukin 17 and interferon gamma production in inflammatory bowel disease.* Gut, 2009. **58**(12): p. 1629-36.

212. Atarashi, K., et al., *ATP drives lamina propria T(H)17 cell differentiation.* Nature, 2008. **455**(7214): p. 808-12.

213. Pelegrin, P., C. Barroso-Gutierrez, and A. Surprenant, *P2X7 receptor differentially couples to distinct release pathways for IL-1beta in mouse macrophage.* J Immunol, 2008. **180**(11): p. 7147-57.

214. Pelegrin, P. and A. Surprenant, *Pannexin-1 mediates large pore formation and interleukin-1beta release by the ATP-gated P2X7 receptor.* EMBO J, 2006. **25**(21): p. 5071-82.

215. Delaloye, J., et al., *Innate immune sensing of modified vaccinia virus Ankara (MVA) is mediated by TLR2-TLR6, MDA-5 and the NALP3 inflammasome.* PLoS Pathog, 2009. **5**(6): p. e1000480.

216. Goonetilleke, N.P., et al., *Enhanced immunogenicity and protective efficacy against Mycobacterium tuberculosis of bacille Calmette-Guerin vaccine using mucosal administration and boosting with a recombinant modified vaccinia virus Ankara.* J Immunol, 2003. **171**(3): p. 1602-9.

217. Tzartos, J.S., et al., *Interleukin-17 production in central nervous system-infiltrating T cells and glial cells is associated with active disease in multiple sclerosis.* Am J Pathol, 2008. **172**(1): p. 146-55.

218. Lowes, M.A., et al., *Psoriasis vulgaris lesions contain discrete populations of Th1 and Th17 T cells.* The Journal of investigative dermatology, 2008. **128**(5): p. 1207-11.

219. Shen, H., J.C. Goodall, and J.S. Hill Gaston, *Frequency and phenotype of peripheral blood Th17 cells in ankylosing spondylitis and rheumatoid arthritis.* Arthritis Rheum, 2009. **60**(6): p. 1647-56.

220. Redford, P.S., P.J. Murray, and A. O'Garra, *The role of IL-10 in immune regulation during M. tuberculosis infection.* Mucosal immunology, 2011. **4**(3): p. 261-70.

221. Yu, J., et al., *Transcriptional regulation of IL-6 in bile duct epithelia by extracellular ATP.* Am J Physiol Gastrointest Liver Physiol, 2009. **296**(3): p. G563-71.

222. Almeida, M.Q., et al., *Protein kinase A regulates caspase-1 via Ets-1 in bone stromal cell-derived lesions: a link between cyclic AMP and pro-inflammatory pathways in osteoblast progenitors.* Hum Mol Genet, 2011. **20**(1): p. 165-75.

223. Campbell, J.D., et al., *Allergic humans are hyporesponsive to a CXCR3 ligand-mediated Th1 immunity-promoting loop.* FASEB J, 2004. **18**(2): p. 329-31.

224. Petrilli, V., et al., *Activation of the NALP3 inflammasome is triggered by low intracellular potassium concentration.* Cell Death Differ, 2007. **14**(9): p. 1583-9.

225. Vordermeier, H.M., et al., *Correlation of ESAT-6-specific gamma interferon production with pathology in cattle following Mycobacterium bovis BCG vaccination against experimental bovine tuberculosis.* Infect Immun, 2002. **70**(6): p. 3026-32.

226. Redford, P.S., et al., *Enhanced protection to Mycobacterium tuberculosis infection in IL-10-deficient mice is accompanied by early and enhanced Th1 responses in the lung.* Eur J Immunol, 2010.

10 PUBLISHED PAPERS

Griffiths, K.L., Pathan, A.A., Minassian, A.M., Sander, C.R., Beveridge, N.E., Hill, A.V., Fletcher, H.A. and McShane, H. *Th1/Th17 cell induction and corresponding reduction in ATP consumption following vaccination with the novel Mycobacterium tuberculosis vaccine MVA85A.* PLoS One, 2011. **6** (8): p. e23463

OPEN ACCESS Freely available online

PLoS one

Th1/Th17 Cell Induction and Corresponding Reduction in ATP Consumption following Vaccination with the Novel *Mycobacterium tuberculosis* Vaccine MVA85A

Kristin L. Griffiths, Ansar A. Pathan¤, Angela M. Minassian, Clare R. Sander, Natalie E. R. Beveridge, Adrian V. S. Hill, Helen A. Fletcher, Helen McShane*

The Jenner Institute, Oxford University, Oxford, United Kingdom

Abstract

Vaccination with Bacille Calmette-Guérin (BCG) has traditionally been used for protection against disease caused by the bacterium *Mycobacterium tuberculosis* (*M.tb*). The efficacy of BCG, especially against pulmonary tuberculosis (TB) is variable. The best protection is conferred in temperate climates and there is close to zero protection in many tropical areas with a high prevalence of both tuberculous and non-tuberculous mycobacterial species. Although interferon (IFN)-γ is known to be important in protection against TB disease, data is emerging on a possible role for interleukin (IL)-17 as a key cytokine in both murine and bovine TB vaccine studies, as well as in humans. Modified Vaccinia virus Ankara expressing Antigen 85A (MVA85A) is a novel TB vaccine designed to enhance responses induced by BCG. Antigen-specific IFN-γ production has already been shown to peak one week post-MVA85A vaccination, and an inverse relationship between IL-17-producing cells and regulatory T cells expressing the ectonucleosidease CD39, which metabolises pro-inflammatory extracellular ATP has previously been described. This paper explores this relationship and finds that consumption of extracellular ATP by peripheral blood mononuclear cells from MVA85A-vaccinated subjects drops two weeks post-vaccination, corresponding to a drop in the percentage of a regulatory T cell subset expressing the ectonucleosidase CD39. Also at this time point, we report a peak in co-production of IL-17 and IFN-γ by $CD4^+$ T cells. These results suggest a relationship between extracellular ATP and effector responses and unveil a possible pathway that could be targeted during vaccine design.

Citation: Griffiths KL, Pathan AA, Minassian AM, Sander CR, Beveridge NER, et al. (2011) Th1/Th17 Cell Induction and Corresponding Reduction in ATP Consumption following Vaccination with the Novel *Mycobacterium tuberculosis* Vaccine MVA85A. PLoS ONE 6(8): e23463. doi:10.1371/journal.pone.0023463

Editor: Ludovic Tailleux, Institut Pasteur, France

Received May 19, 2011; **Accepted** July 18, 2011; **Published** August 26, 2011

Copyright: © 2011 Griffiths et al. This is an open-access article distributed under the terms of the Creative Commons Attribution License, which permits unrestricted use, distribution, and reproduction in any medium, provided the original author and source are credited.

Funding: Funding was provided by KLG's Wellcome Trust studentship (www.wellcome.ac.uk; WT086338RP) and HM's Wellcome Trust Senior Fellowship (www.wellcome.ac.uk; WT076943MA). The funders had no role in study design, data collection and analysis, decision to publish, or preparation of the manuscript.

Competing Interests: The authors have read the journal's policy and have the following conflicts: AVSH, AAP, and HM are named inventors in a patent filing related to MVA85A and are shareholders in a joint venture, OETC, formed for the future development of this vaccine. AVSH and HM are named as co-inventors on patents related to heterologous prime-boost immunization. There are no other conflicts of interest. These conflicts of interest will not in any way interfere with the authors' adherence to the journal's policies on sharing data and materials.

* E-mail: Helen.Mcshane@ndm.ox.ac.uk

¤ Current address: Centre for Infection, Immunity and Disease Mechanisms, Biosciences, School of Health Sciences and Social Care, Brunel University, Uxbridge, West London, United Kingdom

Introduction

Mycobacterium tuberculosis (*M.tb*), the causative agent of tuberculosis (TB), infects ~30% of the World's population and is endemic in Asia and sub-Saharan Africa. *M.tb* is transmitted by aerosol and infects macrophages in the lung. Infection with *M.tb* can result in acute (primary) disease, or, more commonly, remain latent. In 10% of cases, this latent infection reactivates later in life causing disease, which is usually pulmonary but can occur in other organs including spleen, stomach, bowel or brain. Co-infection with HIV, also endemic in TB-endemic areas, results in a significant increase in the risk of reactivation of this latent infection [1,2,3]. Bacille Calmette-Guérin (BCG), the current TB vaccine, is an attenuated form of *M.bovis* and offers varying degrees of protection. Notably, the level of protection is lowest in areas endemic for *M.tb* and the development of a novel, more effective vaccine against TB is urgently needed.

Modified Vaccinia virus Ankara expressing antigen 85A (MVA85A), a secreted and highly immunogenic protein common to both BCG and *M.tb*, is a vaccine designed to enhance the low level of T cell responses induced by BCG through expansion of antigen 85A-specific T cells [4,5]. The MVA85A-induced interferon (IFN)-γ response has been well-characterised across several groups of vaccinated individuals and peaks 1–2 weeks post-vaccination [4,5,6,7,8]. Recently, however, other immunological parameters have been investigated, in particular those pertaining to immune regulation. MVA85A has been shown to induce a reduction in transforming growth factor (TGF)-β in the serum [9] as well as a reduction in percentages of $CD25^+Foxp3^+CD39^+$ Treg in peripheral blood monocytes (PBMC) from vaccinated subjects [10]. CD39, an ectonucleosidase triphosphate diphosphohydrolase (eNDTPase; apyrase) hydrolysing extracellular adenosine triphosphate (ATP) to adenosine monophosphate (AMP) [11], is expressed on leukocytes, including neutrophils and T cells. In humans, $CD4^+$ T cells can be divided according to their expression of CD25, CD39 and Foxp3, with $CD4^+CD25^+CD39^+Foxp3^+$ cells representing a regulatory population [12]. ATP is released into the extracellular

environment as a natural process during inflammation [13] as well as being released by dead cells. It has been identified as a proinflammatory agent and is known to activate the NALP3 inflammasome through binding to the P2X7 receptor and inducing a K^+ efflux, as well as activating the Pannexin-1 channel [14,15]. The combination of these events drives the cleavage of pro-IL-1, induced by Toll-like receptor (TLR) activation, to IL-1β by Caspase-1 [16]. IL-1β, in synergy with IL-6, has in turn been shown to induce IL-17 production by Th17 cells [17]. Reduced percentages of $Foxp3^+CD39^+$ Treg have been described in PBMC of patients with multiple sclerosis compared to healthy donors [18,19], and the $CD39^+$ cells that were present had impaired ATP-hydrolysing capacity [19], providing evidence for a link between CD39 expression on Treg cells and a function in regulating inflammation through controlling extracellular ATP levels.

Here we show that $CD39^+$ Treg percentages drop 2 weeks post-MVA85A vaccination, coincident with a drop in ATP consumption by PBMC from MVA85A-vaccinated subjects. This also coincides with an increase in percentages IFN-γ and IL-17 double-producing $CD4^+$ T cells.

Clearance and control of *M.tb* infection is at least partly dependent upon interferon (IFN)-γ production by $CD4^+$ T helper 1 (Th1) cells [20], however IL-17 has recently been identified as being induced by *M.tb* in murine lungs following vaccination with adjuvanted peptides derived from ESAT-6, an immunodominant secreted protein specific to *M.tb* [21]. Vaccination of mice lacking IL-23 subunits, the cytokine essential for Th17 expansion, resulted in the loss of accelerated vaccine-induced recruitment of Th1 cells to the lungs following *M.tb* infection, suggesting that IL-17-producing cells (Th17) contribute to vaccine-induced protection against *M.tb* challenge through recruitment of Th1 cells to the lung. These hypotheses are supported by a different study in which mice were vaccinated with either BCG or BCG followed by a construct designed to produce anti-IL-12 antibodies within the animal, or with the anti-IL-12-inducing construct alone [22]. Following an *M.tb* challenge, results showed higher bacterial load (cfu) in lungs and spleen from mice with anti-IL-12 antibodies compared to no treatment, but no difference in cfu between BCG or BCG+anti-IL-12 groups, which both had significantly lower cfu than unvaccinated mice. Interestingly, higher IL-17 and IL-6 levels were detected in the vaccinated compared to the unvaccinated groups, suggesting that control during primary intravenous infection depends on a Th1 response, but on an IL-17-driven response following vaccination.

Further support for the involvement of IL-17 in control of *M.tb* infection comes from a recent study comparing cytokine levels in tuberculin skin test (TST) negative and TST positive (considered latently infected) individuals in a TB endemic area. These results showed that IL-17, IL-23 and RORγt, the transcription factor implicated in Th17 development, were downregulated in TST^+ individuals [23] suggesting that higher IL-17 production favours clearance or control of *M.tb*.

MVA85A has previously been shown to increase interleukin (IL)-17 production in both humans and cattle [10,24]. Furthermore, in cattle, vaccine-induced IL-17 production both pre- and post- *M.bovis* challenge has been correlated with vaccine-induced protection against TB disease [24]. IL-17 has also been detected in whole blood of MVA85A-vaccinated adolescents and children, where the $IL\text{-}17^+$ cells were also found to produce IFN-γ, tumour necrosis factor (TNF)-α and IL-2 [25]. Here we suggest a possible link between $CD39^+$ Treg cells and potentially protective MVA85A-induced IFN-γ and IL-17 production.

Results

ATP consumption following MVA85A vaccination follows a distinct pattern and can be inhibited using an apyrase inhibitor

Consumption of extracellular ATP was measured in PBMC from vaccinated subjects at 0, 1, 2, 4 and 24 weeks post-vaccination using the CellTiter-Glo cell viability assay and plotting against a standard curve. There was a significant difference in ATP consumption 2 weeks post-vaccination compared to baseline ($p = 0.008$) (Fig. 1A). Paired analysis between 0 and 2 weeks is shown in figure 2B. In order to verify that ATP consumption was attributable to the action of an apyrase, cells were treated with ARL67156 at the time of ATP addition, which reduced ATP consumption (Fig. 1C).

Regulatory T cells, defined here as $CD4^+CD25^+CD39^{hi}$, have previously been shown to decrease in number post-vaccination with MVA85A [10]. Since CD39 is an eNDTPase metabolising ATP, percentages of these cells in PBMC of vaccinated subjects were compared to levels of ATP consumption. There was a small dip in percentages of $CD39^+$ Treg cells between 1 and 2 weeks post-vaccination and followed the pattern of ATP consumption (Fig. 1D).

IFN-γ and IL-17 double positive cells peak 2 weeks post-vaccination

In PBMC from healthy MVA85A-vaccinated subjects, T cells producing only IL-17 were not detectable by intracellular cytokine staining, using a peptide pool of 66 Ag85A peptides as the stimulant (data not shown). In contrast, $CD4^+$ T cells producing both IFN-γ and IL-17 simultaneously in response to stimulation with Ag85A peptides were readily detected in response to the same stimulant. $IFN\text{-}\gamma^+IL\text{-}17^+$ cells (gating shown in Fig. 2A) peaked 2 weeks post-vaccination (Fig. 2B). Since there appeared to be CD39 activity in the PBMC samples (Fig. 1C), the effect of ARL67156 treatment on antigen-specific cytokine production was examined. Addition of ARL67156 enhanced production of both cytokines both 1 and 2 weeks post-vaccination and the change in cytokine production compared to baseline in this experiment was significant ($p = 0.047$ at 1 week and 0.02 at 2 weeks post-vaccination) (Fig. 2C).

$IL\text{-}17^+$ and $IFN\text{-}\gamma^+IL\text{-}17^+$ cells are present at a higher frequency in whole blood compared to PBMC of vaccinated subjects

Other trials involving vaccination with MVA85A have investigated cytokine responses in whole blood as opposed to PBMC. One marked difference between these two compartments is that IFN-γ-producing $CD8^+$ T cells are readily detectable in whole blood but not in PBMC following vaccination ([5,26] and Satti, I. unpublished data). To directly compare $CD4^+$ T cell cytokine production in these two compartments, we investigated IL-17 and IFN-γ production following stimulation with Ag85A peptides in whole blood and PBMC from the same BCG-vaccinated healthy subjects. Whole blood was stimulated with peptide pools of 85A. Both $IL\text{-}17^+$ and $IFN\text{-}\gamma^+IL\text{-}17^+$ cells peaked 1 week post-vaccination (Figs. 3A & B), in contrast to the undetectable IL-17 response and the peak of $IFN\text{-}\gamma^+IL\text{-}17^+$ cells observed 2 weeks post-vaccination in PBMC. The magnitude of response was also significantly higher one week post-vaccination in whole blood, with a mean of 0.0548% (±0.0355) compared to 0.0065% (±0.0063) for PBMC, $p = 0.002$ following stimulation with the Ag85A peptide pool. Furthermore, there was a significant

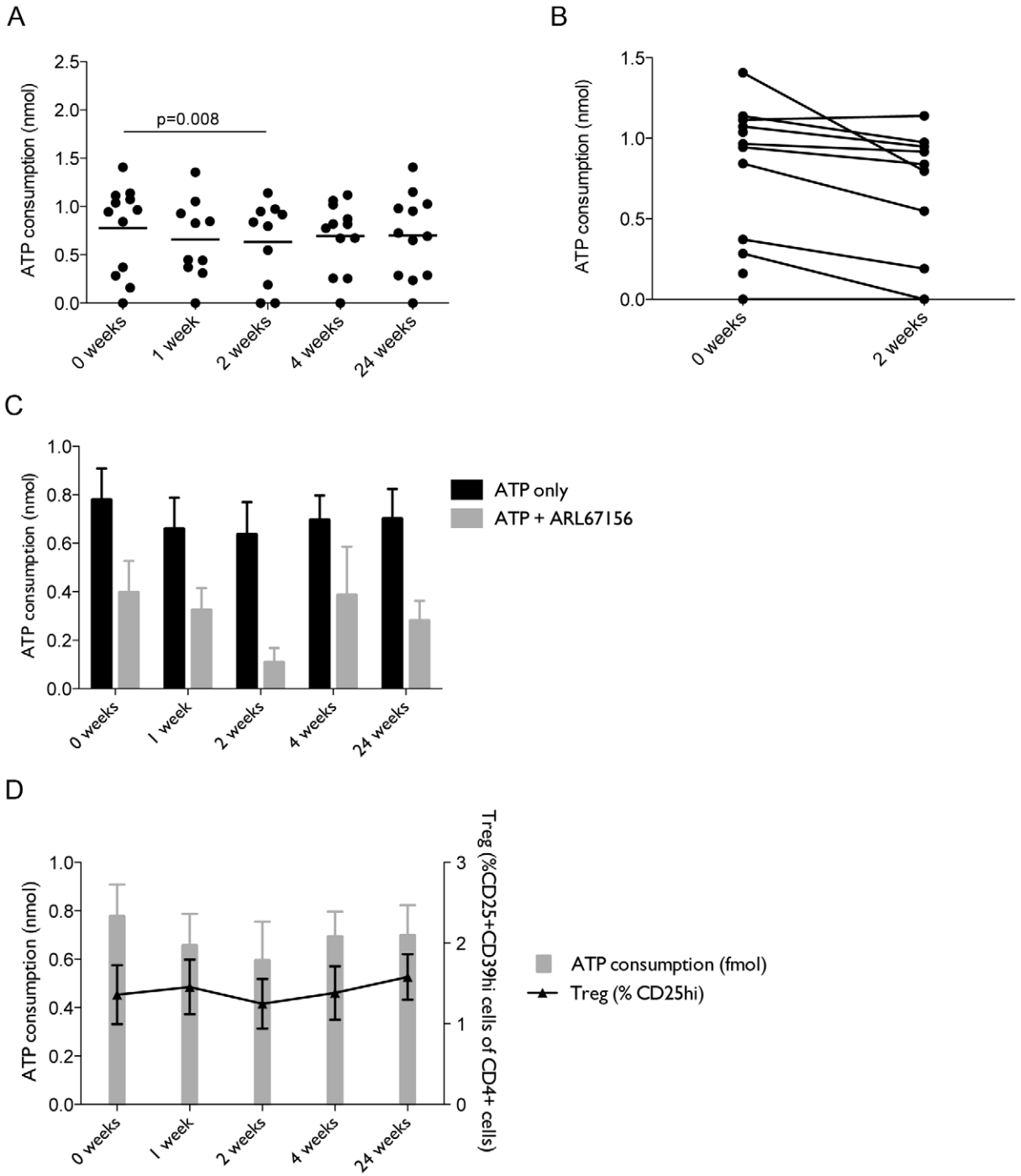


Figure 1. ATP consumption by PBMC and CD39$^+$ Treg percentages dip 2 weeks post-vaccination. PBMC from MVA85A-vaccinated subjects were plated out at 5×10^4 cells/well in 50 μL. Cells were incubated with either 50 μM ATP or 50 μM+100 μM ARL67156 before addition of the luciferase reagent. A standard curve starting at 50 μM ATP was set up and negative controls were cells with no ATP added. (A) Shows change in ATP consumption over time post-vaccination. (B) Paired representation of change in ATP consumption between 0 and 2 weeks post-MVA85A. Effect of addition of ARL67156 is show in (C). (n = 10–12). Note that the observation of a greater effect of the inhibitor is potentially due to saturation of binding sites for ATP by the inhibitor at this timepoint, whereas the greater percentage of CD39$^+$ cells present at other timepoints meant the concentration of ARL67156 was not high enough to completely block all available binding sites. Percentages of CD25$^+$CD39$^+$ Treg in MVA85A-vaccinated subjects were calculated as a percentage of CD4$^+$ T cells and shown in (D), plotted over ATP consumption.
doi:10.1371/journal.pone.0023463.g001

difference in peak response comparing whole blood and PBMC following Ag85A peptide pool stimulation (Fig. 3C) (mean ± SD for WB (1 week post-vaccination): 0.0548% (±0.0355); PBMC (2 weeks post-vaccination): 0.0096% (±0.0083), $p<0.001$).

Discussion

M.tb is a resilient intracellular pathogen that has evolved to survive successfully inside human macrophages in a delicate

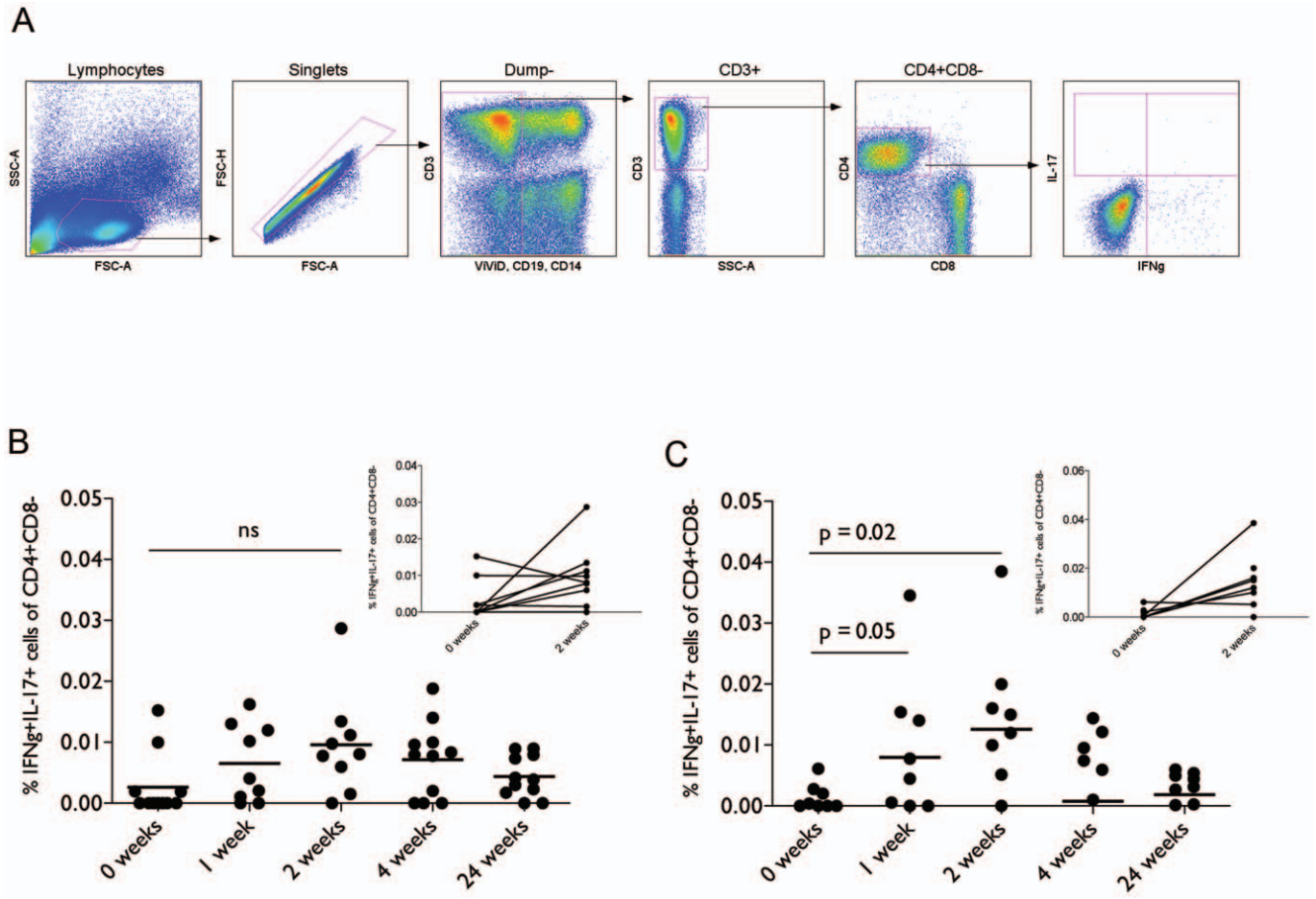


Figure 2. IL-17 and IFN-γ production in PBMC peaks 2 weeks post-vaccination. PBMC from vaccinated subjects were stimulated with Ag85A peptide pools with or without 100 uM ARL67156. No stimulation and phorbol 12-myristate 13-acetate with ionomycin were used as negative and positive controls. Percentages shown are unstimulated subtracted from Ag85A stimulation. Following staining, cells were gated as shown in (A): Lymphocytes were gated for on FSC vs. SSC. Singlets were then gated and dead cells, B cells and monocytes were gated out. $CD3^+$ cells were selected for $CD4^+CD8^-$ cells. Antigen-specific cytokine expression from these cells was evaluated. Cells expressing both IL-17 and IFN-γ were quantified and shown in (B). The effect of ARL67156 on cytokine expression was investigated by addition during ICS stimulation (C).
doi:10.1371/journal.pone.0023463.g002

balance with the host's immune system. Should this balance be tipped in favour of the pathogen, the result is potentially fatal active disease. Vaccination is therefore essential in order to either prevent initial infection or, failing that, to prevent development of active TB disease. Consequently, it is important to understand the types of immune cells that should optimally be induced by vaccination and the mechanisms through which these cells can be induced. As well as measuring effector responses in terms of Th1 immunity, it is also important to measure other types of effector responses as well as the corresponding regulatory response induced by vaccination as protection induced by any vaccine will be the outcome of the balance of all these responses.

Here we show that there is a relationship between ATP consumption, and IFN-γ and IL-17 expression by $CD4^+$ T cells following vaccination with MVA85A, which also relates to percentages of $CD39^+$ Treg in the PBMC. In healthy BCG and MVA85A-vaccinated subjects, $CD39^+$ Treg numbers decrease post-vaccination, with a maximum decrease 2 weeks post-vaccination. This is associated with a decrease in ATP consumption, suggesting that ATP consumption is driven at least in part by $CD39^+$ Treg. Strikingly, at 2 weeks post-vaccination, we also show an increase in the percentage of IFN-γ^+IL-17^+ cells. IFN-γ^+IL-17^+ cells have been previously been described in autoimmune diseases [19] and ulcerative colitis [27] as well as in response to mycobacterial antigens [28]. Our data support the hypothesis that extracellular ATP may help to drive the development of these cells. This hypothesis is supported by the fact that IL-17^+ and IFN-γ^+IL-17^+ cells are more readily detectable in whole blood compared to PBMC; the extracellular environment of whole blood is far more complex than that of PBMC and our experiments have shown a higher concentration of ATP in whole blood compared to PBMC following stimulation. Furthermore, ATP has previously been shown to induce IL-17 production by T cells in mice [29].

The link between these observations following MVA85A vaccination is still under investigation. One mechanism that could contribute to increased cytokine production is activation of the NALP3 inflammasome. This leads to IL-1β production, which in turn acts on induction of $CD4^+$ T cells to produce IL-17 [17]. Since CD39 metabolises ATP, a vaccine-induced reduction in circulating $CD39^+$ Treg may result in increased concentrations of pro-inflammatory extracellular ATP, known to act through the P2X7 receptor to activate the inflammasome [14,30]. Adding to this effect, a decrease in circulating $CD39^+$ Treg would also reduce the concentration of breakdown products of ATP, such as adenosine, which is known to act in an inhibitory fashion through the A2A receptor on activated T cells [31].

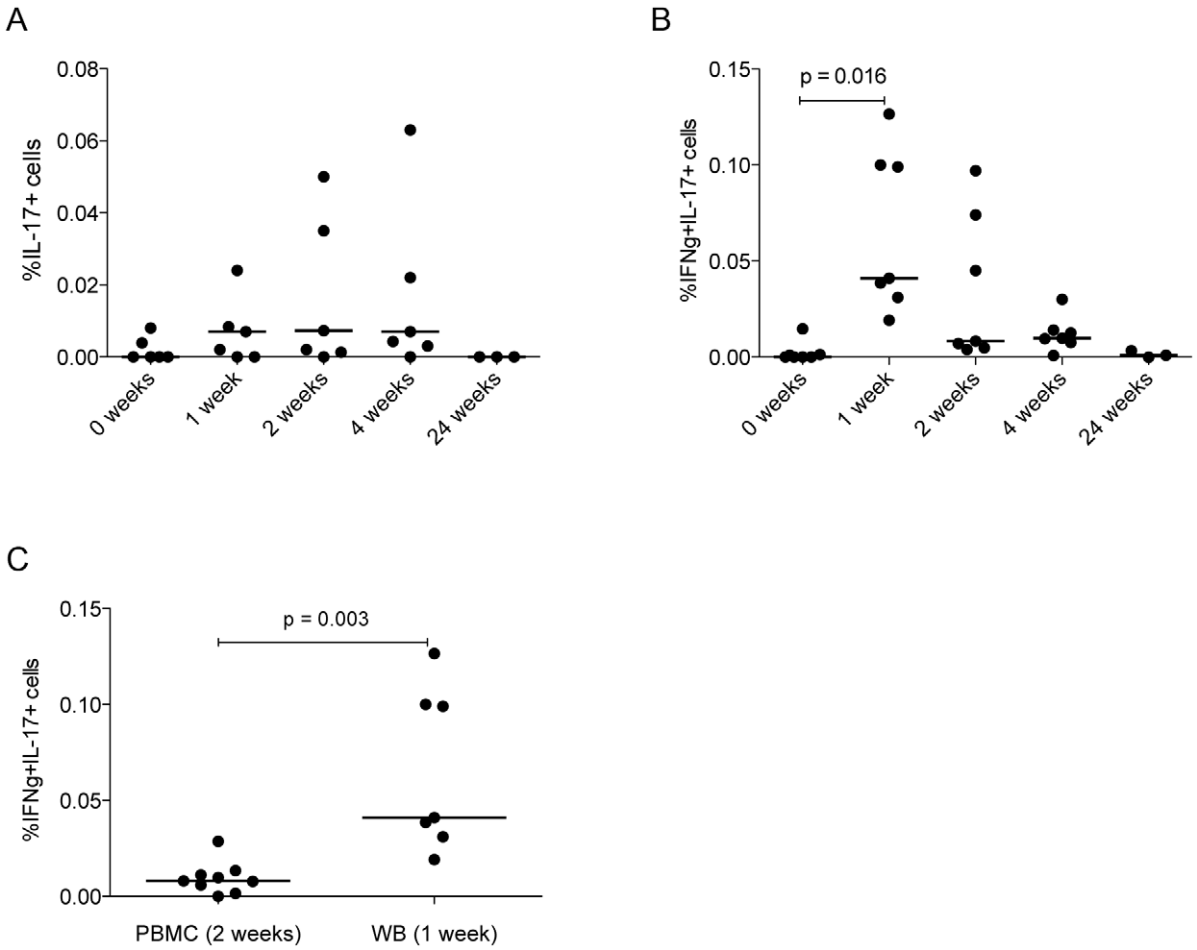


Figure 3. IL-17 and IFN-γ production in whole blood peaks 1 week post-vaccination. Whole blood (WB) from vaccinated subjects was stimulated for 6 h with a pool of 66 Ag85A peptides. Phytohaemagglutinin (PHA)-treated and untreated cells were used as positive and negative controls respectively. Lymphocytes were gated for and cytokine-expressing cells quantified as described above. Percentages of IL-17$^+$ and IFN-γ$^+$IL-17$^+$ cells responding to the Ag85A peptide pool (with the percentages from unstimulated cells subtracted) are shown in (A) and (B). Differences in percentages of cells at the relevant peak time point in PBMC vs. WB is shown in (C). n = 7.
doi:10.1371/journal.pone.0023463.g003

A further contributing factor to inflammasome activation and IL-17 induction might be the viral vector MVA, which has been found to activate the NALP3 inflammasome in THP-1 cells following its endocytosis [32].

The role of IFN-γ$^+$IL-17$^+$ cells in protection against mycobacterial infection is not clear, however both cytokines individually are known to be important in vaccine-induced protection. So far in mice, it has been shown that ablation of an IL-17 response following both vaccination (antigen-specific production) [21] and high-dose *M.tb* challenge (production by innate cells) [33] leads to reduced protection against *M.tb* infection. However, it would also appear that pathology induced as a result of prolonged exposure to mycobacterial antigens is IL-17-dependent [34]. Measurement of IL-17 production in lungs following either vaccination or *M.tb* infection is not possible in human studies so it is difficult to draw comparisons and to predict the role of IL-17, especially since the mouse model of *M.tb* disease is not an ideal representation of human disease. As discussed above, it has been found that IL-17 levels in blood in both humans and cattle correlate with protection against mycobacterial exposure [23] and mycobacterial infection [24] respectively, so it may be, as proposed by Torrado and Cooper [35], that while IL-17 may be essential in vaccine-induced control of TB disease, it needs to be under tight regulation by other aspects of the immune response in order to avoid induction of immunopathology.

These findings demonstrate vaccine-mediated induction of a subset of IFN-γ$^+$IL-17$^+$ cells, whose peak corresponds with a reduction in the ability of these cells to hydrolyse ATP in a CD39-mediated manner. Should this cell subset prove to be protective in vaccine-induce protection against TB disease, this pathway represents a potential target for manipulation for their enhancement.

Knowledge of mechanisms through which IL-17-, and IFN-γ and IL-17-producing cells can be induced is important with regard to vaccine development, with the next step being to determine their role in vaccine-induced protection or pathology.

Furthermore, it is important to investigate regulatory aspects of cellular immunity, as the total outcome of any vaccine-induced immunity will be the result of a balance between both effector and regulatory responses. The work here helps to dissect this interaction between regulatory and effector responses following vaccination and provides potential avenues for manipulation of immune responses in order to provide improved vaccine-induced protection.

Materials and Methods

Vaccine study participants

PBMC were from subjects recruited for a trial approved by the review committees indicated below. Subjects (aged 18–50) were recruited on the basis of prior BCG vaccination (maximum Mantoux test 15 mm, <10 sfc/million ELISpot counts in response to ESAT-6 and CFP10 peptide pools) and were seronegative for HIV and hepatitis B and C viruses. The trial was registered on the clinical trials database (ClinicalTrials.gov ID: NCT00465465). Subjects from whom samples were taken received a dose of MVA85A at 1×10^8 pfu as two intradermal injections, administered simultaneously, one in each arm. The MVA85A vaccine was manufactured to Good Manufacturing Practice (GMP) by Impfstoffwerk Dessau-Tornau (IDT) Biologika GmbH in Germany. Samples from weeks 0, 1, 2, 4 and 24 were investigated.

The efficacy and safety data from this trial is in the process of being written up but has yet to be published; immunological data from the same trial has been published in Beveridge et al. 2008 [26].

Ethics statement

All clincal trials are fully approved by the ethical and regulatory agencies (Centre of Research: Ethical Campaign, and Medicines and Healthcare Products Regulatory Agency), and also local GMO and NHS committees as required (the Gene Therapy Advisory Committee), and full written consent was obtained from each subject prior to enrolment in the trial. Storage of samples for exploratory immunological analyses is fully ethically approved.

PBMC preparation

PBMC from vaccinated subjects were cryopreserved in liquid nitrogen at time of acquisition in aliquots of 5×10^6 cells in 50% fetal bovine serum (FBS; Biosera Ltd.), 40% RPMI 1640, 10% dimethylsulphoxide (DMSO; both from Sigma Aldrich). Prior to use, cells were thawed in 9 mL R10 (10% FBS, 2 mM L-glutamine, 100 U/mL penicillin, 100 ug/mL streptomycin in RPMI 1640). Cells were treated with 67.2 U/mL Benzonase (Novagen) for at least 2 hours at 37°C in 5% CO_2. Cells were washed and resuspended to $\sim1\times10^6$ cells/mL and counted using a CASY cell counter (Schärfe System, GmbH).

Antibodies and reagents

Anti-human antibodies (Pacific blue anti-CD19, eFluor450 anti-CD19, Pacific blue anti-CD14, eFluor450 anti-CD14, PE-Cy5 anti-CD3, APC-AlexaFluor780 anti-CD8, APC anti-CD25, PE-Cy7 anti-CD39, FITC anti-IFN-γ, PE anti-IL-17) were obtained from eBioscience, and Qdot655 anti-CD4 and the ViViD Live/Dead cell stain were from Invitrogen. The Cytofix/Cytoperm intracellular staining kit was from BD Biosciences. ATP was purchased from Millipore, and ARL67156 from Tocris Bioscience. The CellTiter-Glo cell viability kit was from Promega. Brefeldin A was supplied by Sigma Aldrich and GolgiStop by BD.

Intracellular cytokine staining

Cells were resuspended at 1×10^6 cells/mL and each sample divided into seven 1 mL aliquots in 5 mL polystyrene round bottom tubes (BD Falcon). Cells were stimulated for 18 hours at 37°C in 5% CO_2 with one of the following: no stimulation, no stimulation +100 uM ATP, no stimulation +100 uM ARL67156, 0.2 ug/mL phorbol 12-myristate 13-acetate (PMA) and 2 ug/mL ionomycin, 2 ug/mL Ag85A peptide pool, 2 ug/mL Ag85A peptide pool +100 uM ATP, 2 ug/mL Ag85A peptide pool +100 uM ARL67156. After 2 hours, 5 ug/mL Brefeldin A and 0.7 uL GolgiStop (BD Biosciences) were added.

After stimulation, cells were sedimented at 1300 rpm for 5 min at 4°C and transferred to a flexible 96 well plate for staining.

Cells were stained with ViViD Live/Dead cell stain prior to surface staining with eFluor450 anti-CD19, eFluor450 anti-CD14, APC anti-CD25 and PE-Cy7 anti-CD39. Cytofix/Cytoperm was used to permeabilise cells prior to staining intracellularly with PE-Cy5 anti-CD3, Qdot655 anti-CD4, APC-AlexaFluor780 anti-CD8, FITC anti-IFN-γ and PE anti-IL-17. Following permeabilisation, washes between stains included sedimentation for 5 min at 1800 rpm, 4°C.

Staining was analysed using an LSR II flow cytometer (BD Biosciences).

Whole blood ICS

Freshly collected heparinised whole blood from MVA85A-vaccinated volunteers was stimulated for 10–11 hours at 37°C with either recombinant Ag85A, a pool of 66 peptides of Ag85A, PPD or BCG. No stimulation and Phytohaemagglutinin were used as negative and positive controls, respectively. After 5–6 hours, Brefeldin A was added for the final 5 hours. Cells were harvested by adding 1 mL FACS Lysing Solution (BD Bioscience) and sedimenting. Cells were frozen in 10% DMSO in FCS and stored at −80°C.

ATP consumption assay

ATP consumption was measured as described Borsellino *et al.* [18]. Briefly, PBMC from subjects were resuspended at 1×10^6 cells/mL and aliquoted into 6 wells/sample of a white 96 well plate (Nunc) at 5×10^4 cells/well. Cells were treated with either nothing, 50 uM ATP or 50 uM ATP +100 uM ARL67156 for 10 min at room temperature. One volume CellTiter-Glo solution was added to each well and cells were incubated for a further 10 min at room temperature in the dark. Luminescence was recorded using a Varioskan Flash spectral scanning multimode reader (Thermo Scientific). ATP consumption was calculated using a standard curve of known ATP concentrations and expressed in nmol.

Statistical analysis

Given the non-parametric nature of the data, Wilcoxon Sign Rank Tests and Mann-Whitney Tests were performed as appropriate tests for statistical analysis.

Acknowledgments

The authors thank the volunteers who took part in the clinical trials reported here, and Ian Poulton and Alison Lawrie for assistance with the clinical trials administration.

Author Contributions

Conceived and designed the experiments: KLG HAF HM. Performed the experiments: KLG. Analyzed the data: KLG HAF. Contributed reagents/materials/analysis tools: AAP AMM CRS NERB HAF. Wrote the paper: KLG. Head of the laboratory: AVSH.

References

1. Churchyard GJ, Kleinschmidt I, Corbett EL, Mulder D, De Cock KM (1999) Mycobacterial disease in South African gold miners in the era of HIV infection. Int J Tuberc Lung Dis 3: 791–798.
2. WHO (2010) Global Tuberculosis Control. World Health Organisation.
3. Dye C, Williams BG (2010) The population dynamics and control of tuberculosis. Science 328: 856–861.

4. McShane H, Pathan AA, Sander CR, Goonetilleke NP, Fletcher HA, et al. (2005) Boosting BCG with MVA85A: the first candidate subunit vaccine for tuberculosis in clinical trials. Tuberculosis (Edinb) 85: 47–52.
5. McShane H, Pathan AA, Sander CR, Keating SM, Gilbert SC, et al. (2004) Recombinant modified vaccinia virus Ankara expressing antigen 85A boosts BCG-primed and naturally acquired antimycobacterial immunity in humans. Nat Med 10: 1240–1244.
6. Sander CR, Pathan AA, Beveridge NE, Poulton I, Minassian A, et al. (2009) Safety and immunogenicity of a new tuberculosis vaccine, MVA85A, in Mycobacterium tuberculosis-infected individuals. Am J Respir Crit Care Med 179: 724–733.
7. Minassian A, Rowland R, Beveridge NE, Poulton I, Satti I, et al. (Under submission) MVA85A, a candidate TB vaccine, is safe and immunogenic in HIV-infected adults.
8. Brookes RH, Hill PC, Owiafe PK, Ibanga HB, Jeffries DJ, et al. (2008) Safety and immunogenicity of the candidate tuberculosis vaccine MVA85A in West Africa. PLoS One 3: e2921.
9. Fletcher HA, Pathan AA, Berthoud TK, Dunachie SJ, Whelan KT, et al. (2008) Boosting BCG vaccination with MVA85A down-regulates the immunoregulatory cytokine TGF-beta1. Vaccine 26: 5269–5275.
10. De Cassan S, Pathan A, Sander C, Minassian A, Hill AV, et al. (2010) Investigating the induction of vaccine induced Th17 and regulatory T cells in healthy, BCG immunised adults vaccinated with a new tuberculosis vaccine, MVA85A. Clin Vaccine Immunol 17: 1066–1073.
11. Robson SC, Sevigny J, Zimmermann H (2006) The E-NTPDase family of ectonucleotidases: Structure function relationships and pathophysiological significance. Purinergic Signal 2: 409–430.
12. Dwyer KM, Hanidziar D, Putheti P, Hill PA, Pommey S, et al. (2010) Expression of CD39 by human peripheral blood CD4+ CD25+ T cells denotes a regulatory memory phenotype. Am J Transplant 10: 2410–2420.
13. Corriden R, Chen Y, Inoue Y, Beldi G, Robson SC, et al. (2008) Ecto-nucleoside triphosphate diphosphohydrolase 1 (E-NTPDase1/CD39) regulates neutrophil chemotaxis by hydrolyzing released ATP to adenosine. J Biol Chem 283: 28480–28486.
14. Pelegrin P, Surprenant A (2006) Pannexin-1 mediates large pore formation and interleukin-1beta release by the ATP-gated P2X7 receptor. EMBO J 25: 5071–5082.
15. Pelegrin P, Surprenant A (2009) The P2X(7) receptor-pannexin connection to dye uptake and IL-1beta release. Purinergic Signal 5: 129–137.
16. Petrilli V, Papin S, Dostert C, Mayor A, Martinon F, et al. (2007) Activation of the NALP3 inflammasome is triggered by low intracellular potassium concentration. Cell Death Differ 14: 1583–1589.
17. Acosta-Rodriguez EV, Napolitani G, Lanzavecchia A, Sallusto F (2007) Interleukins 1beta and 6 but not transforming growth factor-beta are essential for the differentiation of interleukin 17-producing human T helper cells. Nat Immunol 8: 942–949.
18. Borsellino G, Kleinewietfeld M, Di Mitri D, Sternjak A, Diamantini A, et al. (2007) Expression of ectonucleotidase CD39 by Foxp3+ Treg cells: hydrolysis of extracellular ATP and immune suppression. Blood 110: 1225–1232.
19. Fletcher JM, Lonergan R, Costelloe L, Kinsella K, Moran B, et al. (2009) CD39+Foxp3+ regulatory T Cells suppress pathogenic Th17 cells and are impaired in multiple sclerosis. J Immunol 183: 7602–7610.
20. Altare F, Durandy A, Lammas D, Emile JF, Lamhamedi S, et al. (1998) Impairment of mycobacterial immunity in human interleukin-12 receptor deficiency. Science 280: 1432–1435.
21. Khader SA, Bell GK, Pearl JE, Fountain JJ, Rangel-Moreno J, et al. (2007) IL-23 and IL-17 in the establishment of protective pulmonary CD4+ T cell responses after vaccination and during Mycobacterium tuberculosis challenge. Nat Immunol 8: 369–377.
22. Freches D, Romano M, Korf H, Renauld JC, Van Snick J, et al. (2011) Increased pulmonary TNF-{alpha}, IL-6 and IL-17A responses compensate for decreased IFN-{gamma} production in anti-IL-12 auto-vaccine treated, BCG vaccinated mice. Clin Vaccine Immunol 18: 95–104.
23. Babu S, Bhat SQ, Kumar NP, Kumaraswami V, Nutman TB (2010) Regulatory T cells modulate Th17 responses in patients with positive tuberculin skin test results. J Infect Dis 201: 20–31.
24. Vordermeier HM, Villarreal-Ramos B, Cockle PJ, McAulay M, Rhodes SG, et al. (2009) Viral booster vaccines improve Mycobacterium bovis BCG-induced protection against bovine tuberculosis. Infect Immun 77: 3364–3373.
25. Scriba TJ, Tameris M, Mansoor N, Smit E, van der Merwe L, et al. (2010) Modified vaccinia Ankara-expressing Ag85A, a novel tuberculosis vaccine, is safe in adolescents and children, and induces polyfunctional CD4+ T cells. Eur J Immunol 40: 279–290.
26. Beveridge NE, Fletcher HA, Hughes J, Pathan AA, Scriba TJ, et al. (2008) A comparison of IFNgamma detection methods used in tuberculosis vaccine trials. Tuberculosis (Edinb) 88: 631–640.
27. Rovedatti L, Kudo T, Biancheri P, Sarra M, Knowles CH, et al. (2009) Differential regulation of interleukin 17 and interferon gamma production in inflammatory bowel disease. Gut 58: 1629–1636.
28. Acosta-Rodriguez EV, Rivino L, Geginat J, Jarrossay D, Gattorno M, et al. (2007) Surface phenotype and antigenic specificity of human interleukin 17-producing T helper memory cells. Nat Immunol 8: 639–646.
29. Atarashi K, Nishimura J, Shima T, Umesaki Y, Yamamoto M, et al. (2008) ATP drives lamina propria T(H)17 cell differentiation. Nature 455: 808–812.
30. Pelegrin P, Barroso-Gutierrez C, Surprenant A (2008) P2X7 receptor differentially couples to distinct release pathways for IL-1beta in mouse macrophage. J Immunol 180: 7147–7157.
31. Deaglio S, Dwyer KM, Gao W, Friedman D, Usheva A, et al. (2007) Adenosine generation catalyzed by CD39 and CD73 expressed on regulatory T cells mediates immune suppression. J Exp Med 204: 1257–1265.
32. Delaloye J, Roger T, Steiner-Tardivel QG, Le Roy D, Knaup Reymond M, et al. (2009) Innate immune sensing of modified vaccinia virus Ankara (MVA) is mediated by TLR2-TLR6, MDA-5 and the NALP3 inflammasome. PLoS Pathog 5: e1000480.
33. Okamoto Yoshida Y, Umemura M, Yahagi A, O'Brien RL, Ikuta K, et al. (2010) Essential role of IL-17A in the formation of a mycobacterial infection-induced granuloma in the lung. J Immunol 184: 4414–4422.
34. Cruz A, Fraga AG, Fountain JJ, Rangel-Moreno J, Torrado E, et al. (2010) Pathological role of interleukin 17 in mice subjected to repeated BCG vaccination after infection with Mycobacterium tuberculosis. J Exp Med 207: 1609–1616.
35. Torrado E, Cooper AM (2010) IL-17 and Th17 cells in tuberculosis. Cytokine Growth Factor Rev 21: 455–462.